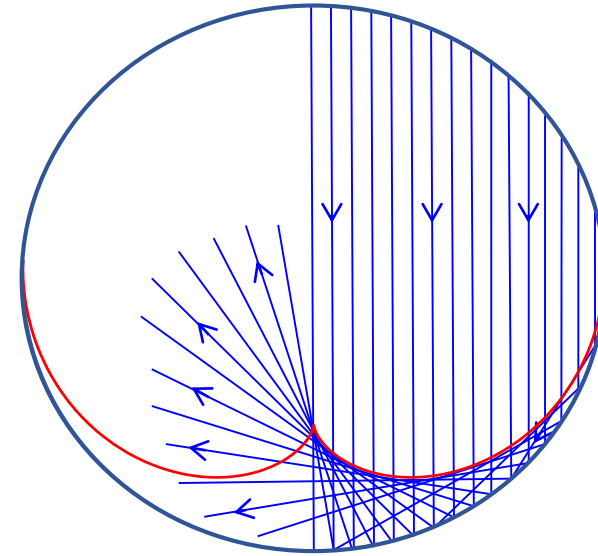


Caustics: Singularities in particle trajectory densities

Tessa Charles ^{1,2}

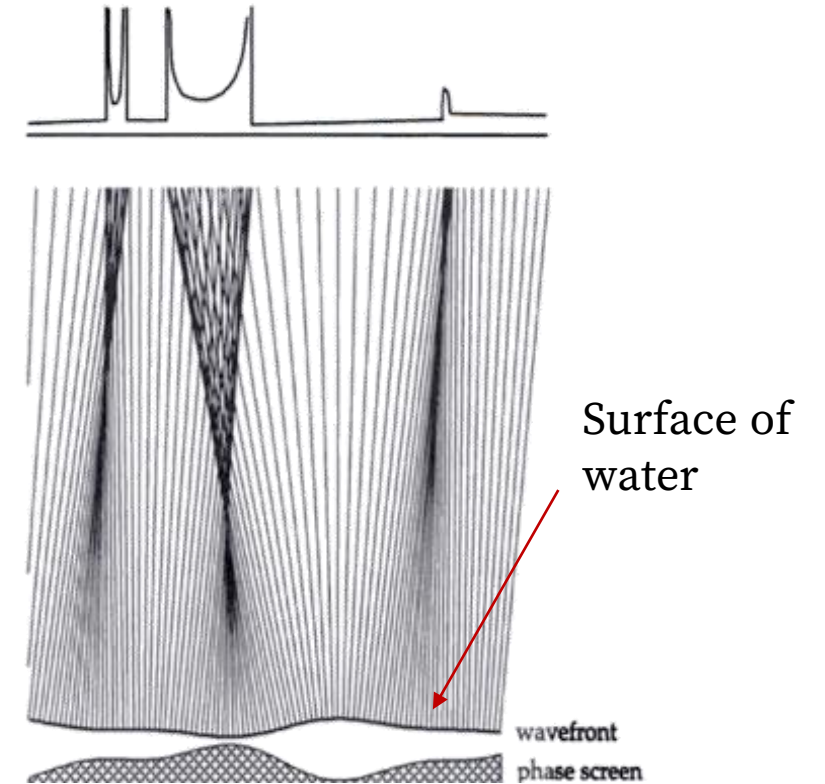
1. University of Liverpool,
2. Cockcroft Institute





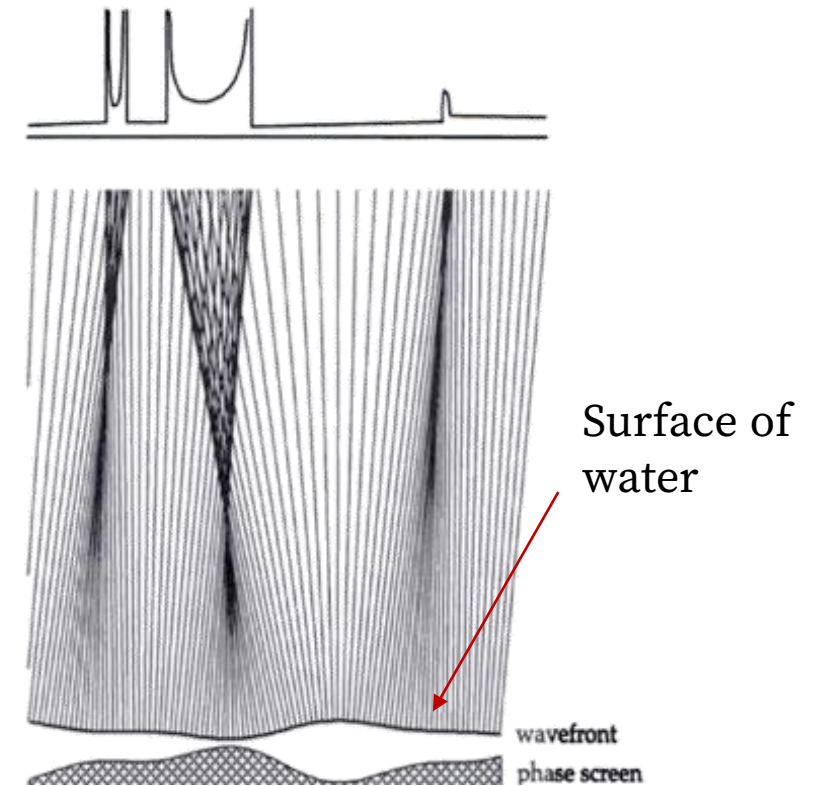
The envelope of trajectories forms the caustics lines.

Caustics lines are an envelope of trajectories,
or the projection of that envelope on another surface.



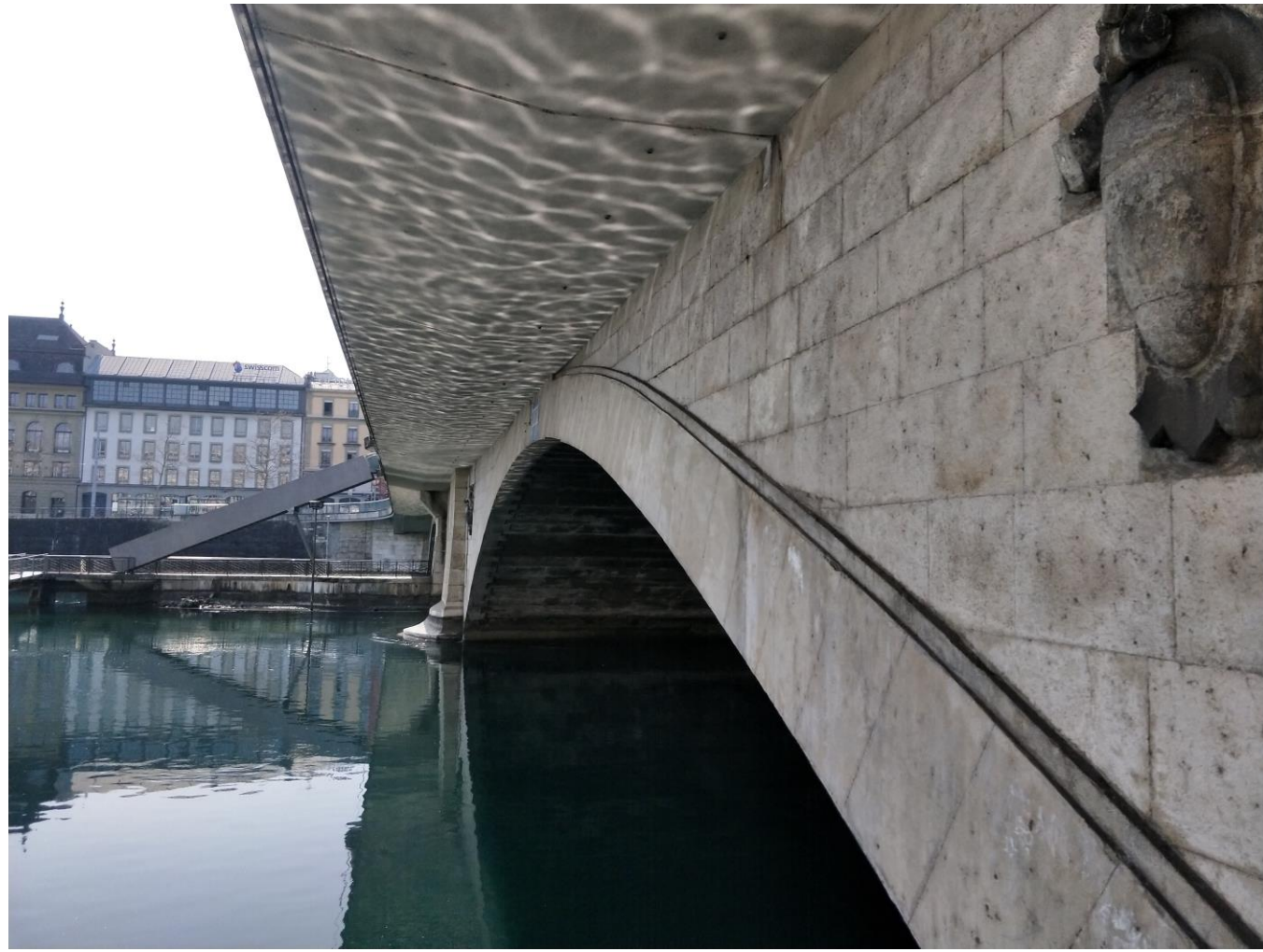
J.F. Nye "Natural Focusing and Fine Structure of Light: Caustics and Wave Dislocations", (Taylor & Francis, Philadelphia, 1999).

Caustics lines are an envelope of trajectories,
or the projection of that envelope on another surface.



J.F. Nye "Natural Focusing and Fine Structure of Light: Caustics and Wave Dislocations", (Taylor & Francis, Philadelphia, 1999).

Caustics lines are an envelope of trajectories,
or the projection of that envelope on another surface.



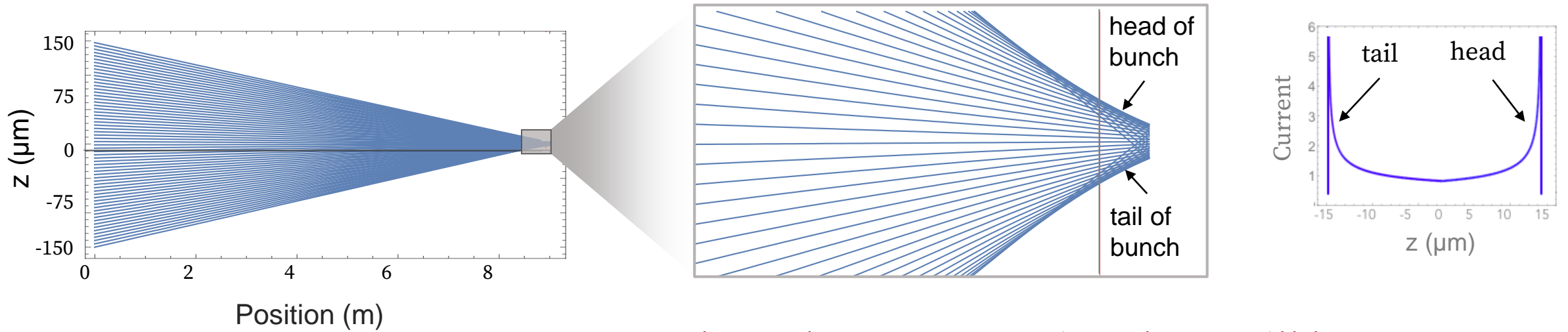
Outline

1. Introduction of caustics
2. Current horn suppression
3. MAX IV experimental measurements
4. Longitudinal Phase Space manipulation in recirculating machines
5. Microbunching instability

Outline

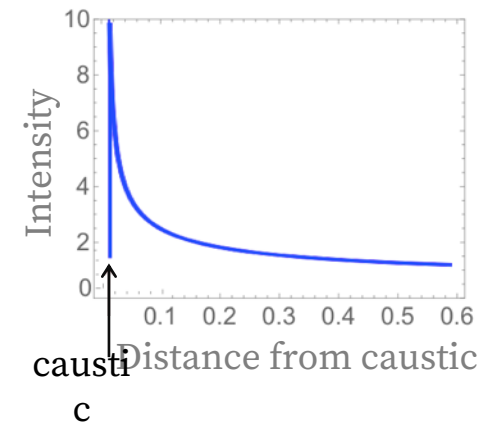
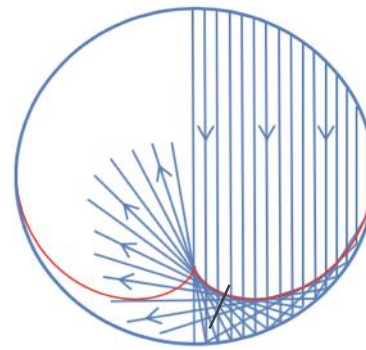
1. Introduction of caustics
2. Current horn suppression (*example of the usefulness of caustics*)
3. MAX IV experimental measurements
4. Longitudinal Phase Space manipulation in recirculating machines (*example of the usefulness of caustics*)
5. Microbunching instability (*example of the usefulness of caustics*)

Electron trajectories in a bunch compressor:



Where there are caustics, there will be current spikes.

Optical caustics example:



Caustics are singularities in the density of families of trajectories.

Caustics fall into catastrophe theory

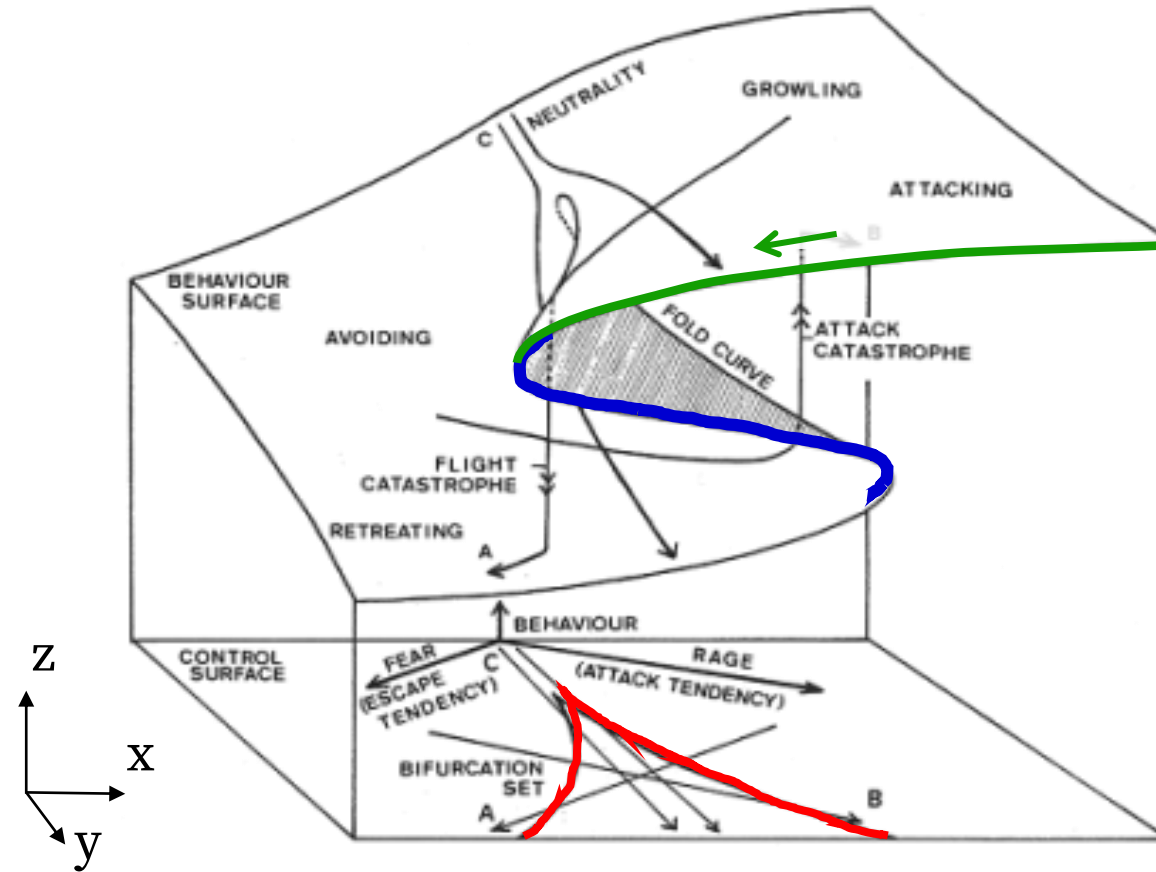
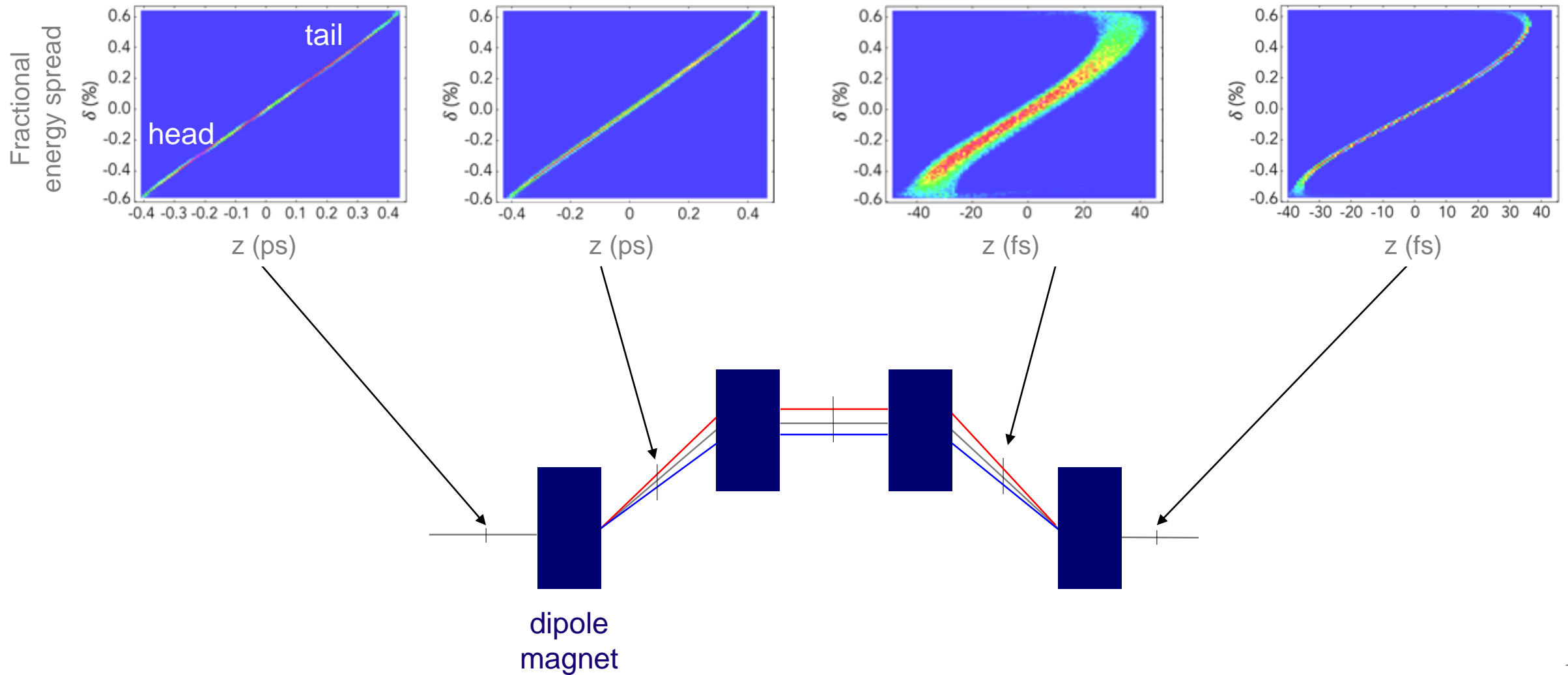


Figure: EC Zeeman (1976) Catastrophe Theory in Scientific American.

Longitudinal phase space evolution through a bunch compression

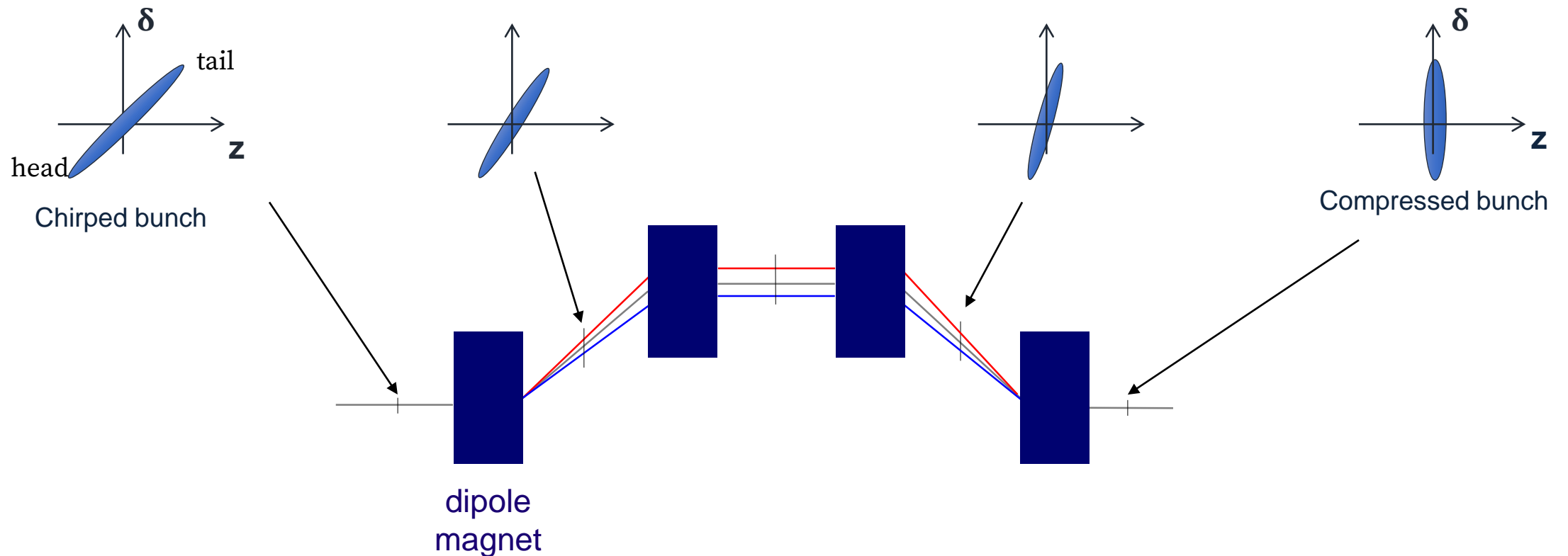


A brief aside: how bunch compressors work

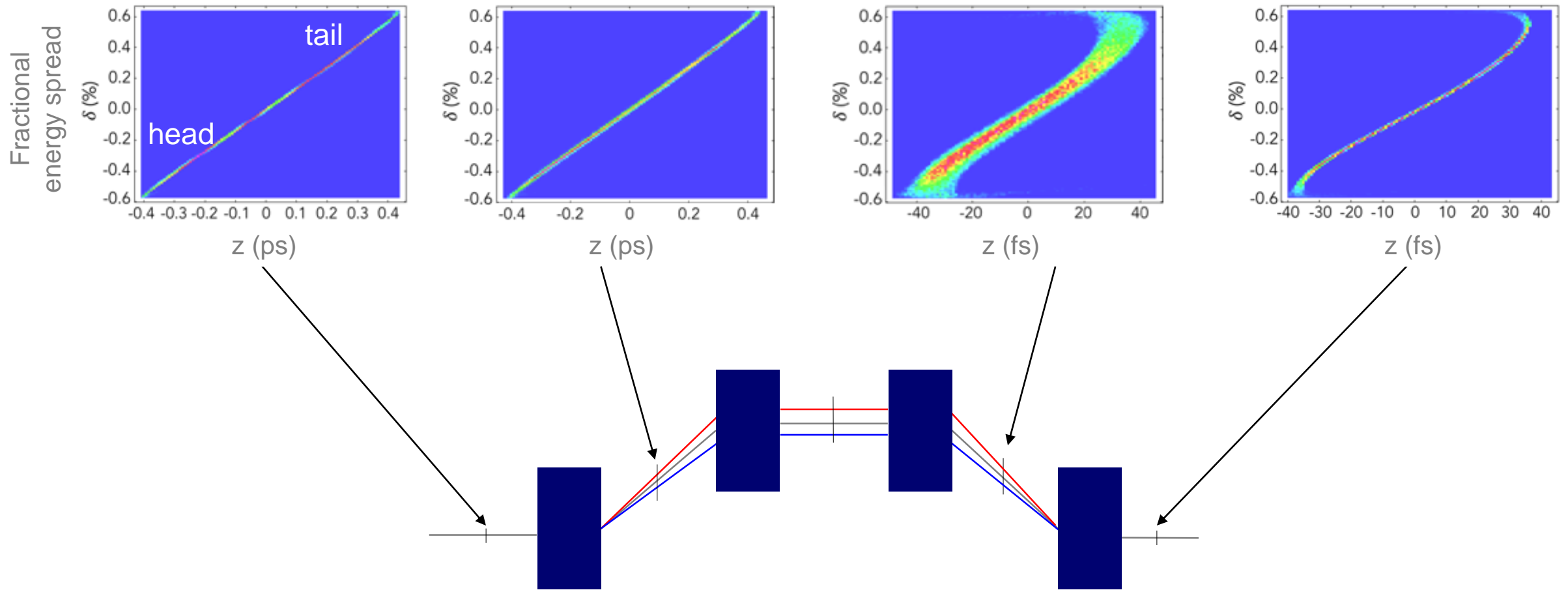
$$z_f = R_{55}z_i + R_{56}\delta + T_{566}\delta^2 + U_{5666}\delta^3 + \dots$$

R_{56} longitudinal dispersion

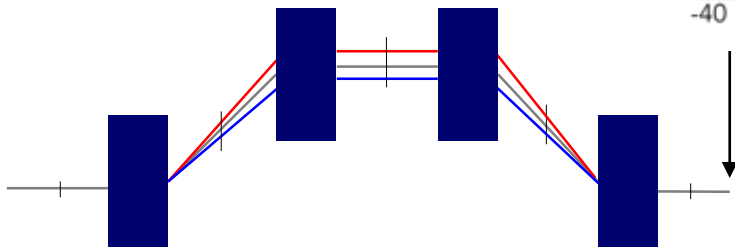
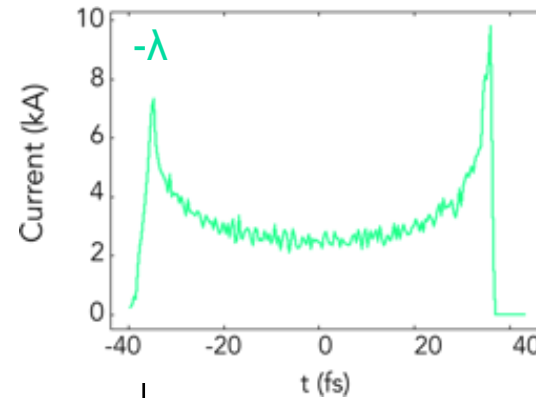
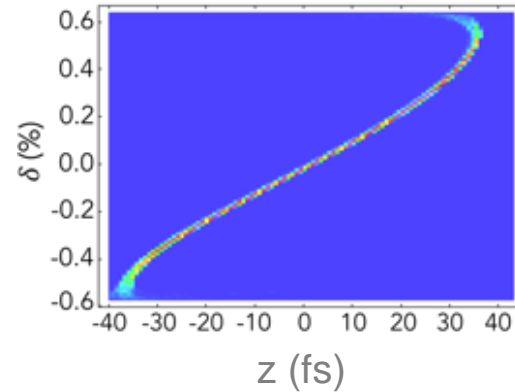
T_{566} second-order longitudinal dispersion



Phase space evolution through a bunch compression



Longitudinal phase space dist. at bunch compression exit



Energy spread induced by Coherent Synchrotron Radiation (CSR):

$$\frac{dE}{cdt} = \frac{-2e^2}{4\pi\epsilon_0(3R^2)^{1/3}} \int_{\tilde{z}-z_L}^{\tilde{z}} \frac{d\lambda}{dz} \left(\frac{1}{\tilde{z}-z} \right)^{1/3} dz$$

$\lambda = \text{linear charge density}$

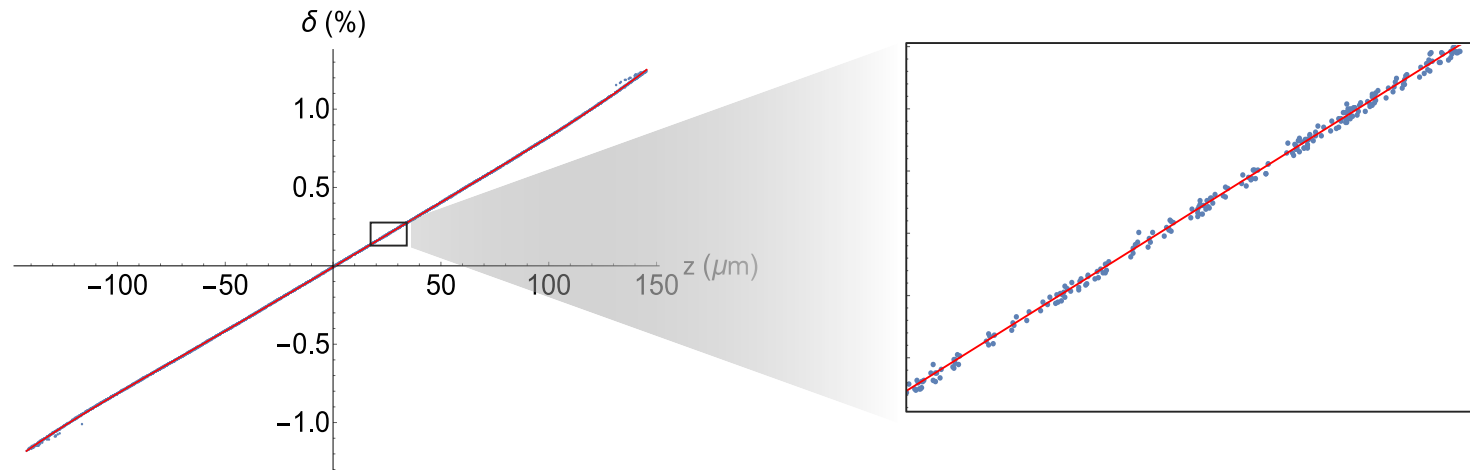
Current spikes are problematic, leading to **CSR-induced emittance growth.**

Caustic expression:

$$\tilde{z}_c(z_i) = z_i + \frac{\delta(z_i)(-1 + T_{566}(-2 + \delta(z_i))\delta'(z_i) + U_{5666}(-3 + \delta(z_i)^2)\delta'(z_i))}{\delta'(z_i)}$$

$$\tilde{R}_{56}(z_i) = \frac{-1 - 2T_{566}\delta'(z_i) - 3U_{5666}\delta'(z_i)}{\delta'(z_i)}$$

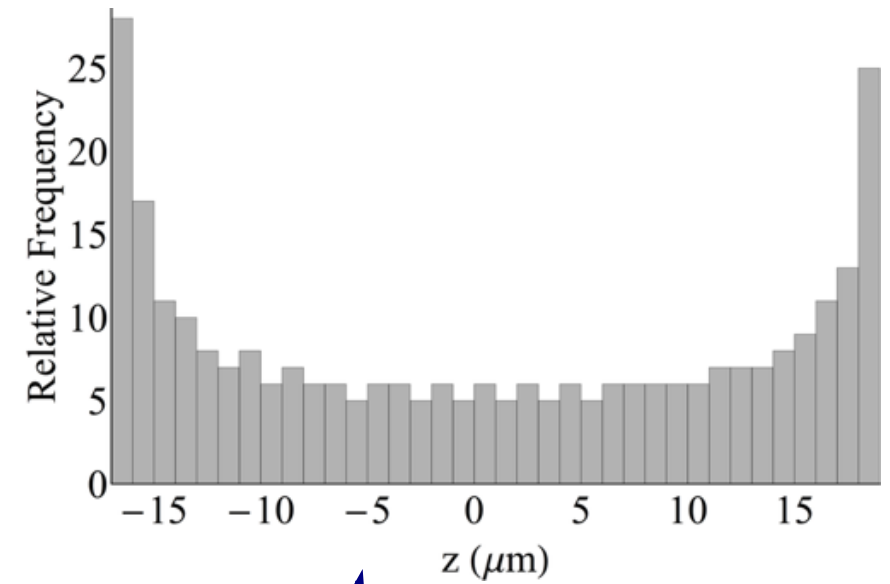
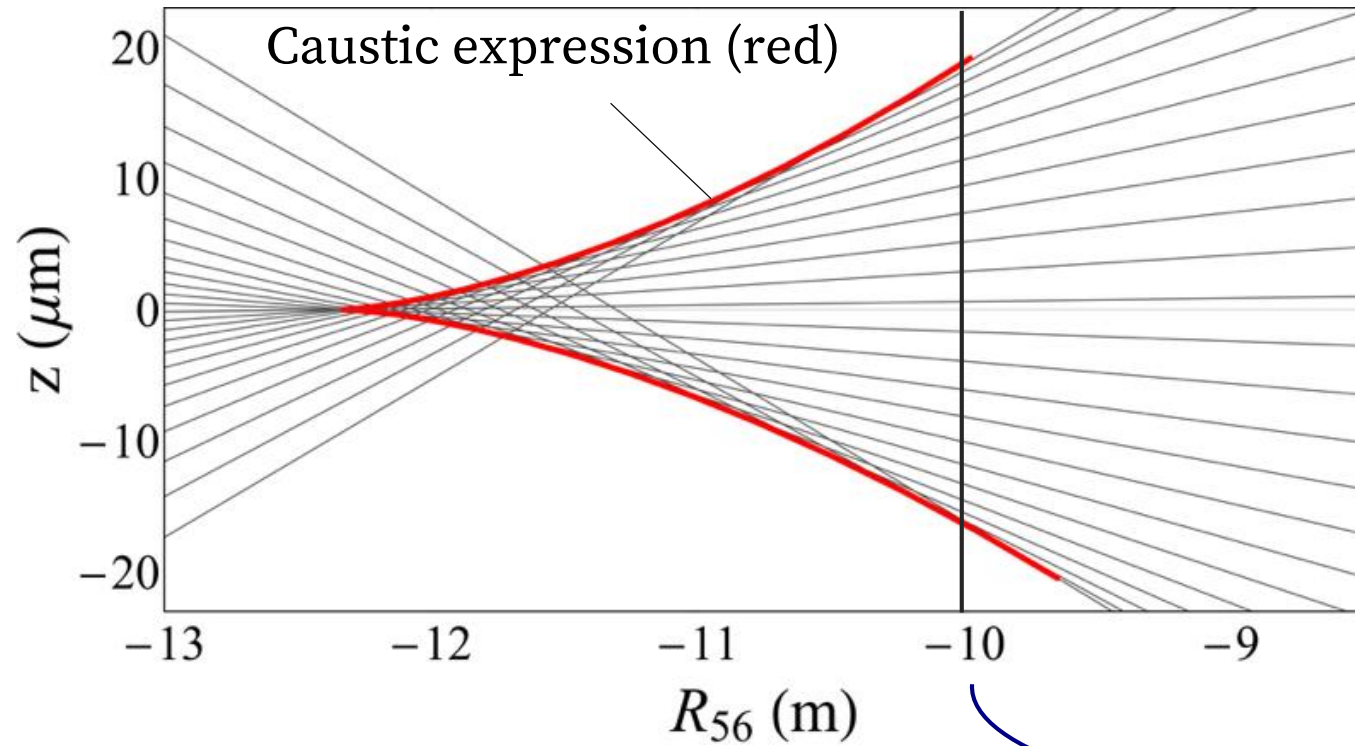
Initial phase space distribution, :



$$\delta(z_i) = h_1 z_i + h_2 z_i^2 + h_3 z_i^3$$

T.K.Charles et al. Phys. Rev. Accel. Beams, (2016) **19**, 104402

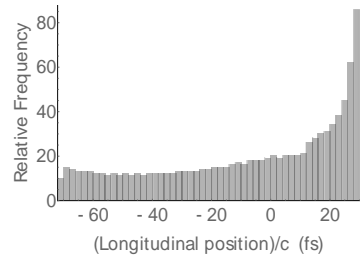
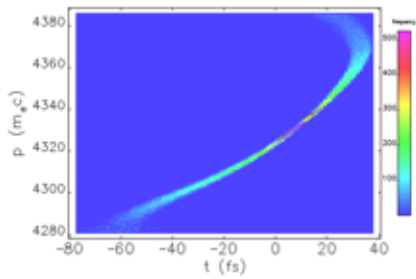
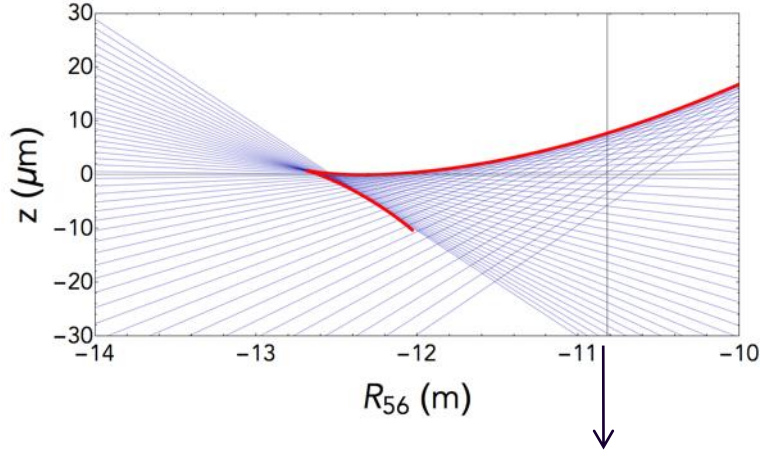
Caustic expression for a chicane



$R_{56} = -10$ mm

Fold

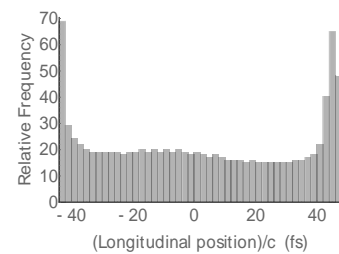
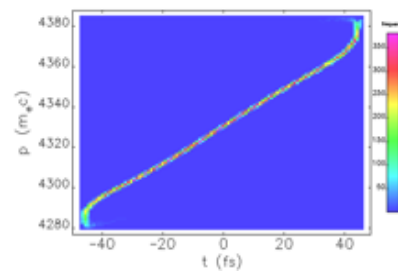
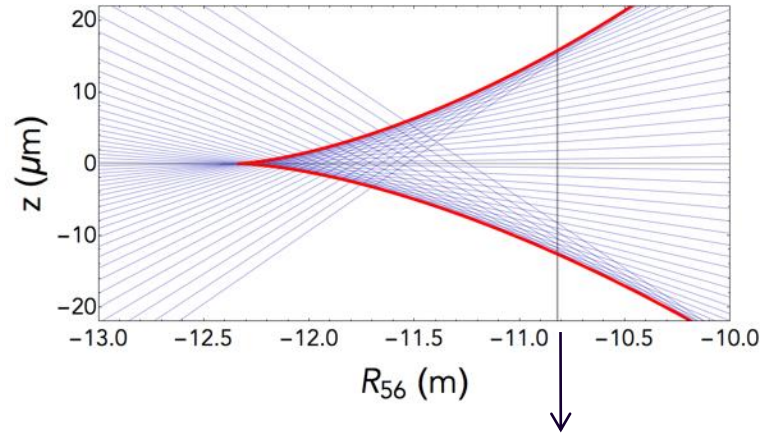
$$T_{566} = 18.1 \text{ mm}, U_{5666} = -24 \text{ mm}$$



E.g. single spike bunch compression [S. Huang *et al.*, Phys. Rev. AB (2014) 17 120703]

Cusp

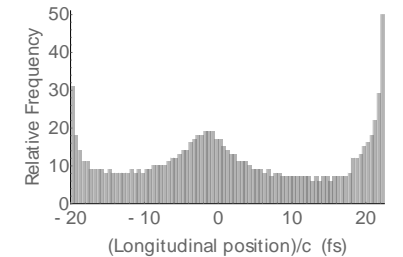
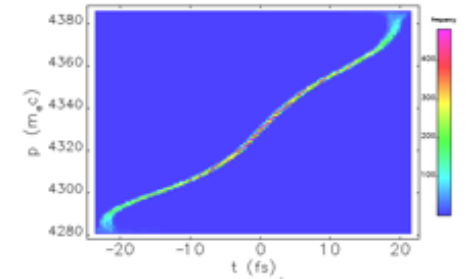
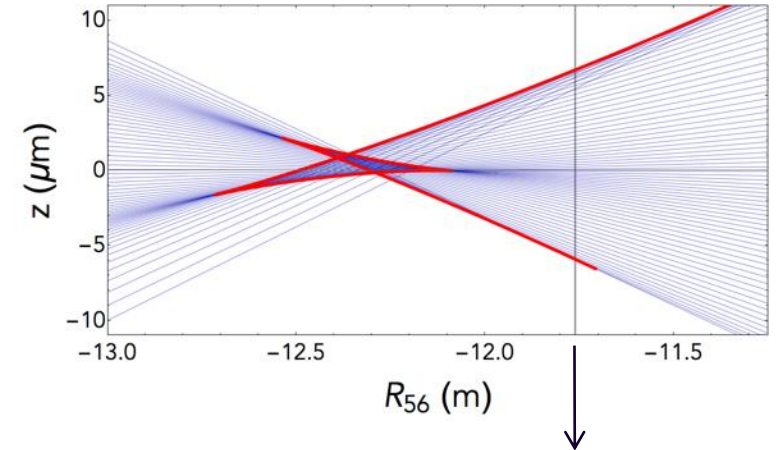
$$T_{566} = 16.4 \text{ mm}, U_{5666} = -11.4 \text{ mm}$$



E.g. LCLS [Y. Ding *et al.* Phys. Rev. AB 19, 100703]

Butterfly

$$T_{566} = 16.1 \text{ mm}, U_{5666} = 2.6 \text{ m}$$



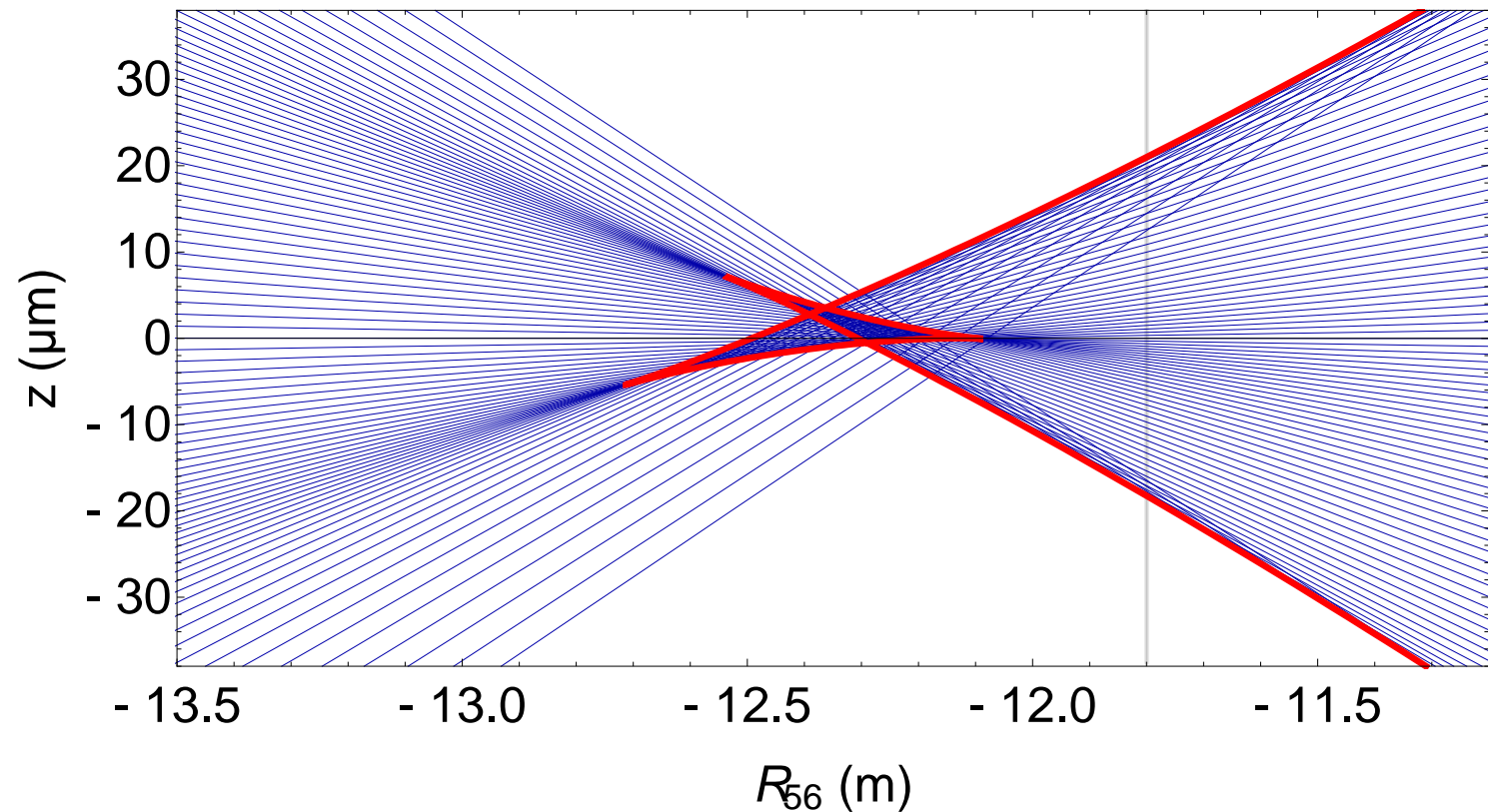
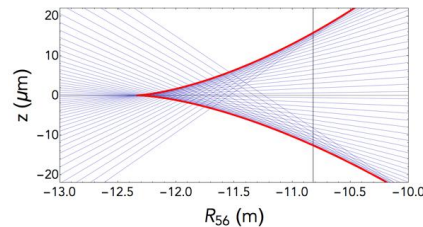
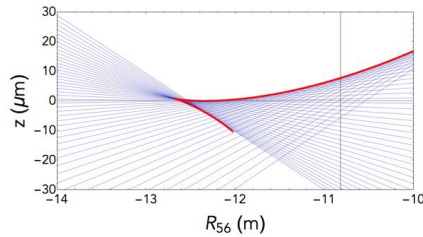
E.g. MAX IV [S. Thorin *et al.* FEL2010, WEPB34]

A closer look...

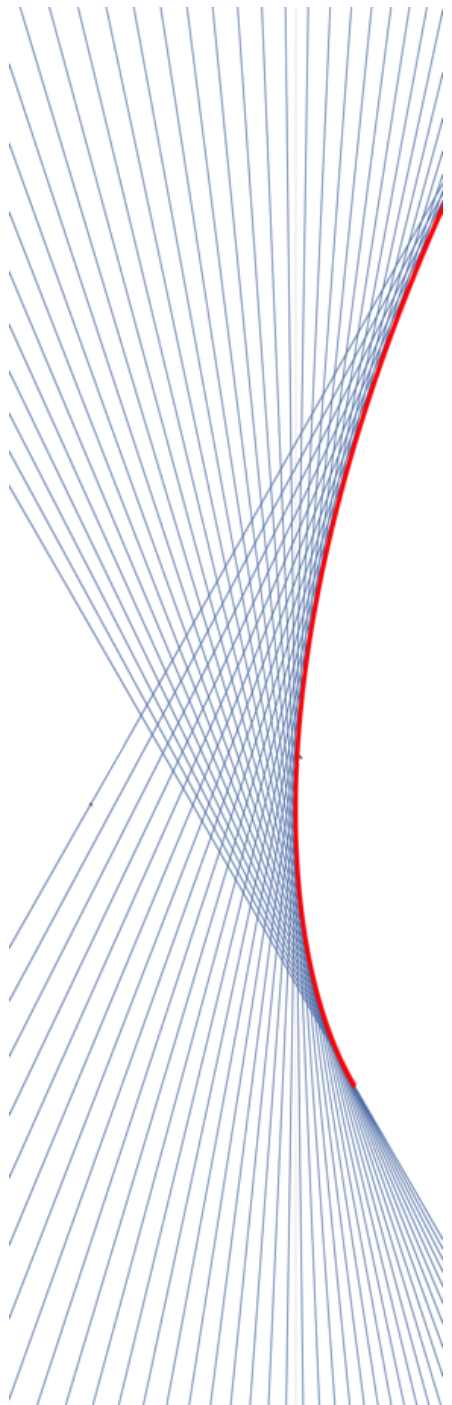
3 types of catastrophes, but all described by the same parametric expression.

$$\tilde{z}(z_i) = z_i + \frac{\delta(z_i)(-1 + T_{566}(-2 + \delta(z_i))\delta'(z_i) + U_{5666}(-3 + \delta(z_i)^2)\delta'(z_i))}{\delta'(z_i)}$$

$$\tilde{R}_{56}(z_i) = \frac{-1 - 2T_{566}\delta'(z_i) - 3U_{5666}\delta'(z_i)}{\delta'(z_i)}$$



“If one must choose between rigour and meaning, I shall unhesitatingly choose the latter.” – René Thom

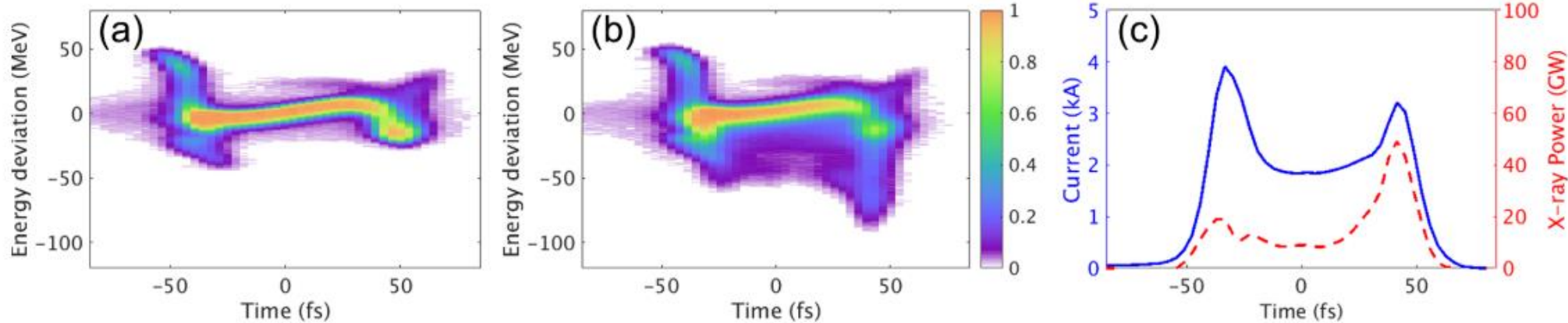


Current horn suppression

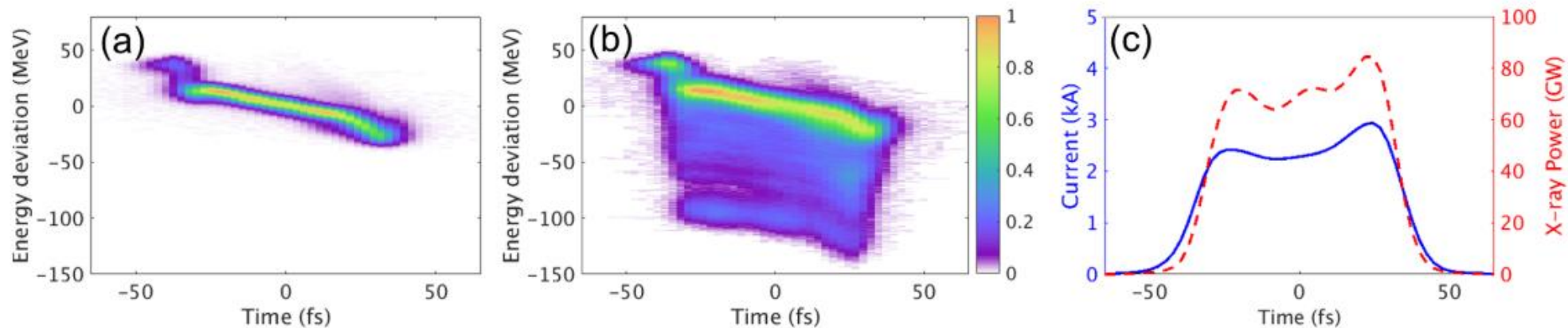
Example of the usefulness of caustics

LSLC's experience - current spikes diminish FEL performance

Before collimation

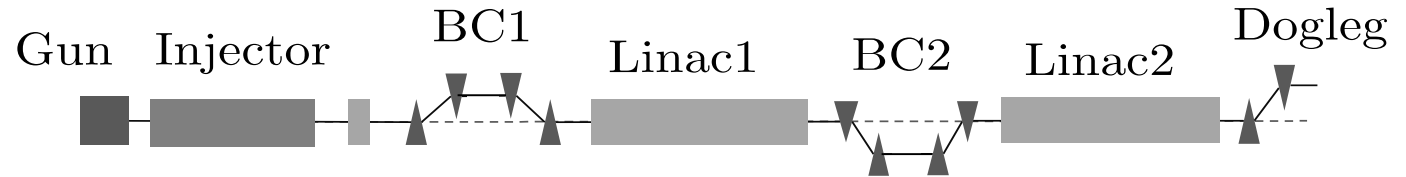
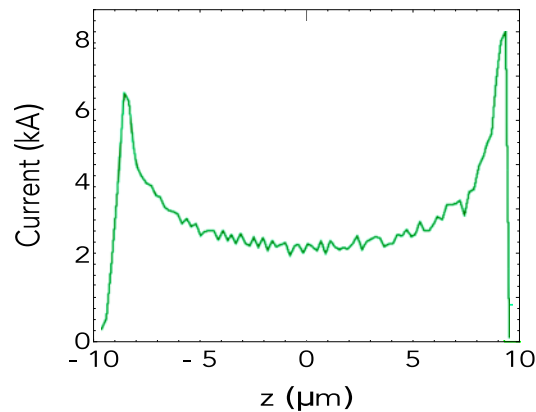
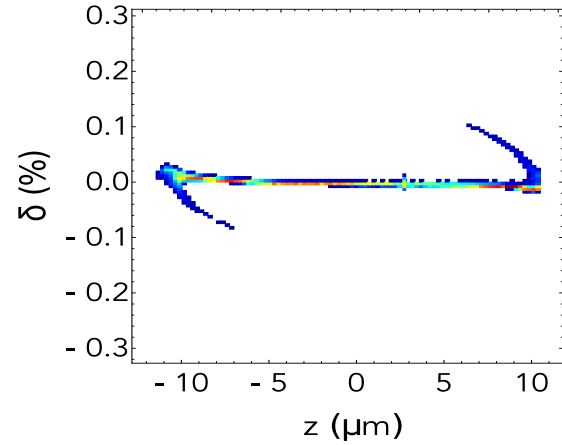


After collimation



FEL power increased from ~3.5 mJ to 4-5 mJ.

Current horn suppression - an S-band FEL Linac example



Elegant simulations of longitudinal phase space and current profile at the end of Linac2.

Caustic condition

$$R_{56} s \frac{d(\delta(z))}{dz} \Big|_{z=z_i} + T_{566} s \frac{d}{dz} (\delta^2(z)) \Big|_{z=z_i} + U_{5666} s \frac{d}{dz} (\delta^3(z)) \Big|_{z=z_i} + s_{BC} = 0.$$

where,

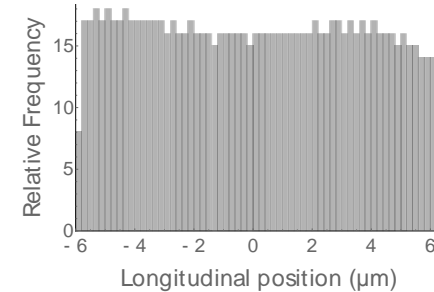
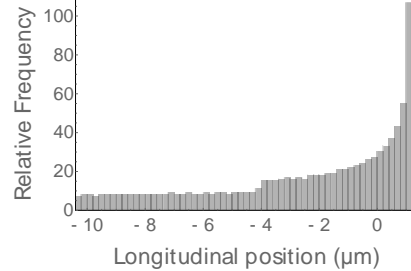
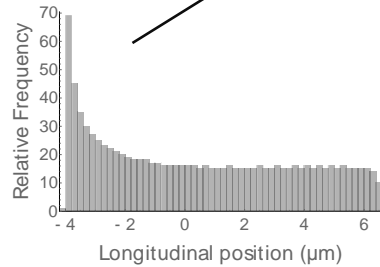
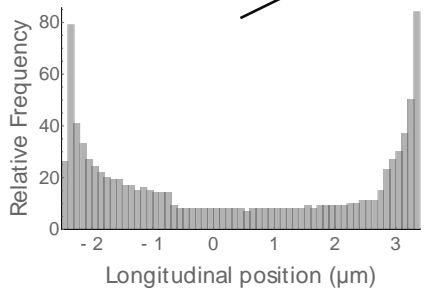
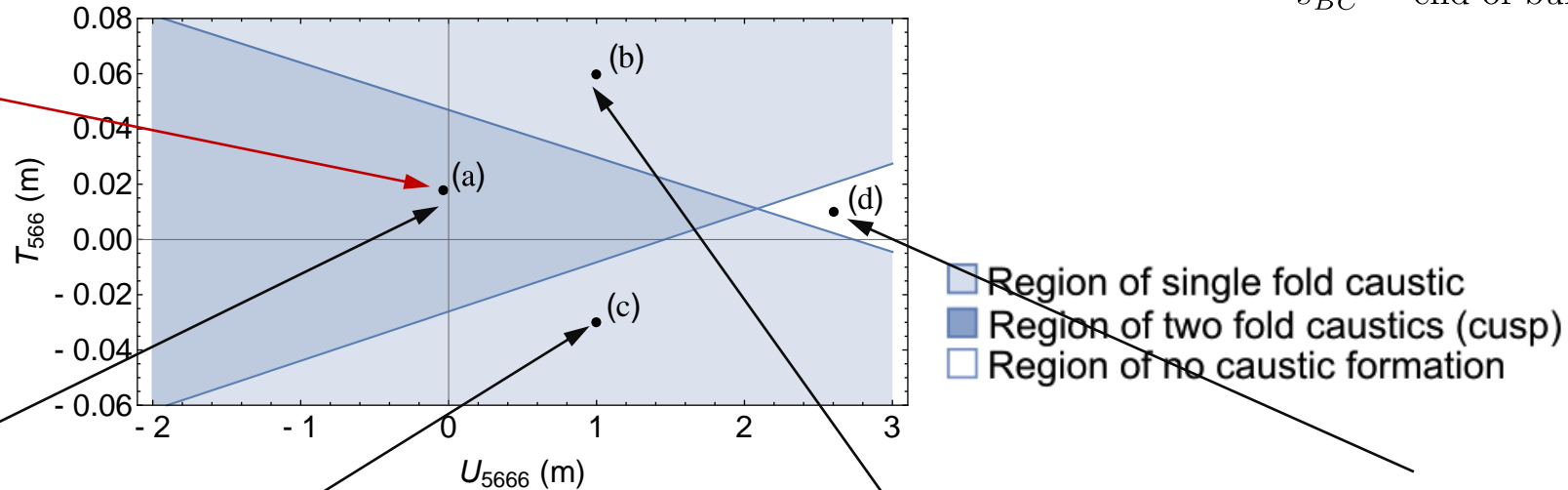
δ = energy spread

z_i = initial longitudinal position

s = position along accelerator

s_{BC} = end of bunch compressor position

Point (a) is the working point of the S-band linac example



Caustic condition

$$R_{56} s \frac{d(\delta(z))}{dz} \Big|_{z=z_i} + T_{566} s \frac{d}{dz} (\delta^2(z)) \Big|_{z=z_i} + U_{5666} s \frac{d}{dz} (\delta^3(z)) \Big|_{z=z_i} + s_{BC} = 0.$$

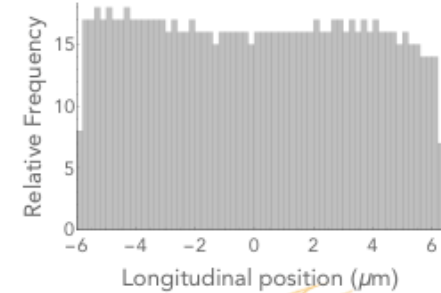
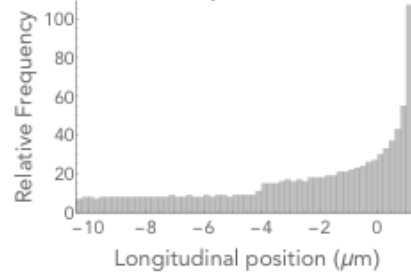
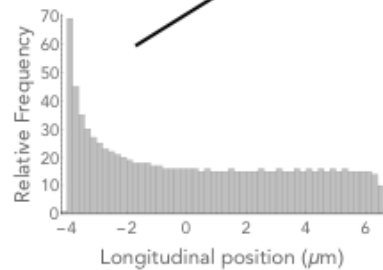
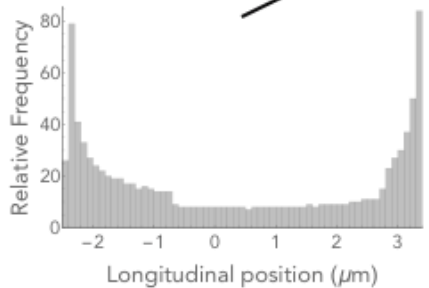
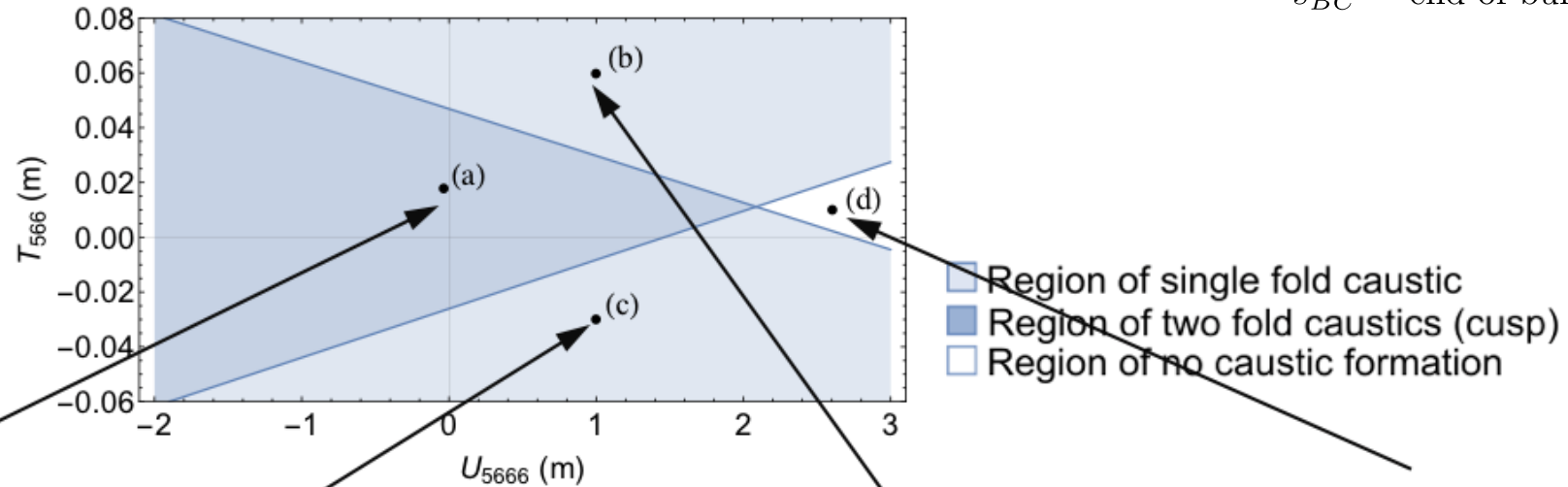
where,

δ = energy spread

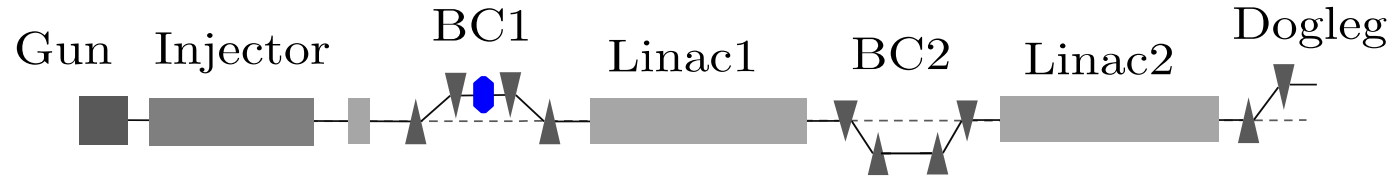
z_i = initial longitudinal position

s = position along accelerator

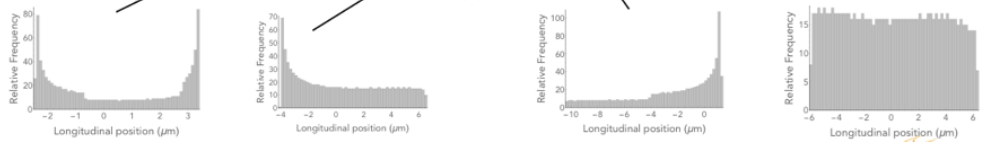
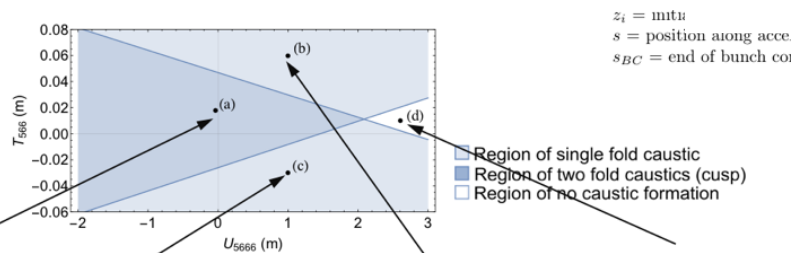
s_{BC} = end of bunch compressor position



Caustic current horn suppression - S-band FEL linac



Octupole added to BC1 to vary U_{5666} .



Caustic condition

$$R_{56} s \frac{d(\delta(z))}{dz} \Big|_{z=z_i} + T_{566} s \frac{d}{dz} (\delta^2(z)) \Big|_{z=z_i} + U_{5666} s \frac{d}{dz} (\delta^3(z)) \Big|_{z=z_i} + s_{BC} = 0.$$

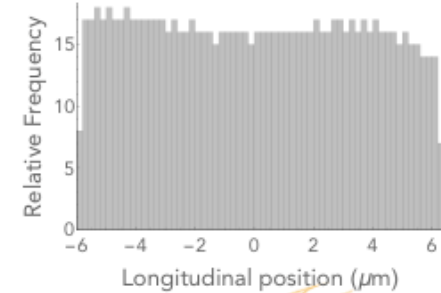
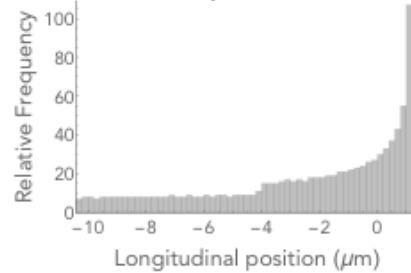
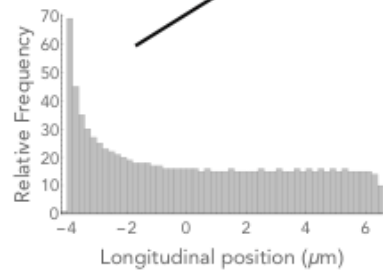
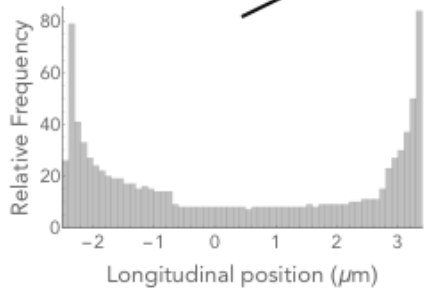
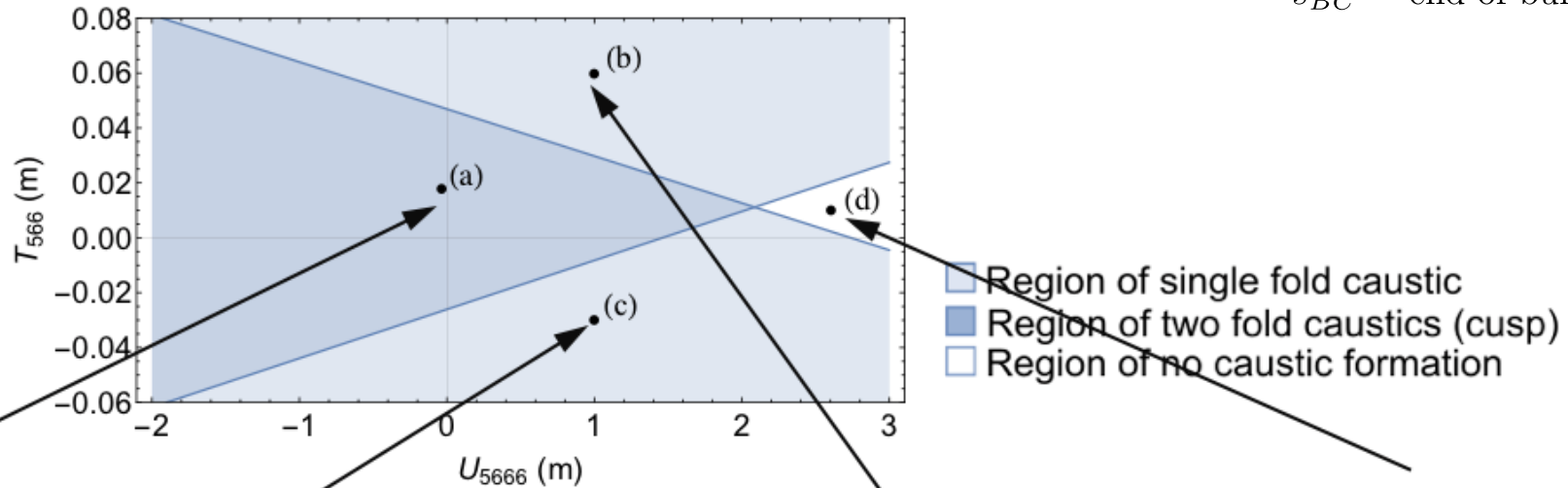
where,

δ = energy spread

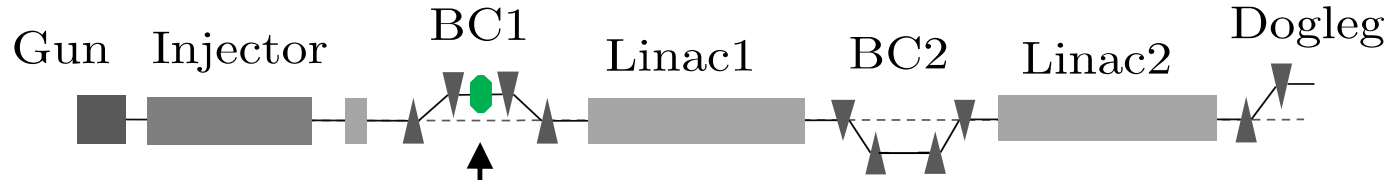
z_i = initial longitudinal position

s = position along accelerator

s_{BC} = end of bunch compressor position

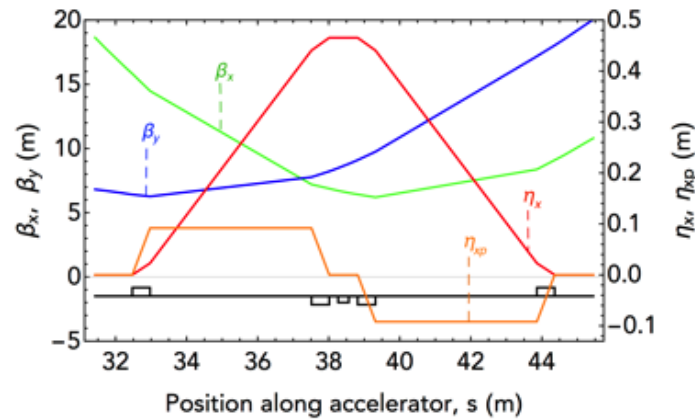


Caustic current horn suppression - S-band FEL linac

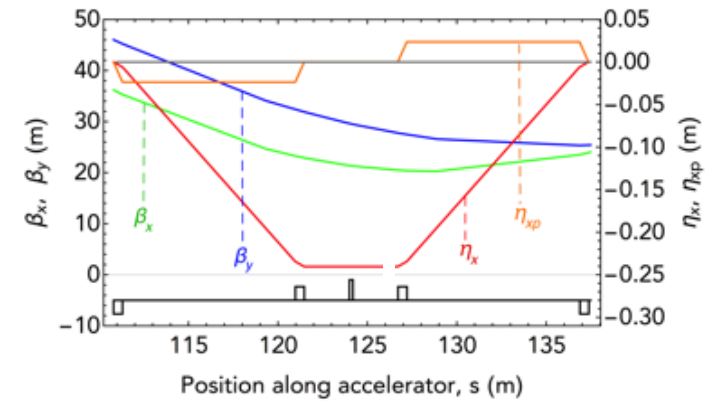


Octupole added to BC1 to vary U5666.

Bunch Compressor 1



Bunch Compressor 2



BC1:

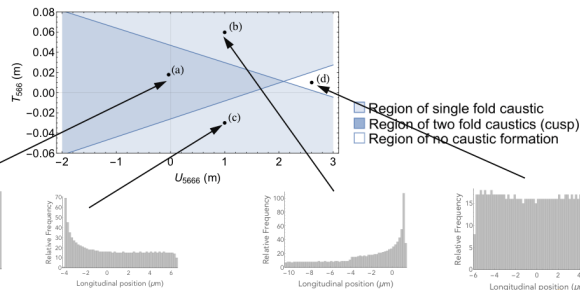
R56 = -82.36 mm
 T566 = 102.40 mm
 U5666 = -5.23 m

Dipole bending angle, $\theta = 5.25^\circ$
 Octupole strength, $K3 = 2061 \text{ m}^{-4}$

BC2:

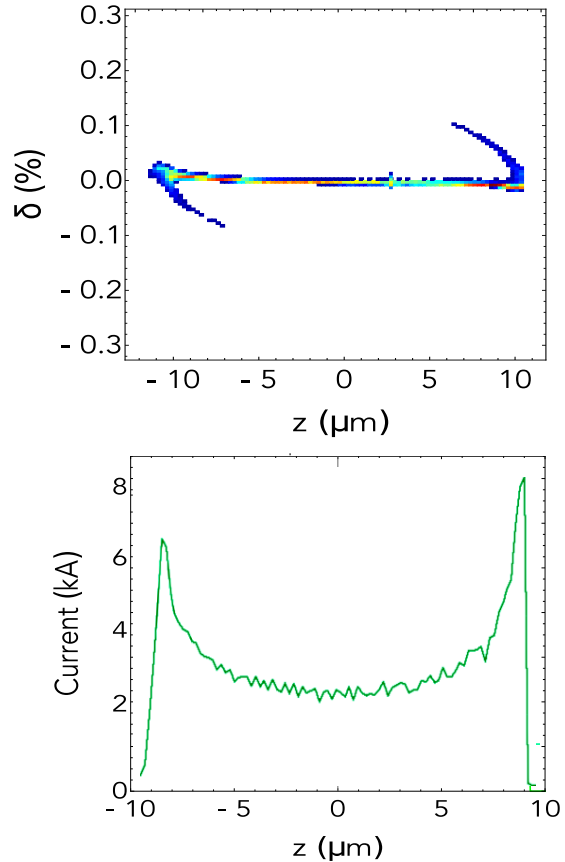
R56 = -11.18 mm
 T566 = 32.10 mm
 U5666 = -72.19 mm

Dipole bending angle, $\theta = 1.35^\circ$
 Sextupole 1 strength, $K2 = 11.03 \text{ m}^{-3}$



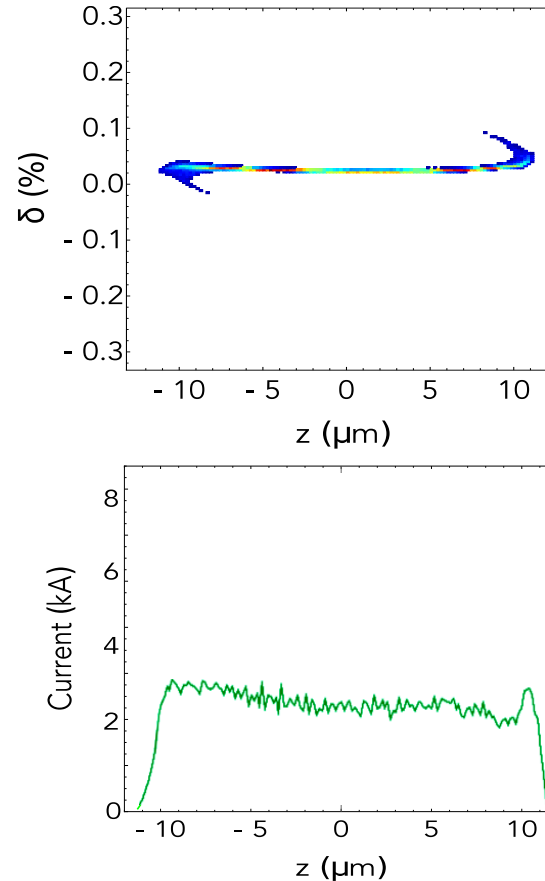
Caustic current horn suppression

Without octupole:



$$\epsilon_{nx} = 1.359 \text{ mm mrad}$$

With octupole:



$$\epsilon_{nx} = 0.762 \text{ mm mrad}$$

63% reduction in
the CSR-induced
emittance growth.

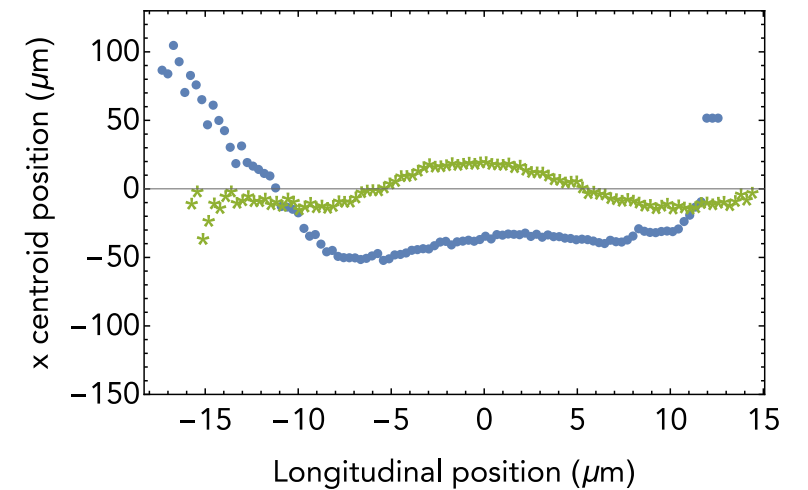
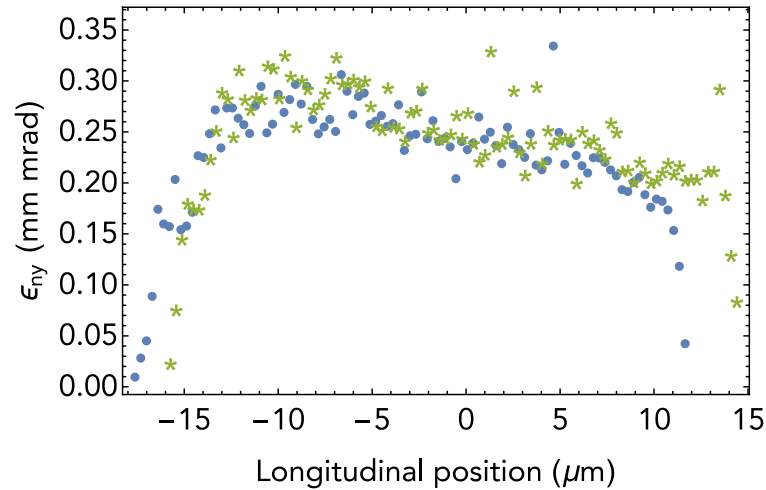
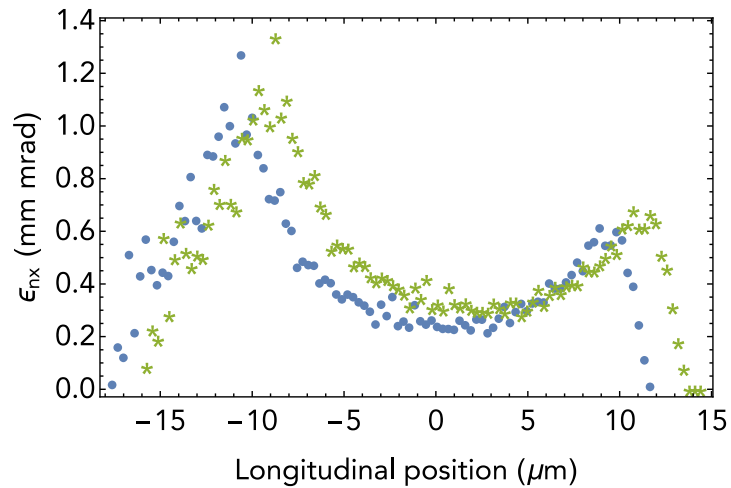
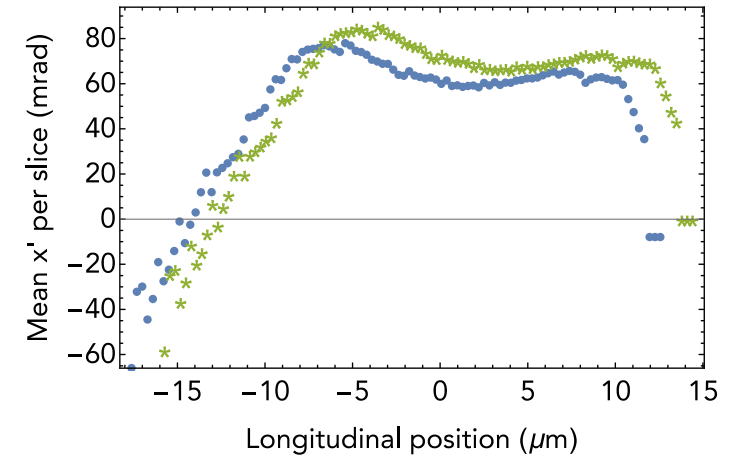
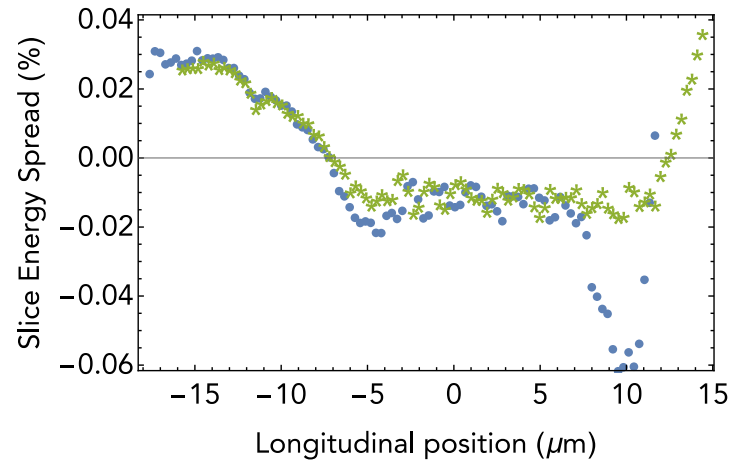
T.K.Charles et al. Phys. Rev.
Accel. Beams, (2017) **20**, 030705

Final bunch slice properties



Without octupole: *

With octupole: •

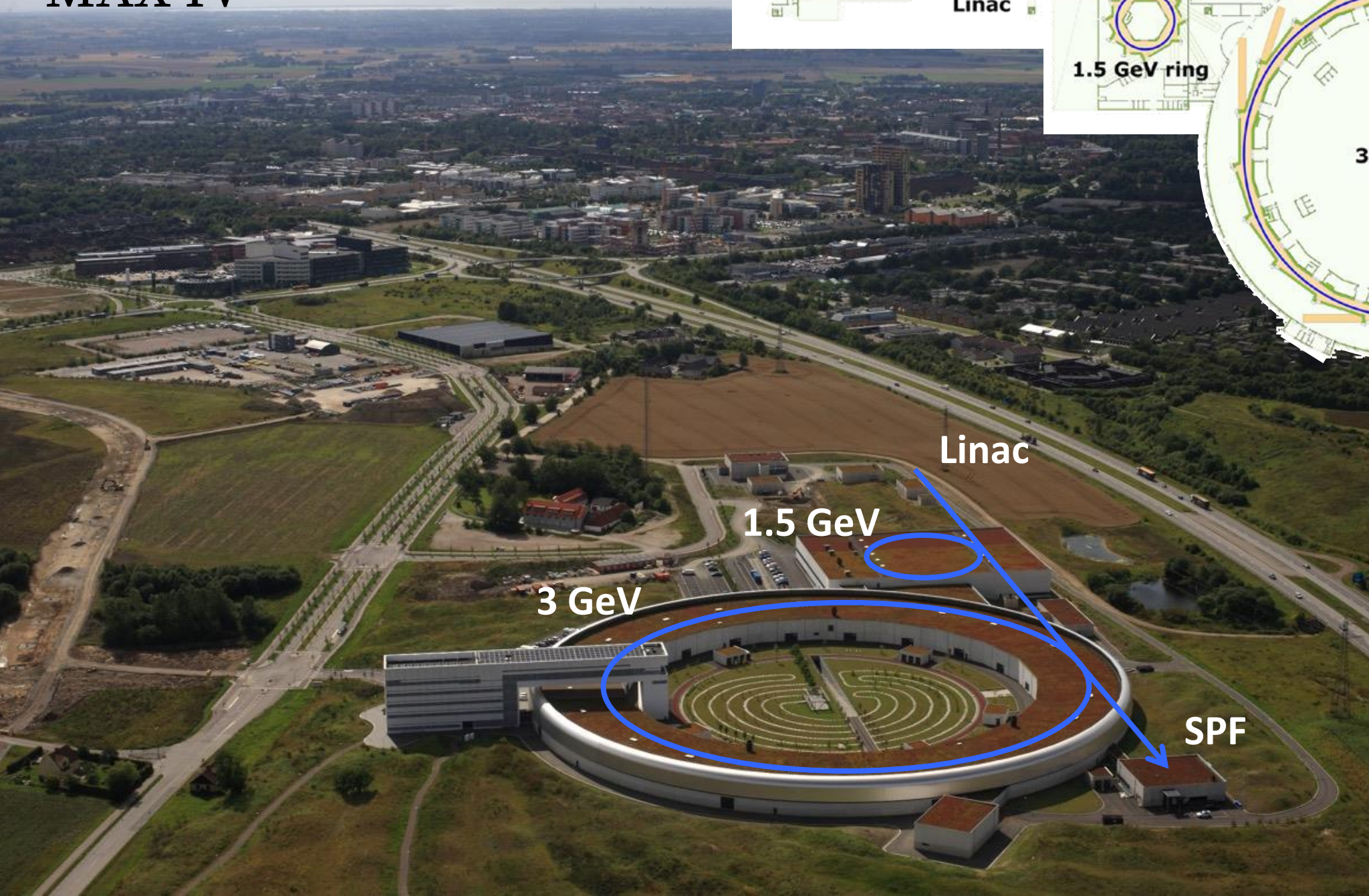
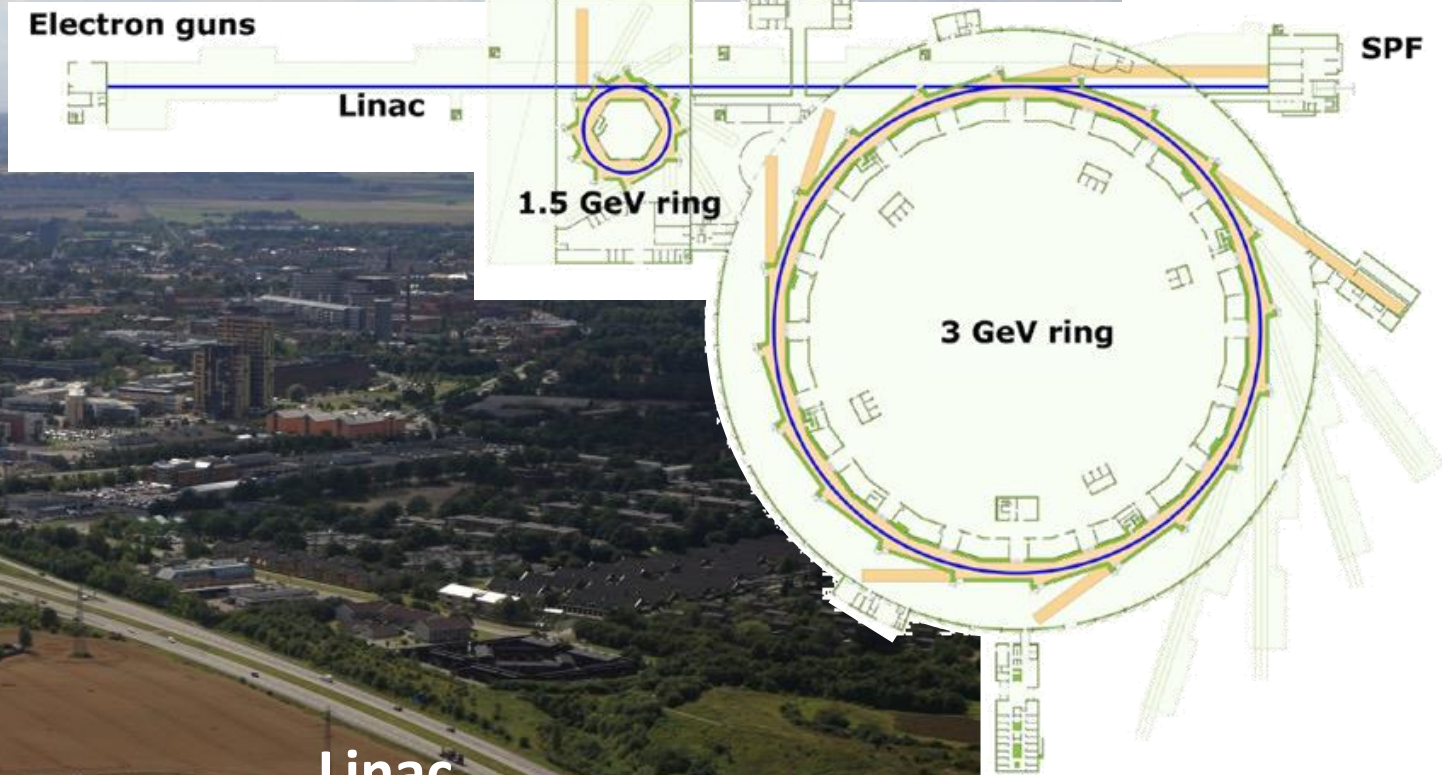




Experimental results from MAX IV

with Andrea Latina (CERN), Sara Thorin (MAX IV), Jonas Björklund Svensson (MAX IV)

MAX IV



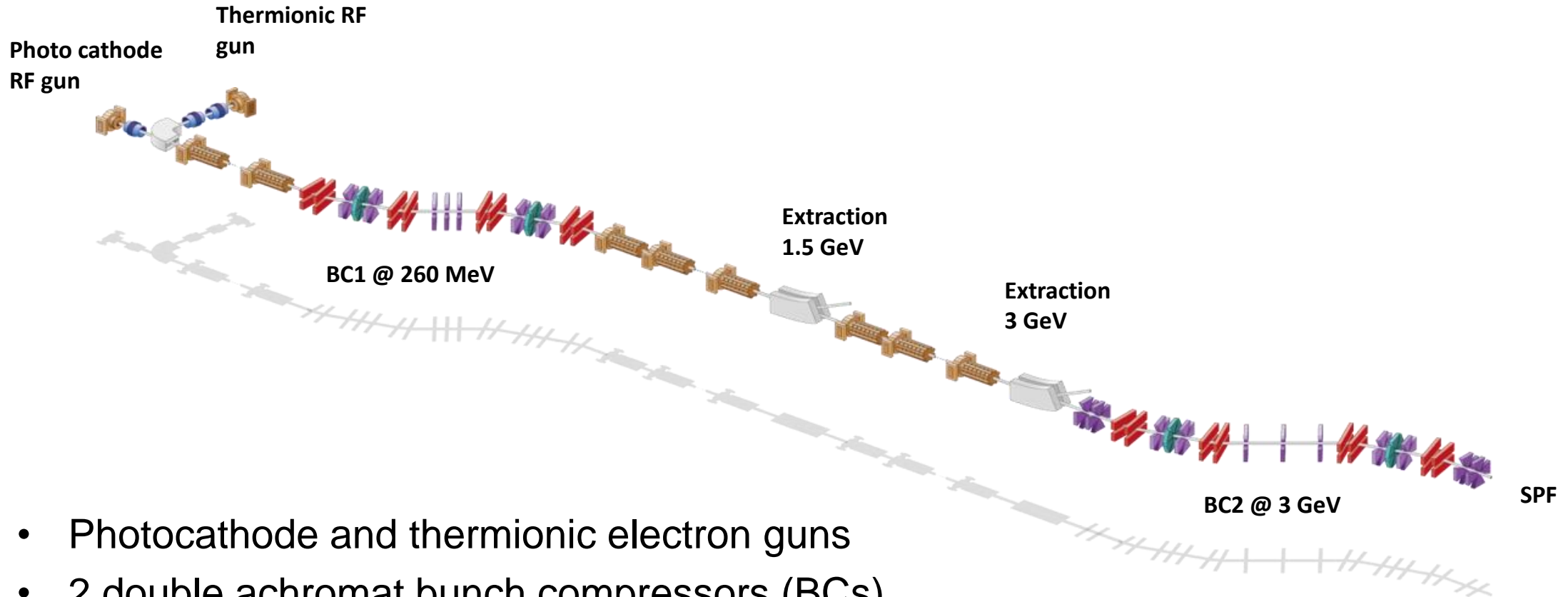
Linac

1.5 GeV

3 GeV

SPF

MAX IV Linac

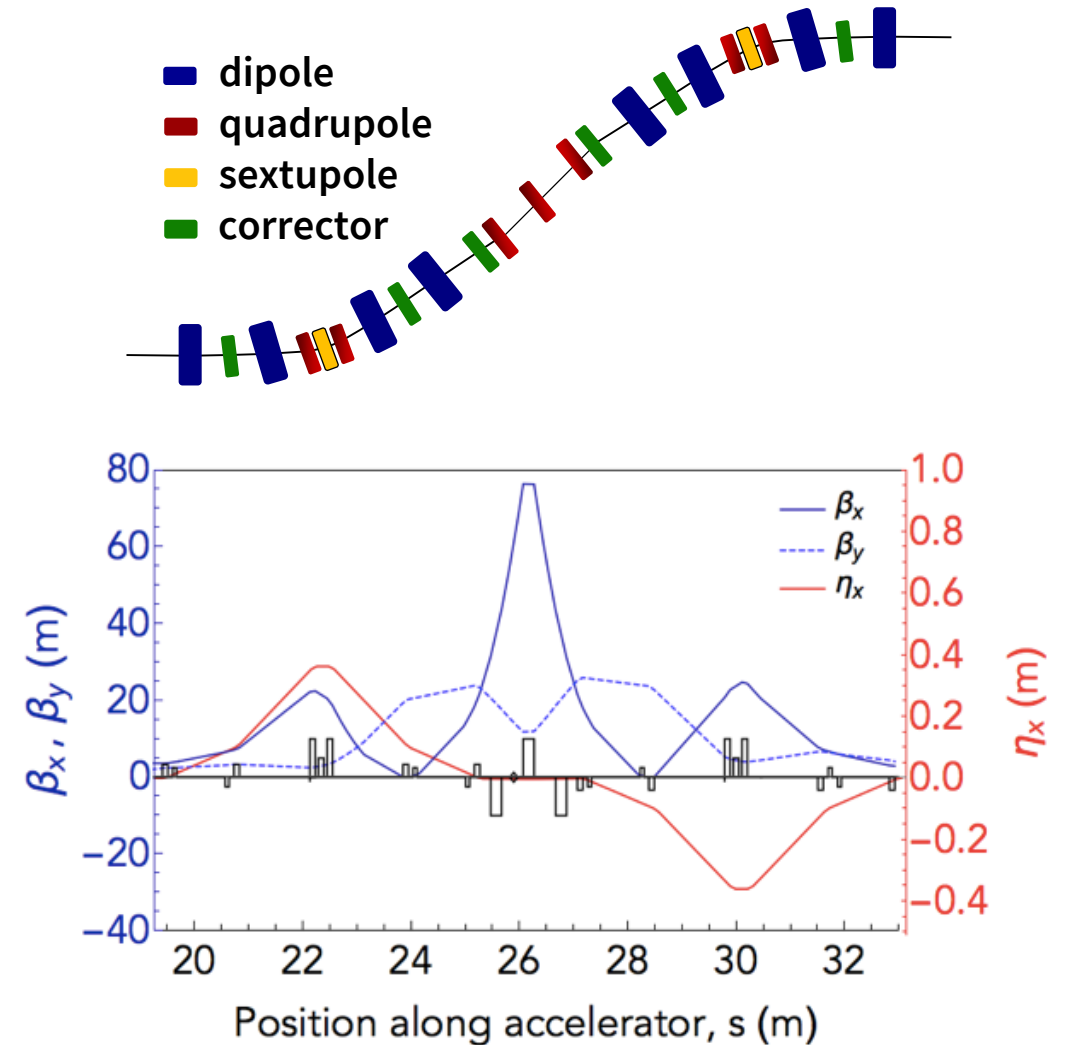


- Photocathode and thermionic electron guns
- 2 double achromat bunch compressors (BCs)
- RF frequency 2.998 GHz

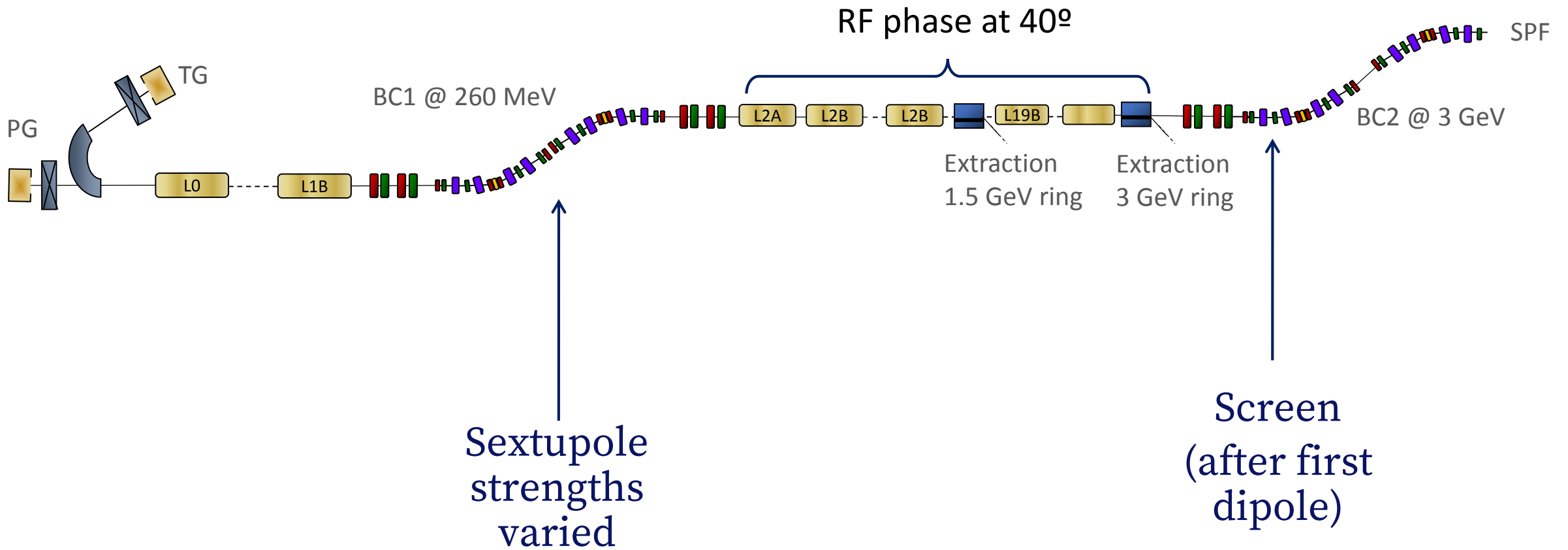
MAX IV Bunch Compressors

Double achromat bunch compressors:

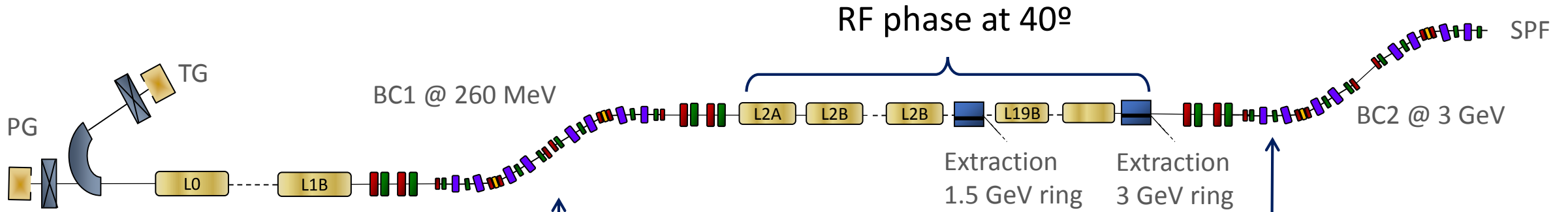
- positive fixed R56 (energy chirp from falling falling RF slope)
- natural T566 used for linearization, **self-linearizing**
- weak sextupoles at the center of each achromat used for fine tuning T566



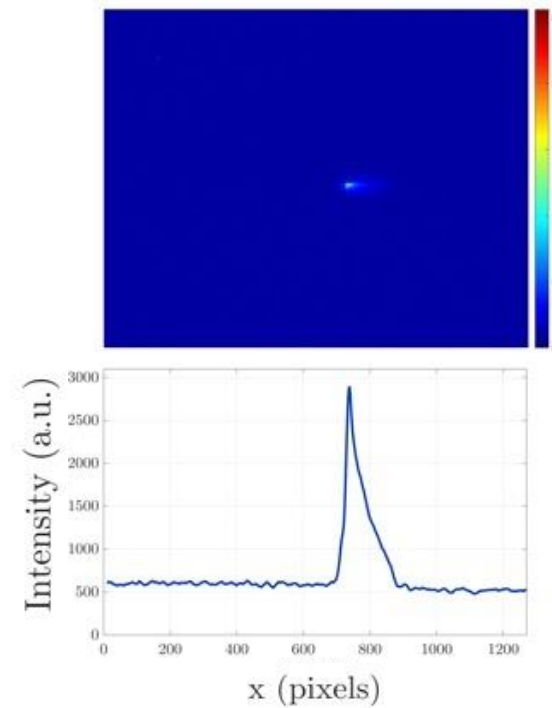
Zero-crossing method



Zero-crossing method



Sextupole strengths varied



Experimental results – linearly ramped current profiles

Sextupole strengths [m^{-3}]:

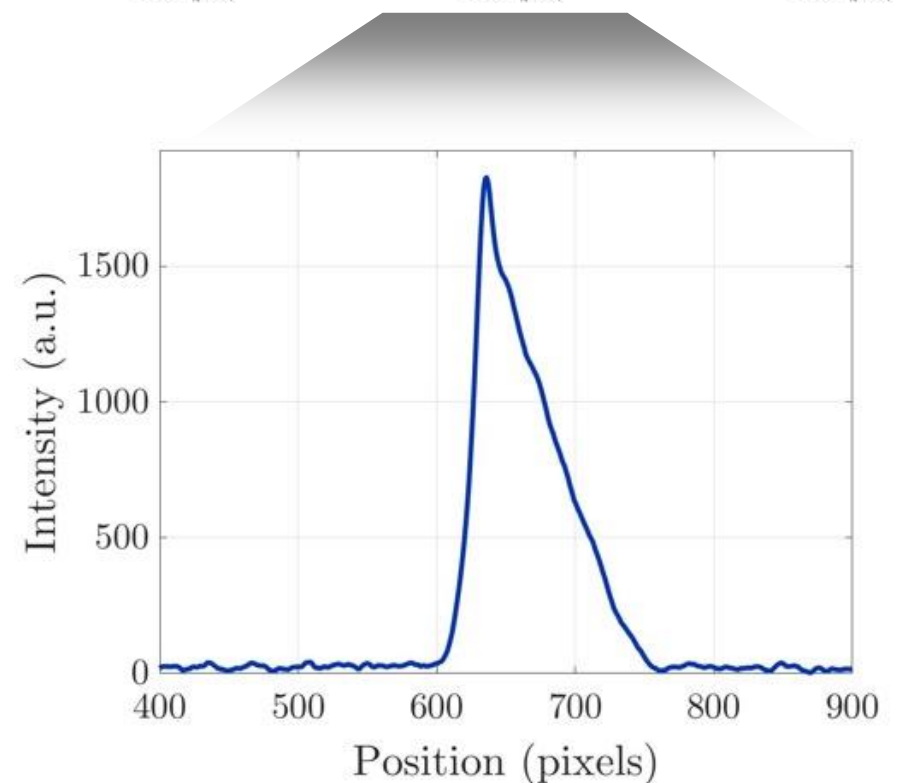
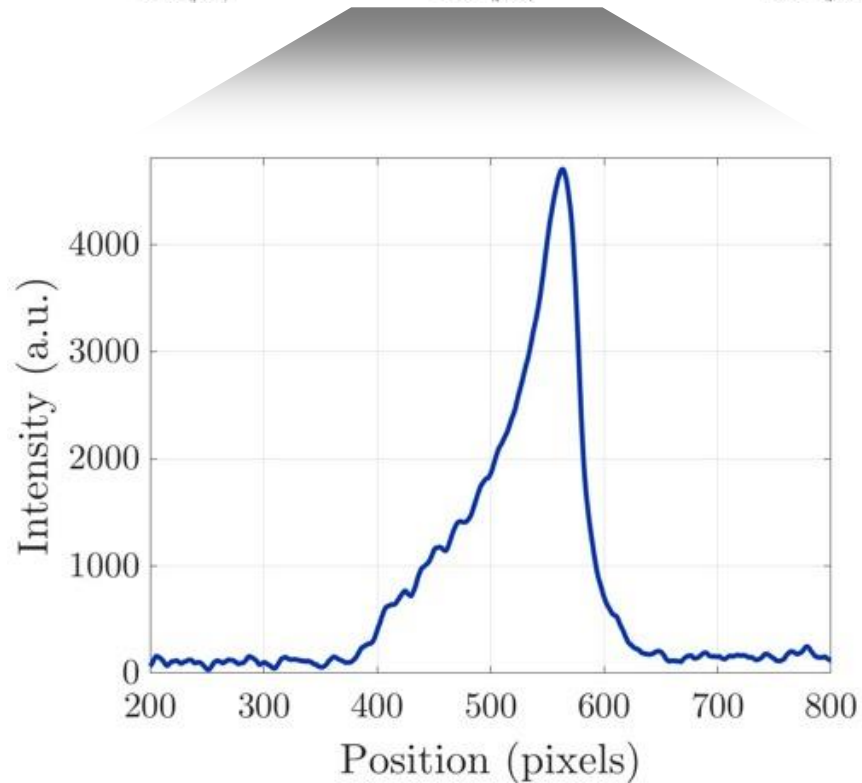
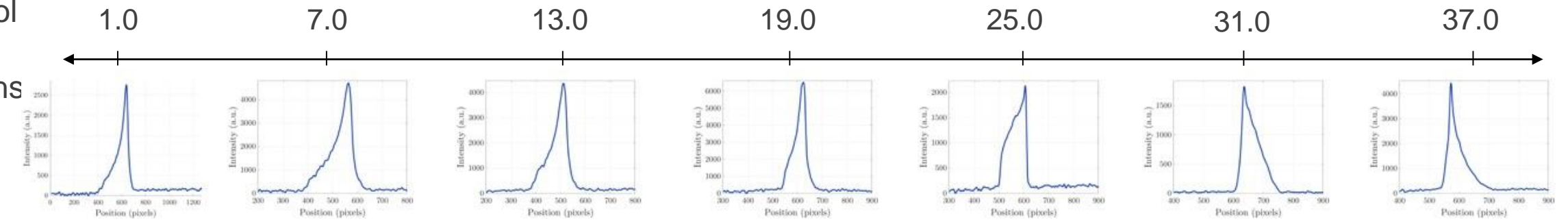
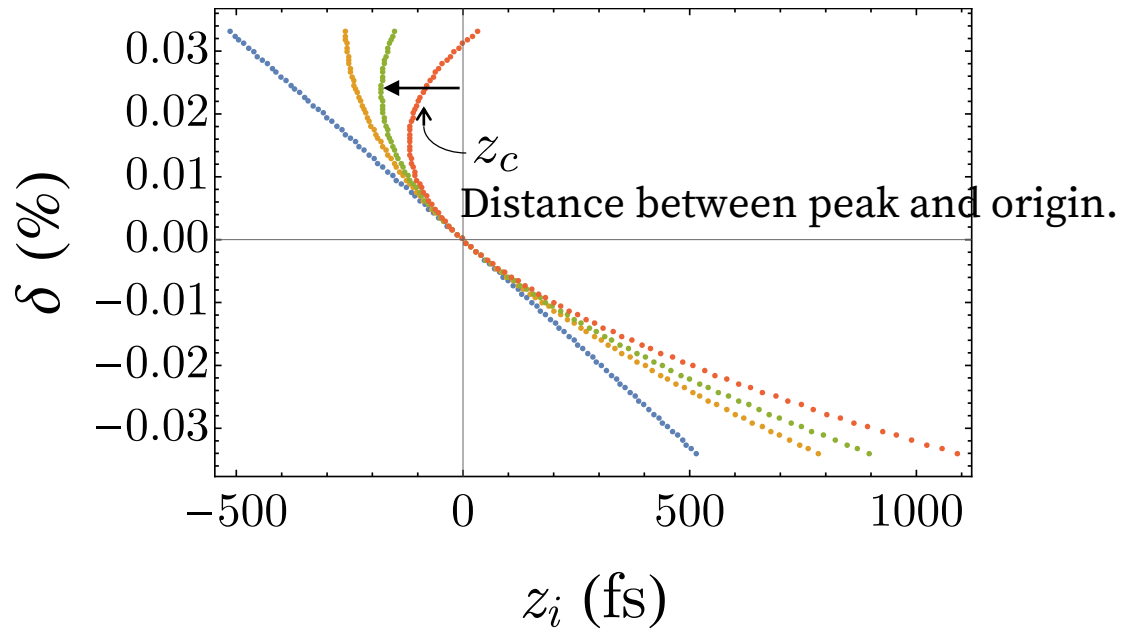


Illustration of compressed bunches LPS



The origin is found as being the distance from one bunch edge to the position within the bunch where the accumulated integrated charge equals half of the total charge.

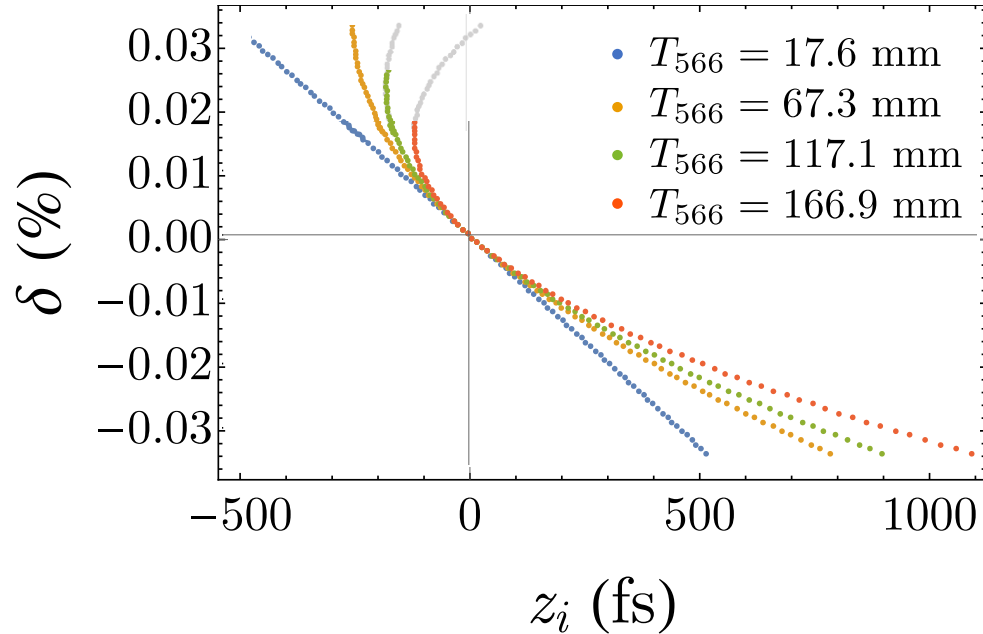
Caustic expression:

$$z_c(z_i) = -z_i - \frac{R_{56}\delta(z_i)}{2} + \frac{U_{5666}}{2} \frac{\delta^3(z_i)}{\delta'(z_i)} + \frac{\delta(z_i)}{2\delta'(z_i)}$$

$$\tilde{T}_{566}(z_i) = \frac{1}{2\delta(z_i)} \left(-R_{56} - \frac{1}{\delta'(z_i)} - 3U_{5666} \delta^2(z_i) \right)$$

(Same expression as shown on slide 15, simply re-arranged)

Illustration of compressed bunches LPS



The light grey portion of the distribution will be mapped to a smaller x value, lengthening out the bunch on the screen.

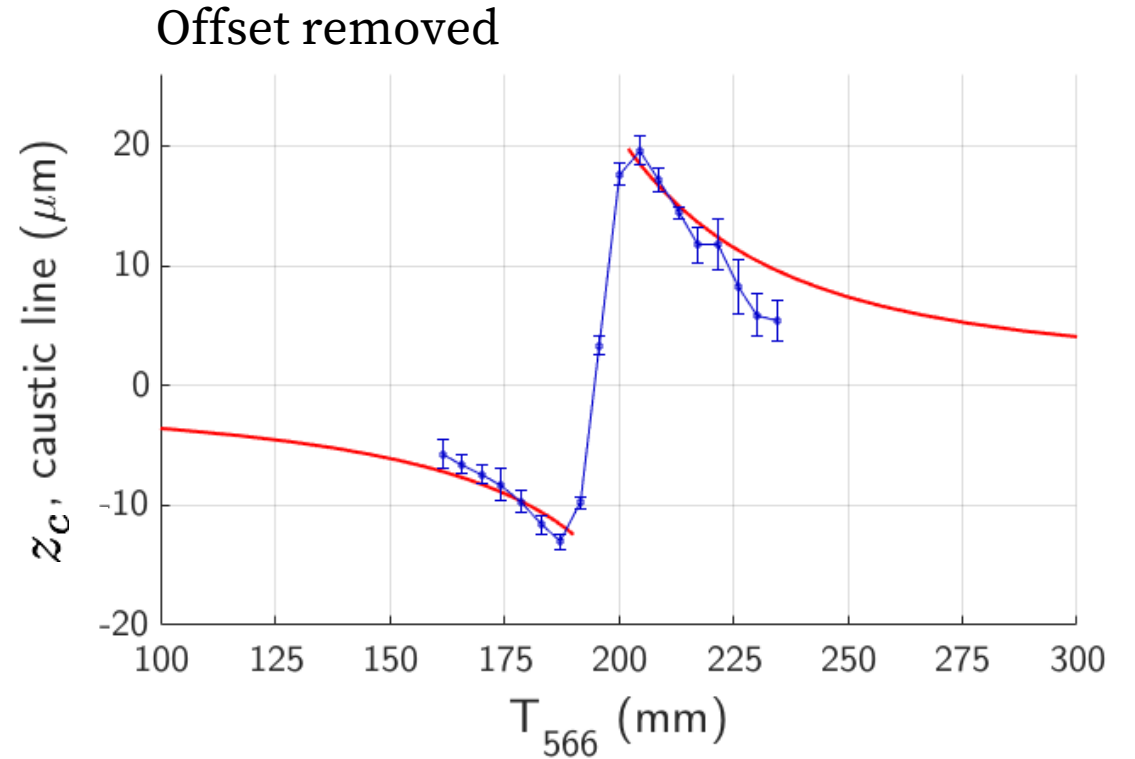
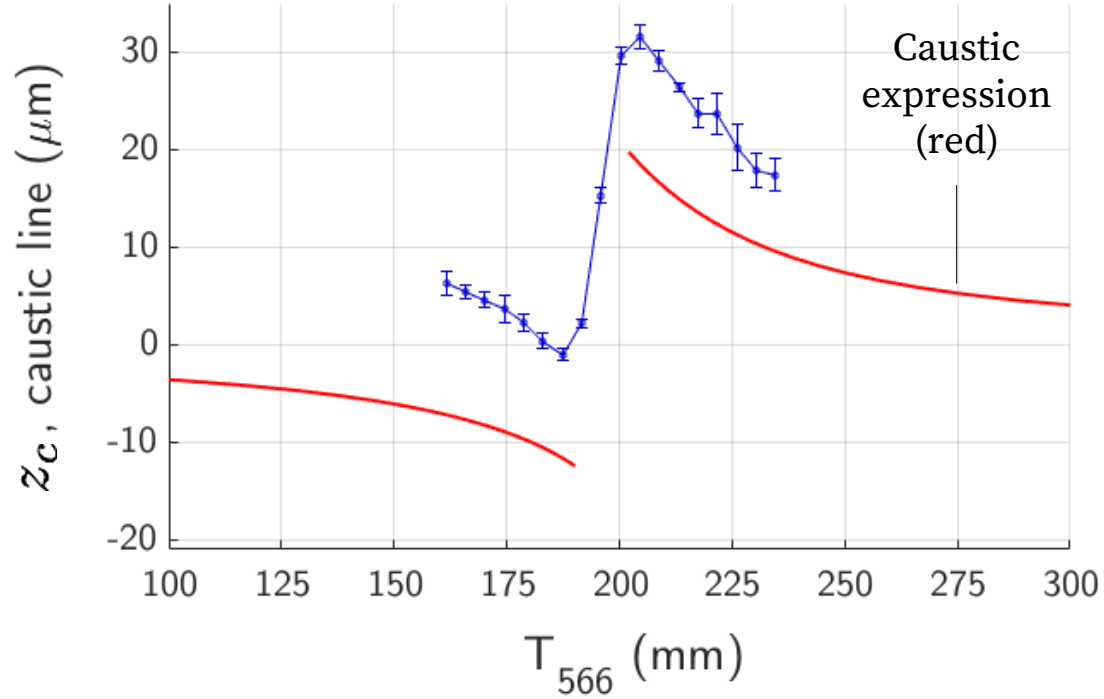
Caustic expression:

$$z_c(z_i) = -z_i - \frac{R_{56}\delta(z_i)}{2} + \frac{U_{5666}}{2} \frac{\delta^3(z_i)}{\delta'(z_i)} + \frac{\delta(z_i)}{2\delta'(z_i)}$$

$$\tilde{T}_{566}(z_i) = \frac{1}{2\delta(z_i)} \left(-R_{56} - \frac{1}{\delta'(z_i)} - 3U_{5666} \delta^2(z_i) \right)$$

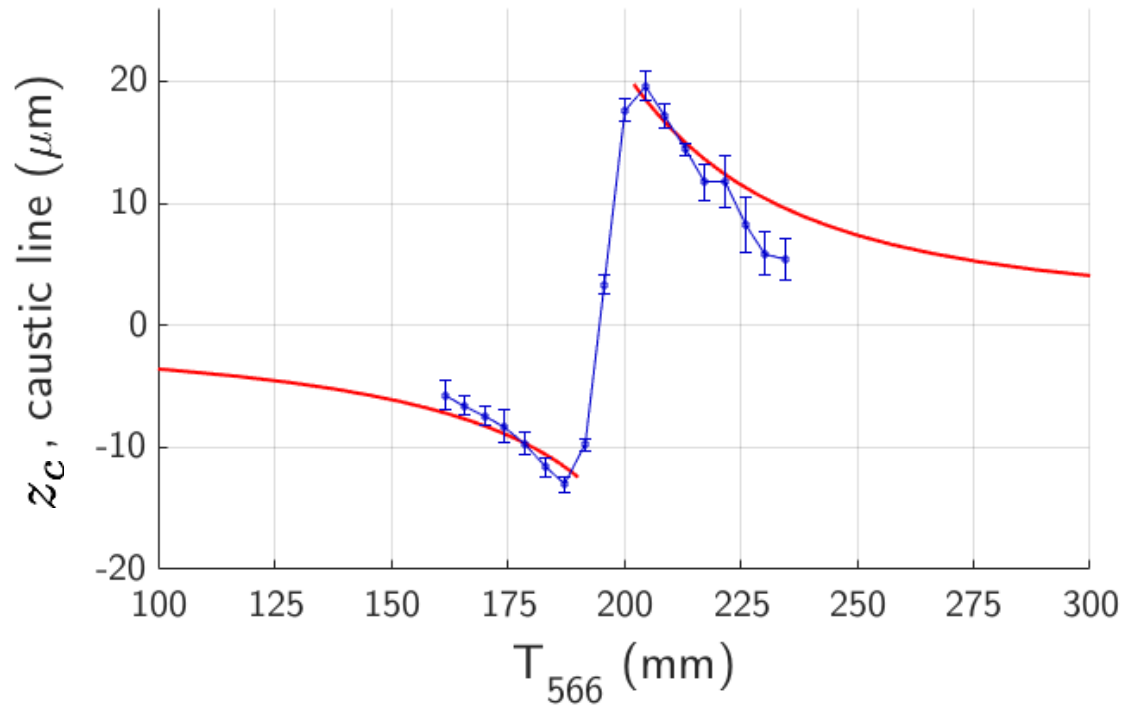
(Same expression as shown on slide 15, simply re-arranged)

Mapping out caustic lines



Offset due to the combined effects of wakefields and curvature of the phase space distribution.

Mapping out caustic lines



Offset of 14 micrometers removed

Where the caustic expression is undefined, the longitudinal phase space is considered well linearized, resulting in a short bunch with a symmetrical current profile.

$$z_c(z_i) = -z_i - \frac{R_{56}\delta(z_i)}{2} + \frac{U_{5666}}{2} \frac{\delta^3(z_i)}{2} + \frac{\delta(z_i)}{2\delta'(z_i)}$$

$$\tilde{T}_{566}(z_i) = \frac{1}{2\delta(z_i)} \left(-R_{56} - \frac{1}{\delta'(z_i)} - 3U_{5666} \delta^2(z_i) \right)$$



Longitudinal Phase Space manipulation in recirculating machines

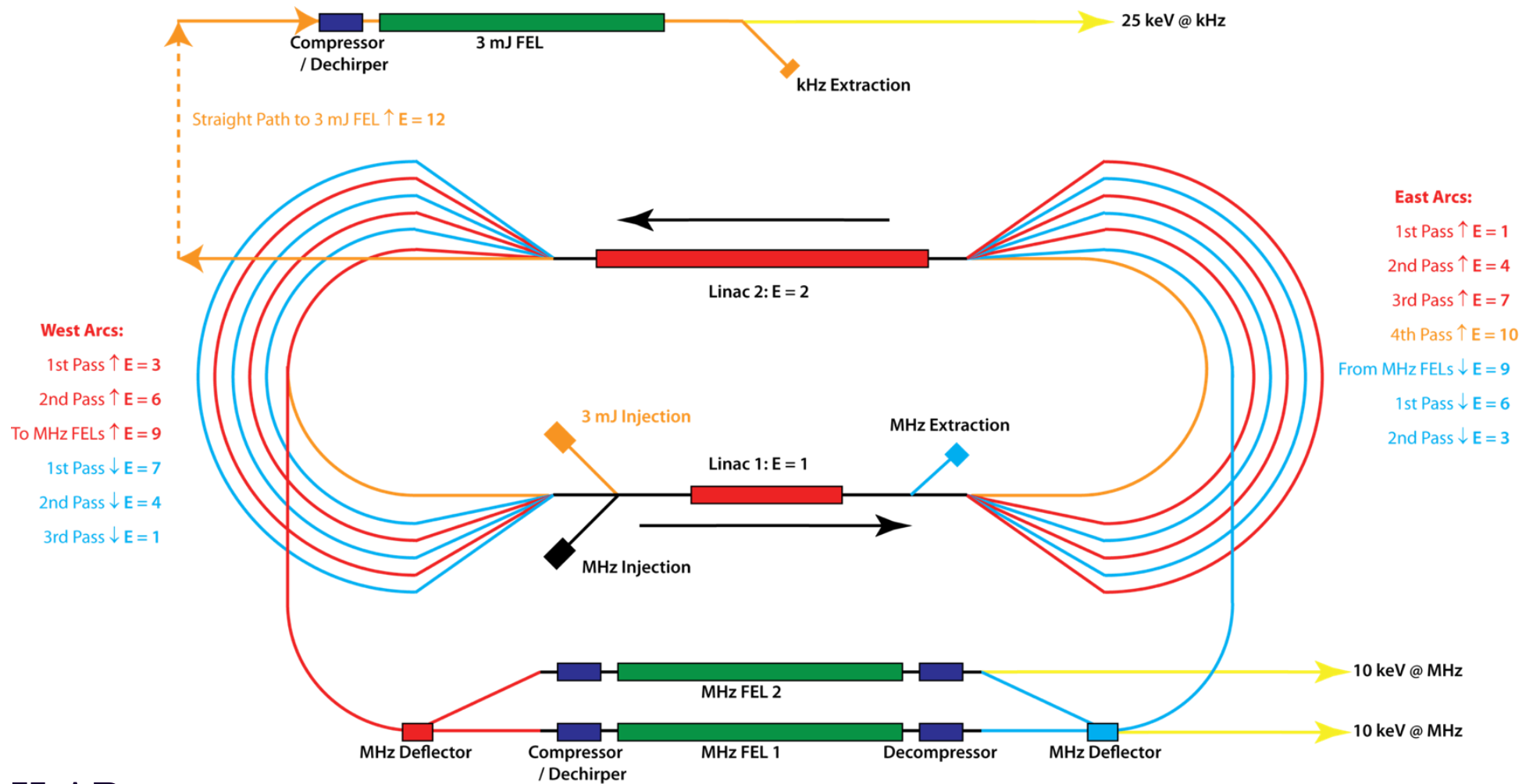
Example of the usefulness of caustics

with

Dave Douglas, JLAB

Peter Williams, Cockcroft Institute

A UK recirculating FEL concept



with
 Dave Douglas, JLAB
 Peter Williams, Cockcroft Institute

Caustic exclusion plots for each arc of a recirculating machine during acceleration

Arc no.

1

2

3

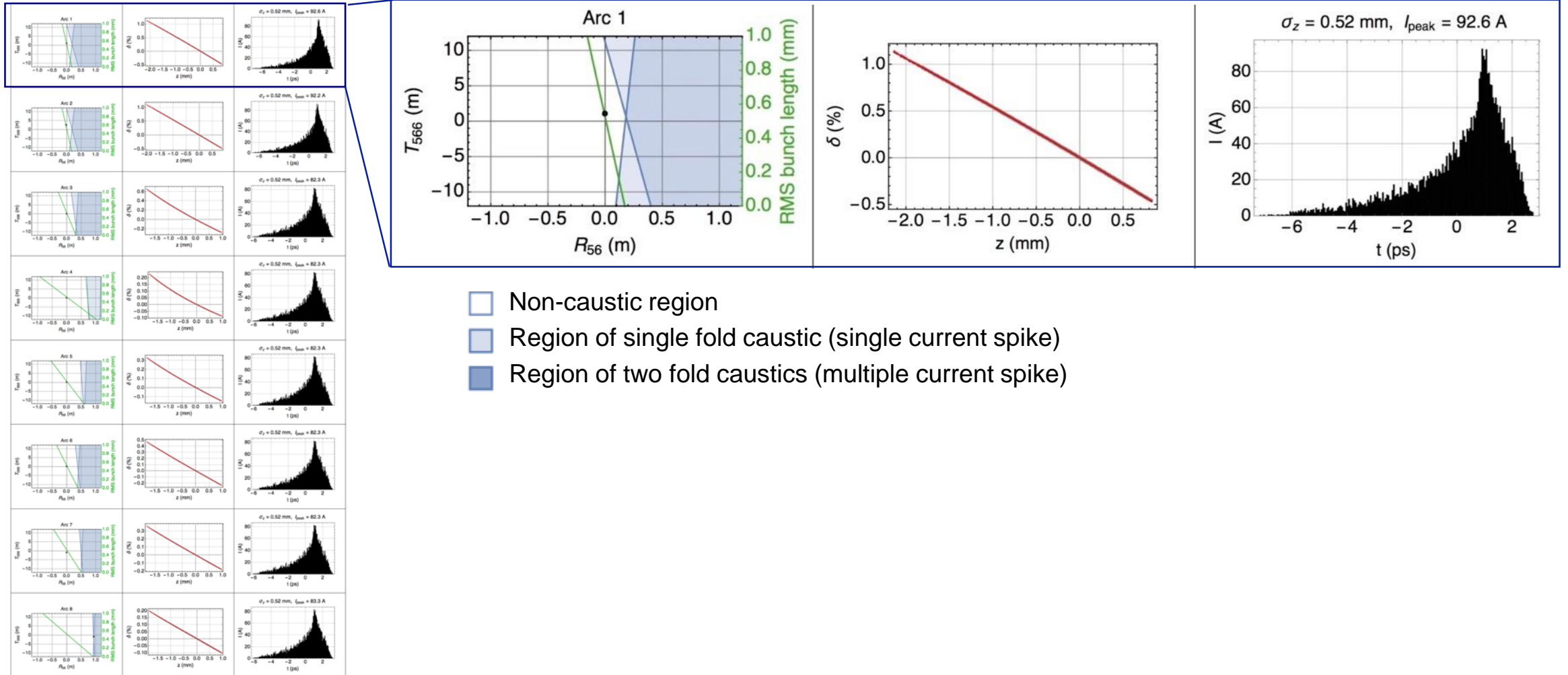
4

5

6

7

8



- Non-caustic region
- Region of single fold caustic (single current spike)
- Region of two fold caustics (multiple current spike)

Caustic exclusion plots for each arc of a recirculating machine during acceleration

Arc no.

1

2

3

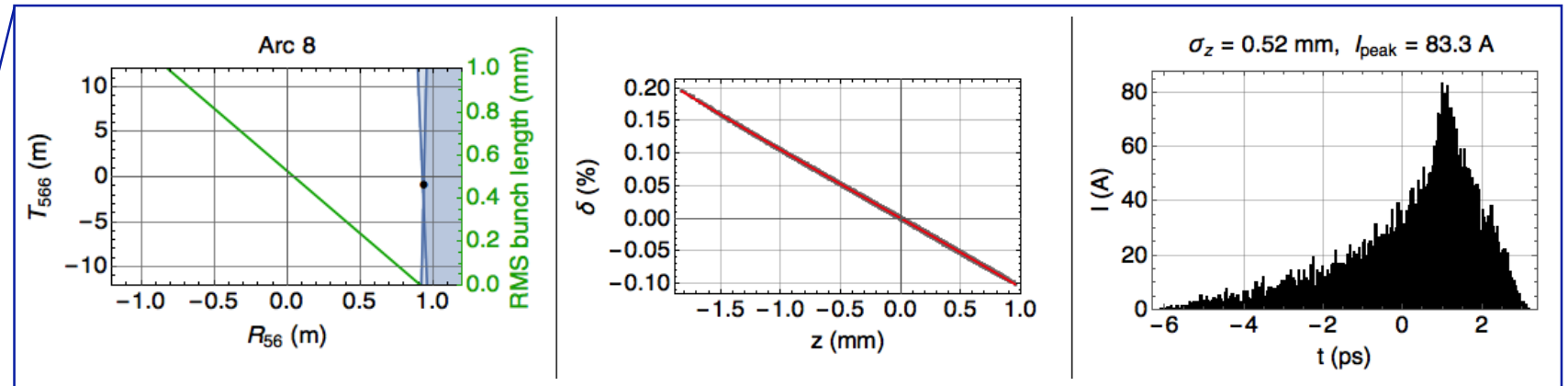
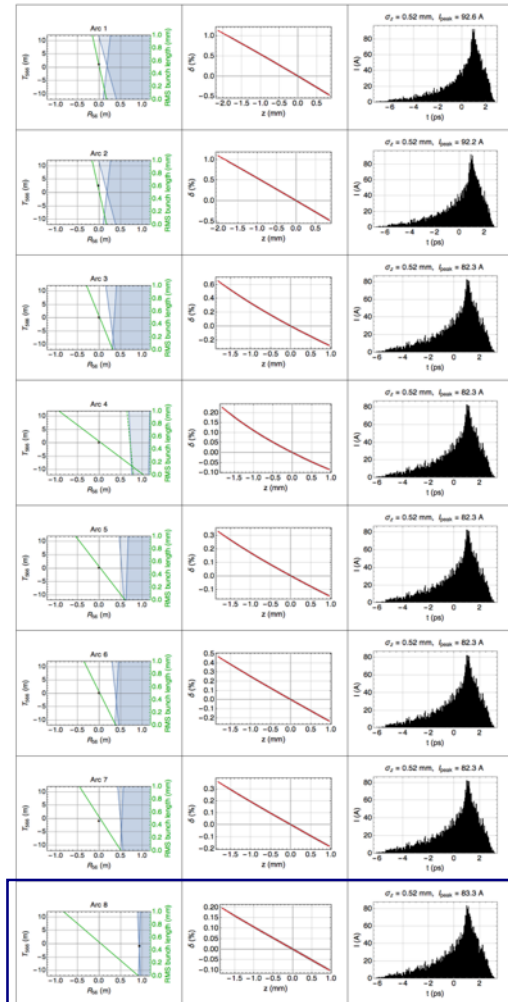
4

5

6

7

8

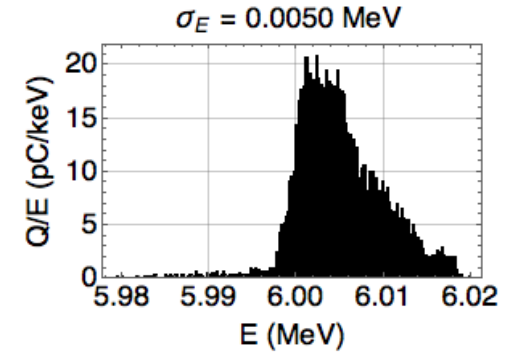
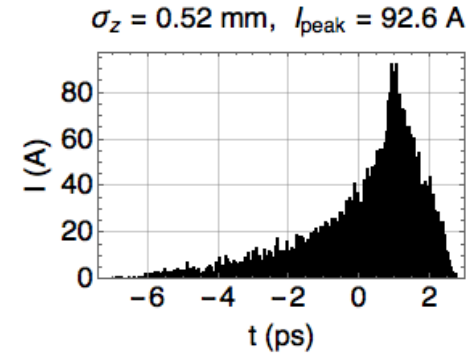
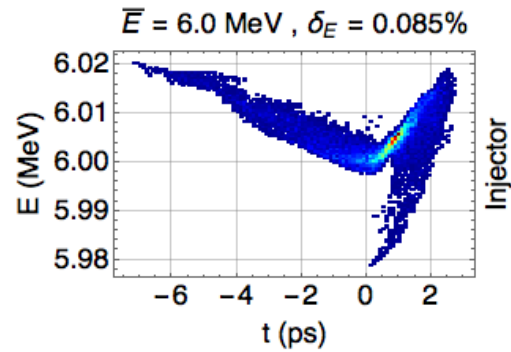


- Non-caustic region
- Region of single fold caustic (single current spike)
- Region of two fold caustics (multiple current spike)

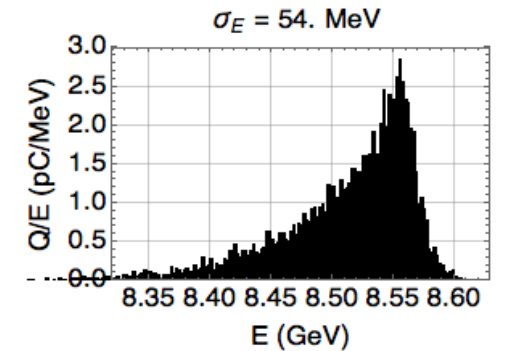
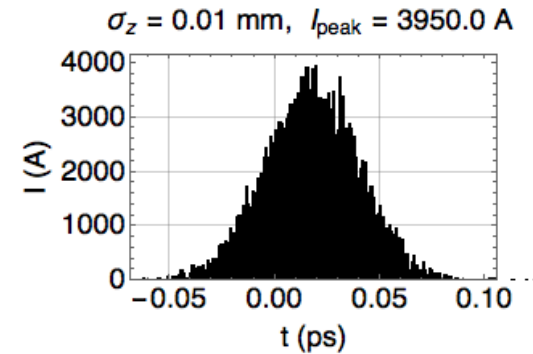
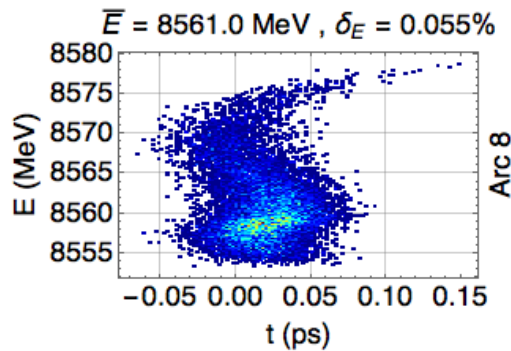
Bunch distributions at various positions around the accelerator

Bunch Distribution from gun:

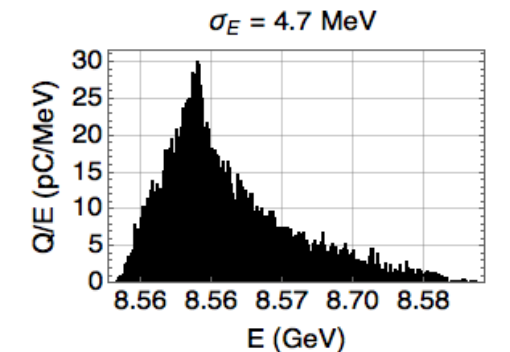
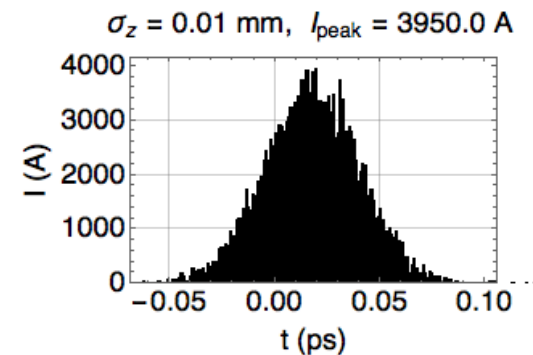
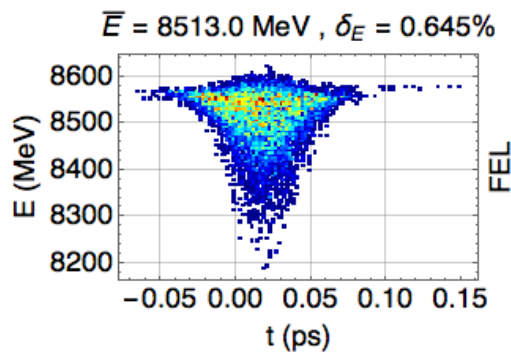
With thanks to **Julian McKenzie** (Daresbury, UK) for this distribution.



Distribution at end of arc 8:



Distribution after lasing:



Caustic exclusion plots for each arc of a recirculating machine during deceleration

Arc no.

9

10

11

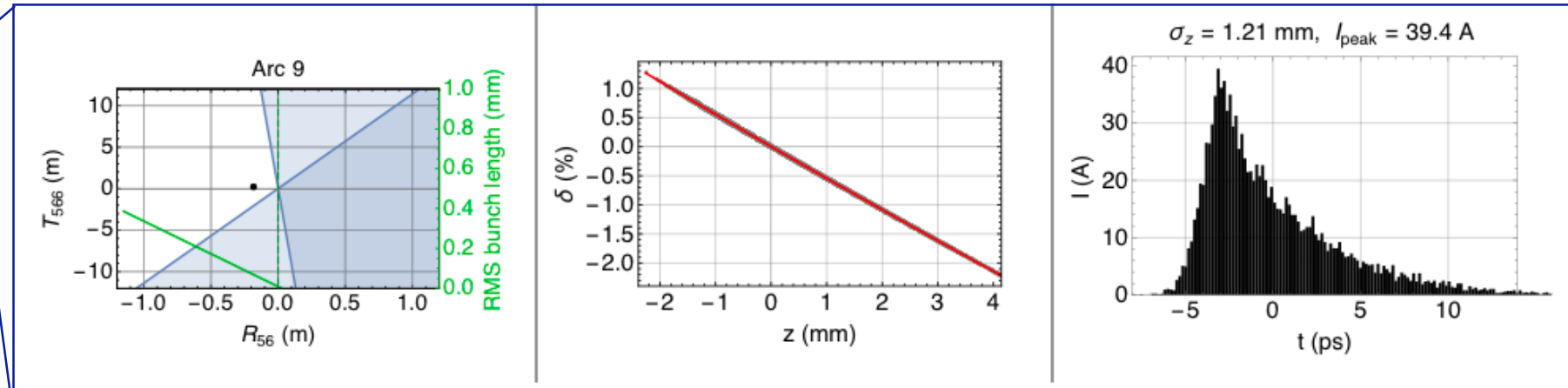
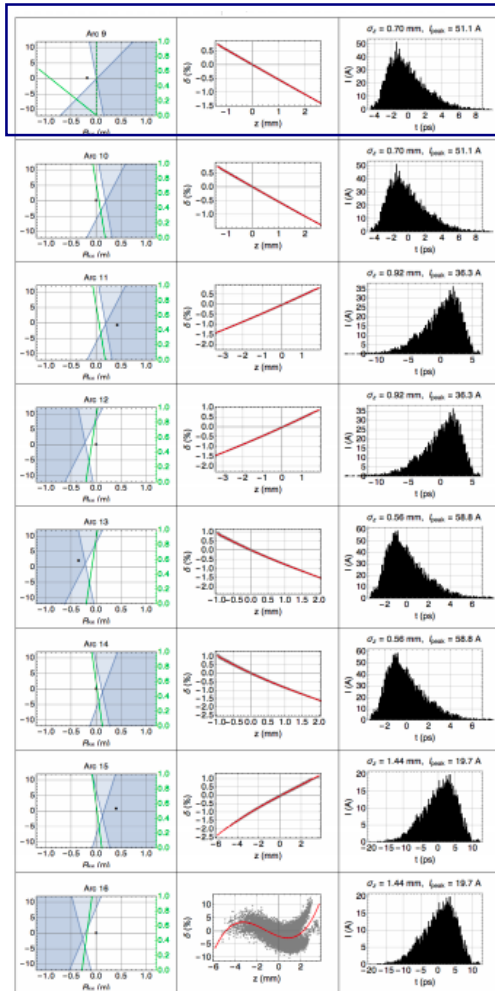
12

13

14

15

16



- Non-caustic region
- Region of single fold caustic (single current spike)
- Region of two fold caustics (multiple current spike)

Caustic exclusion plots for each arc of a recirculating machine during deceleration

Arc no.

9

10

11

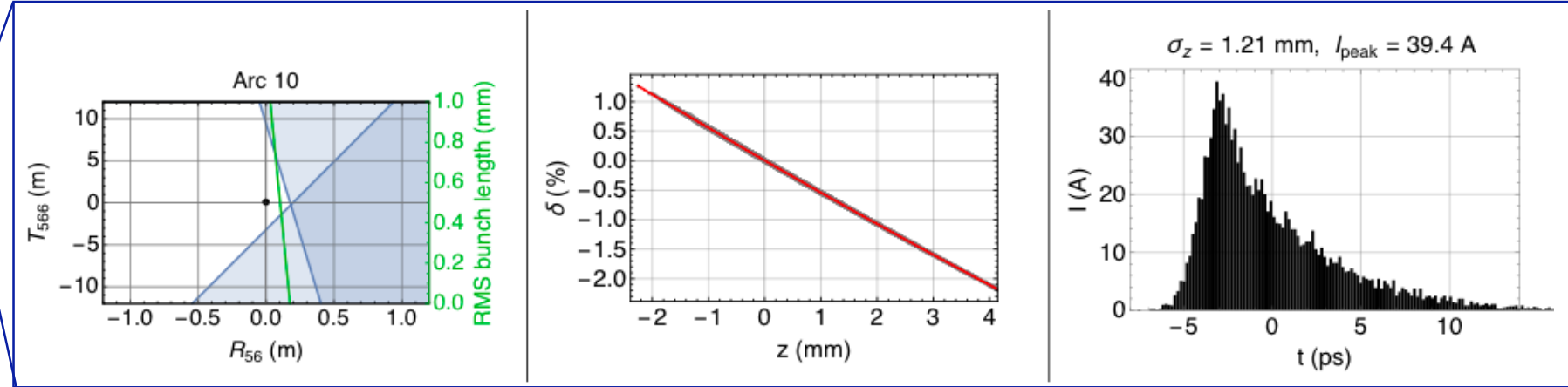
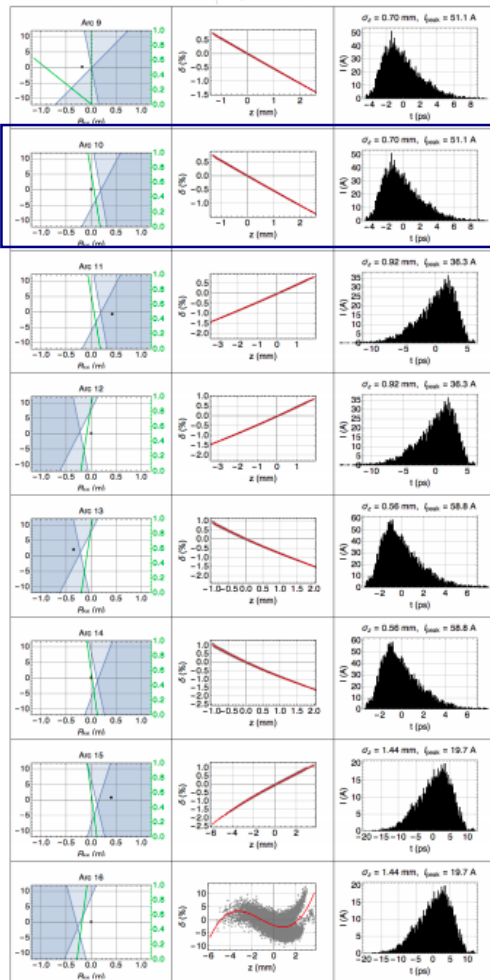
12

13

14

15

16



- Non-caustic region
- Region of single fold caustic (single current spike)
- Region of two fold caustics (multiple current spike)

Caustic exclusion plots for each arc of a recirculating machine during deceleration

Arc no.

9

10

11

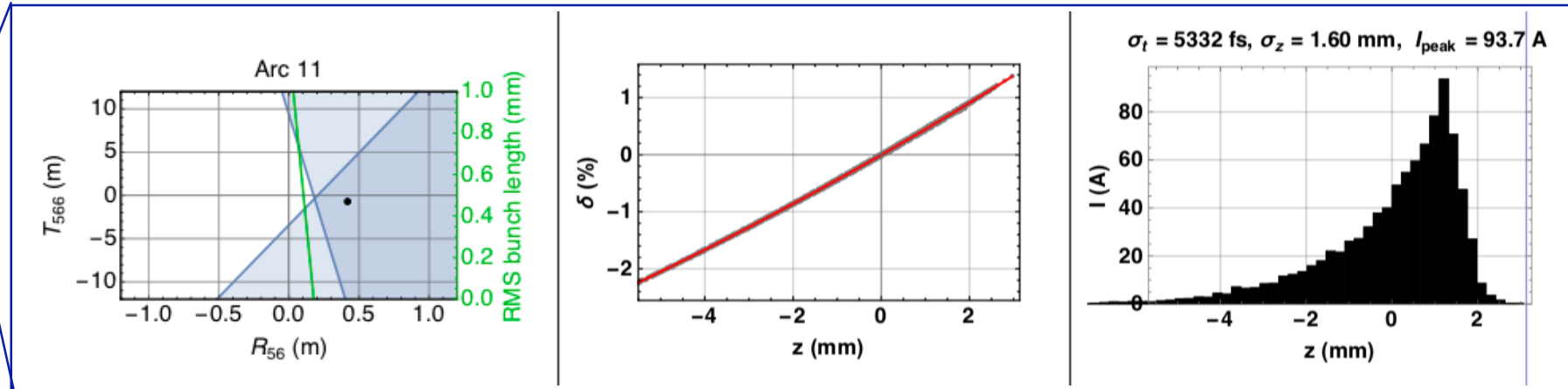
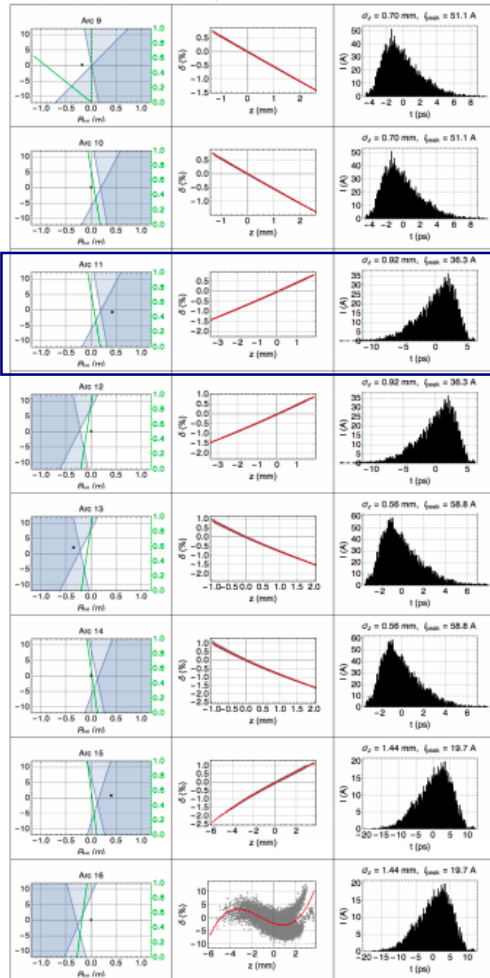
12

13

14

15

16



- Non-caustic region
- Region of single fold caustic (single current spike)
- Region of two fold caustics (multiple current spike)

Caustic exclusion plots for each arc of a recirculating machine during deceleration

Arc no.

9

10

11

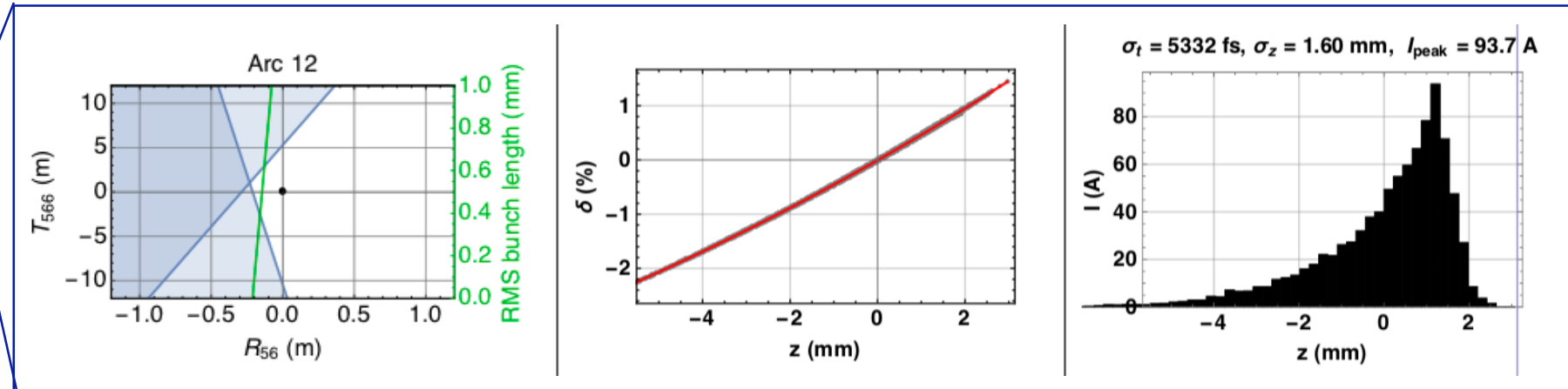
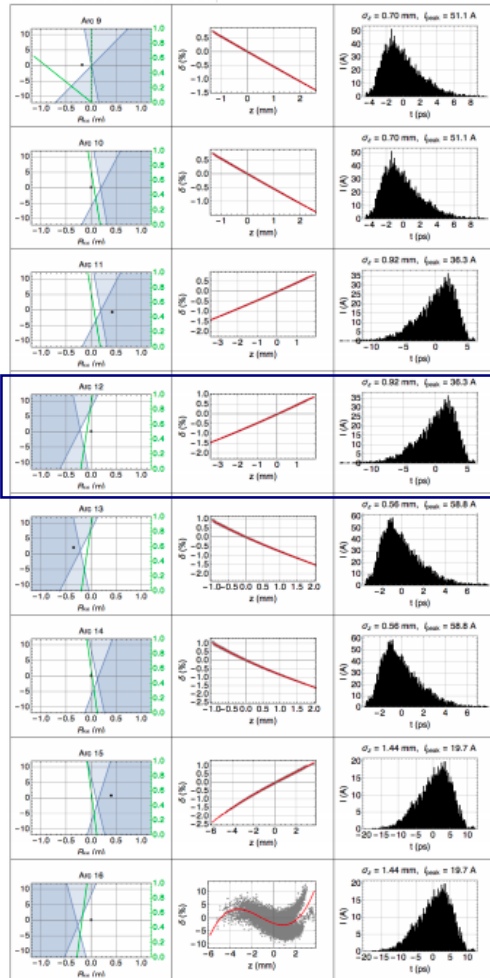
12

13

14

15

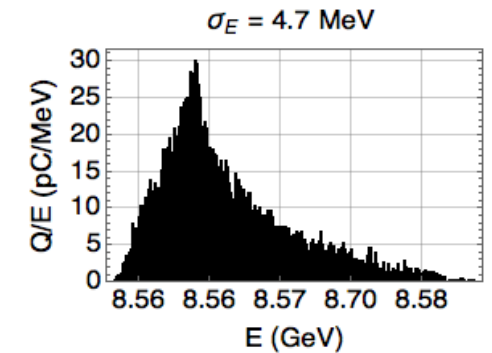
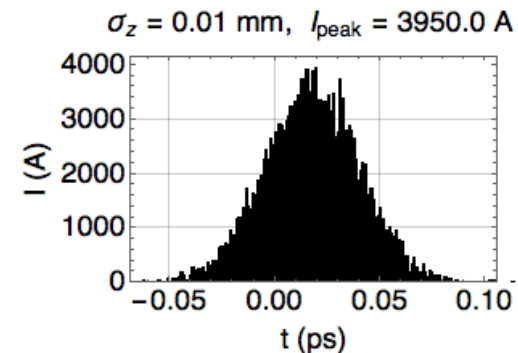
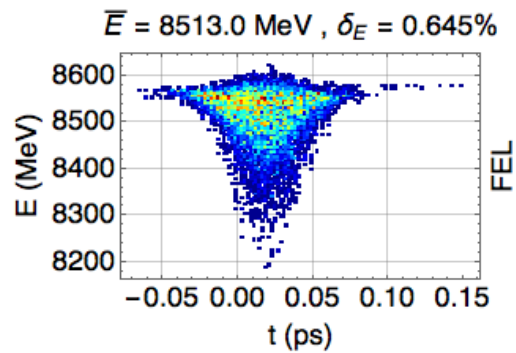
16



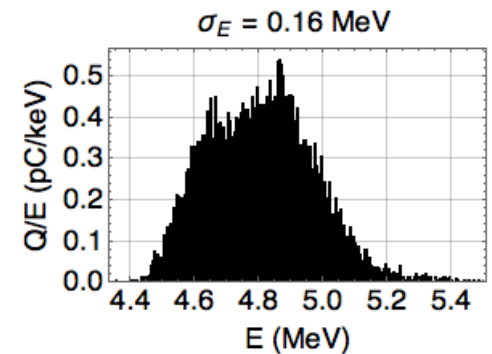
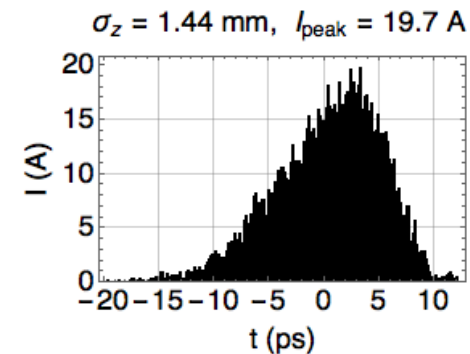
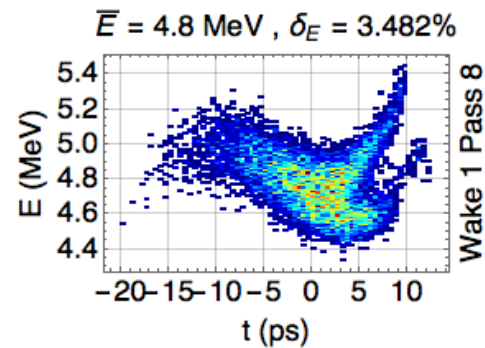
- Non-caustic region
- Region of single fold caustic (single current spike)
- Region of two fold caustics (multiple current spike)

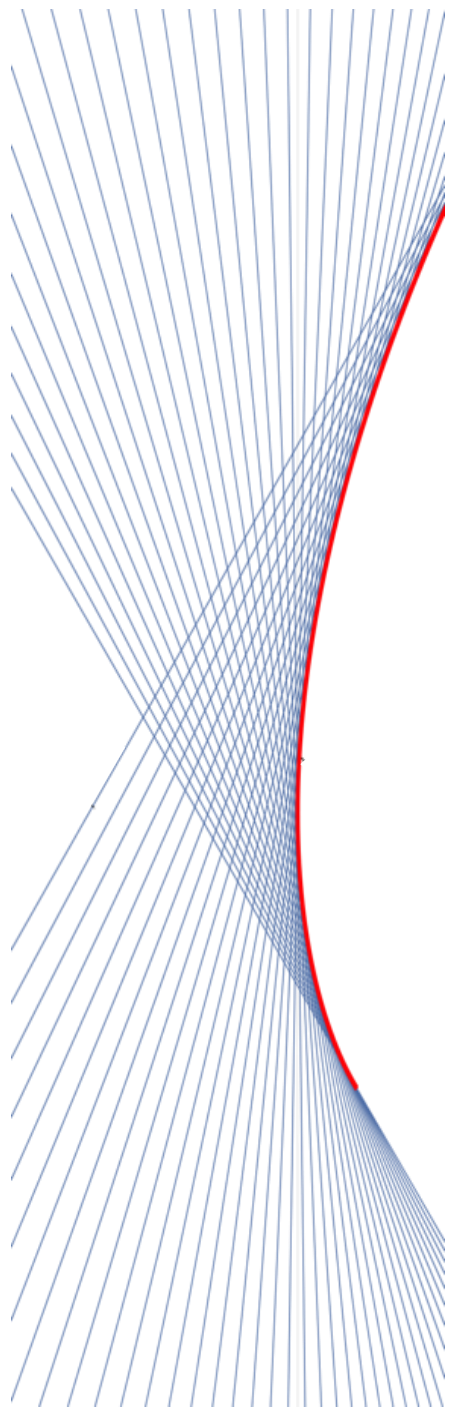
Bunch distributions at various positions around the accelerator

Distribution after lasing:



Distribution at dump:



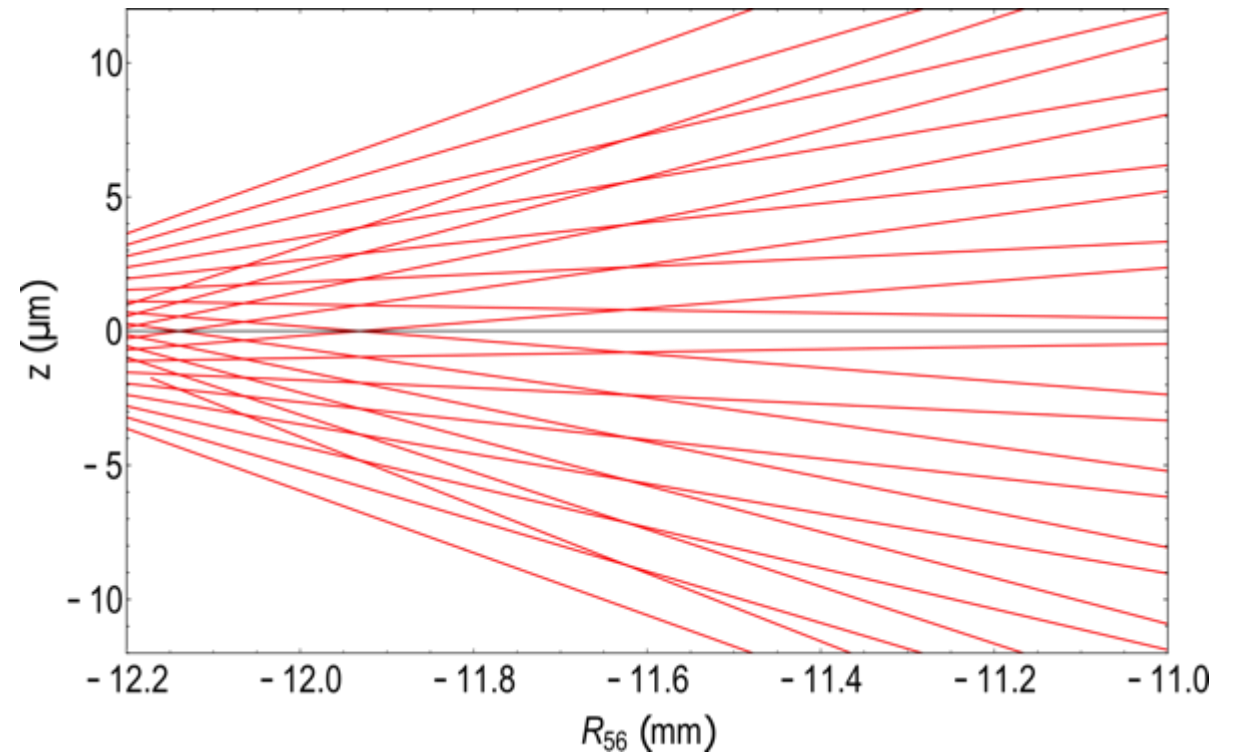
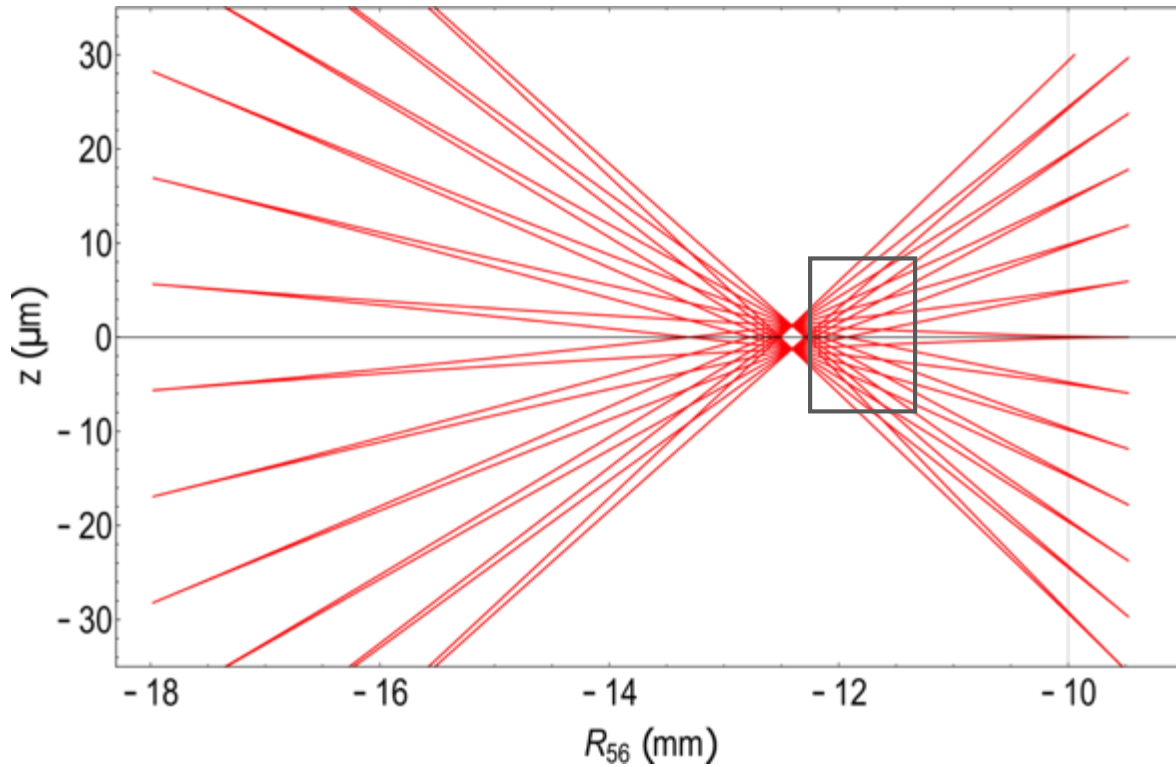


Microbunching instability

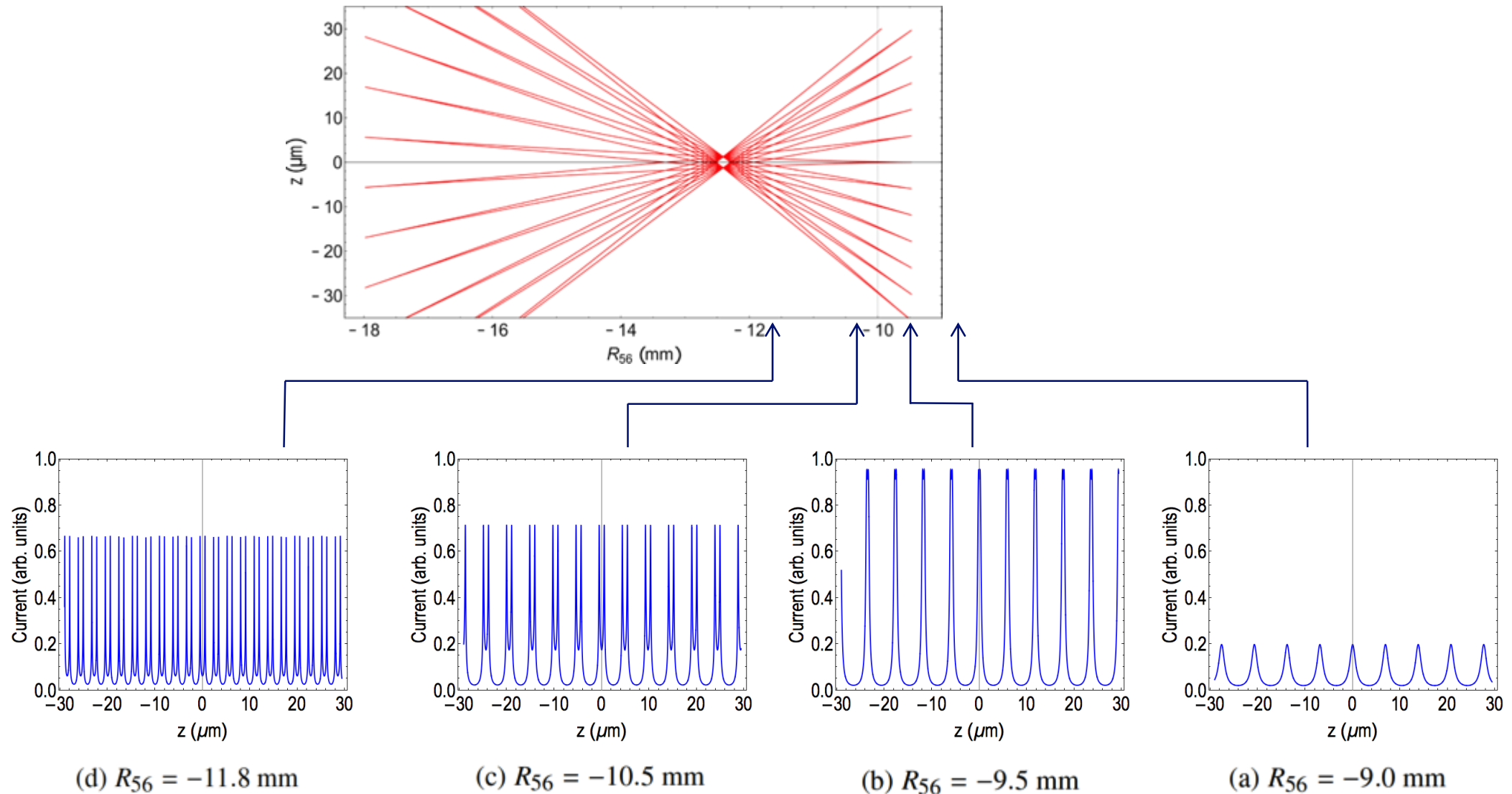
Example of the usefulness of caustics

Micro-bunching caustics

A caustic expression can also be derived for micro-bunching. Each line shows where a current spike will be seen.

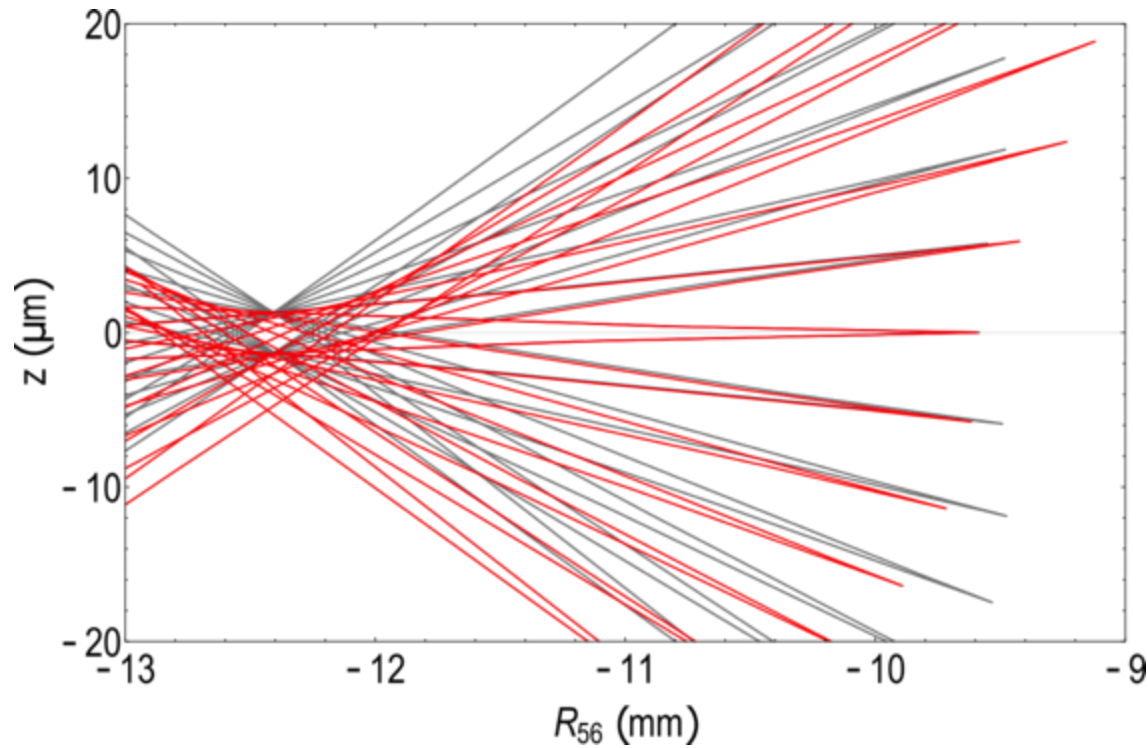


Caustic nature leads to bifurcated current peaks

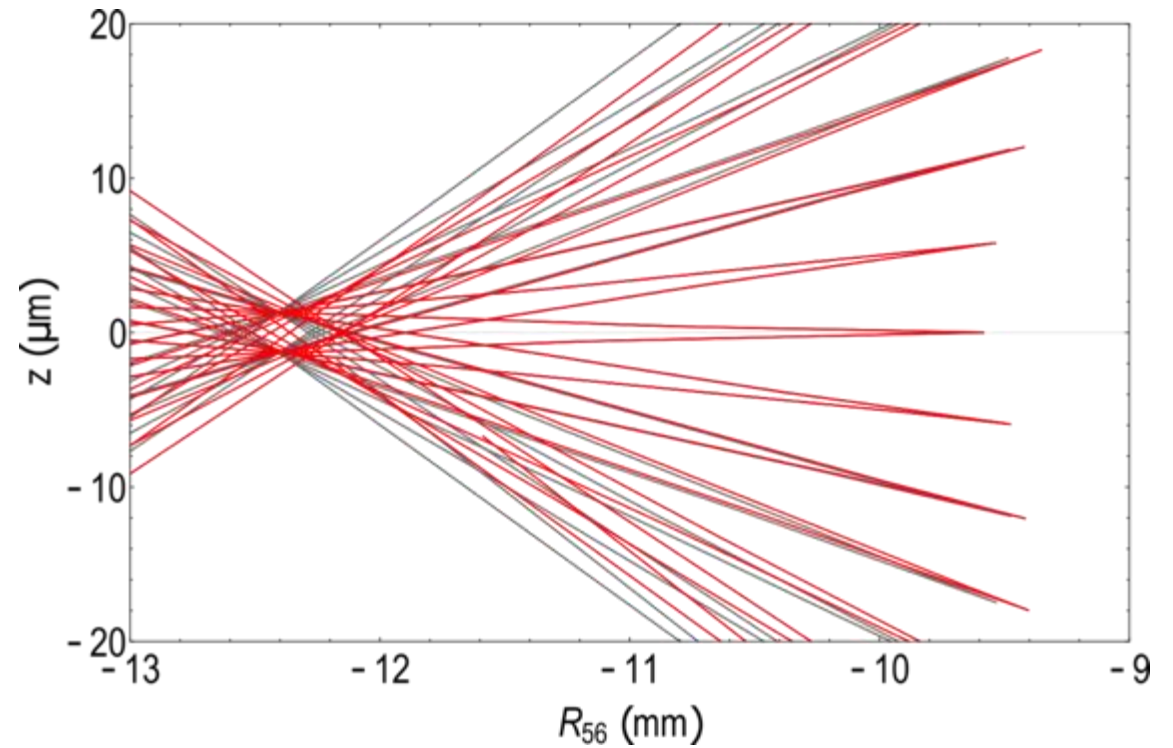


Micro-bunching with higher-order effects

Hyper-caustics 'caustics of caustics'



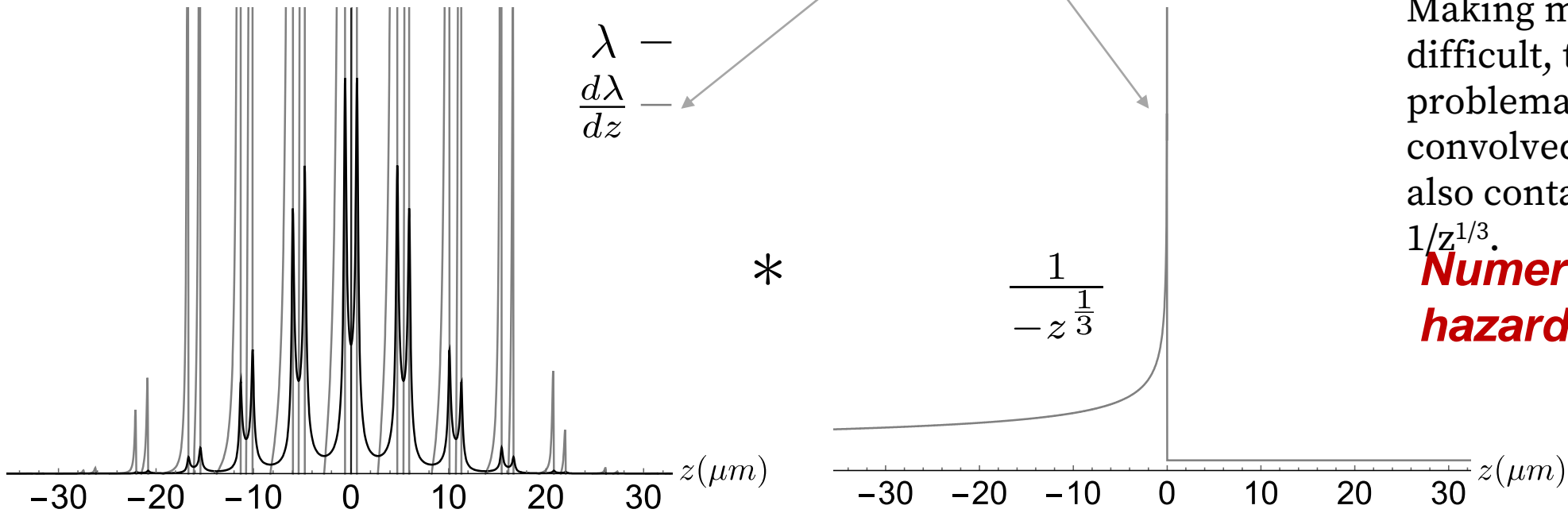
grey: $T_{566} = 0$, $U_{5666} = 0$ mm
red: $T_{566} = -30$ mm, $U_{5666} = 0$ mm



grey: $T_{566} = 0$, $U_{5666} = 0$ mm
red: $T_{566} = -2$ m, $U_{5666} = 0$ mm

CSR with microbunching

$$\frac{dE}{cdt} = \frac{-2e^2}{4\pi\epsilon_0(3R^2)^{1/3}} \int_{\tilde{z}-z_L}^{\tilde{z}} \frac{d\lambda}{dz} \left(\frac{1}{\tilde{z}-z} \right)^{1/3} dz$$



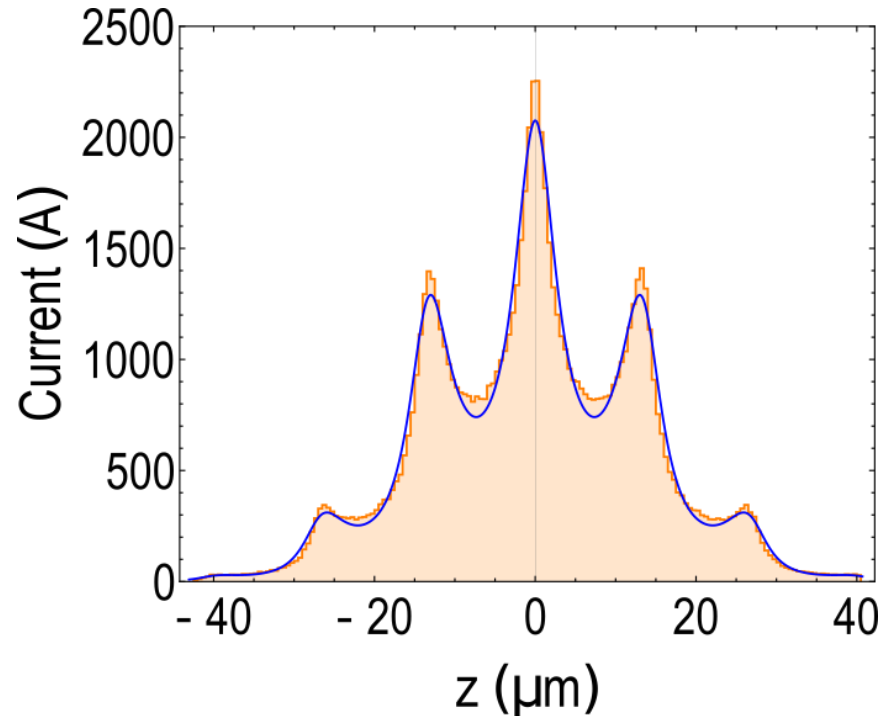
The caustic nature of microbunching results in sharp peaks in the linear charge density function, $\lambda(z)$, which means the numerical evaluation of $d\lambda/dz$ is risky. Making matters even more difficult, this numerically problematic data set is then convolved with a function that also contains a singularity, $1/z^{1/3}$.

Numerically hazardous!

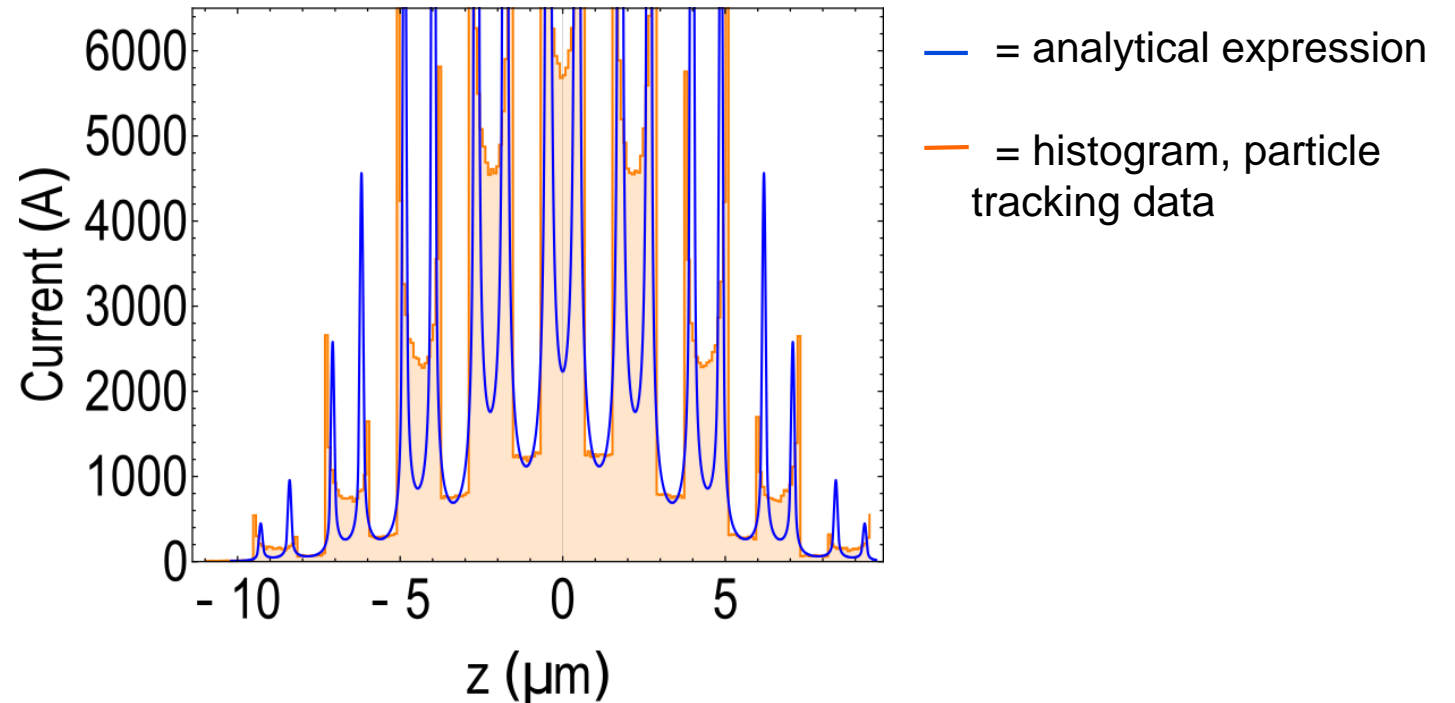
Current profile analytical expression

$$\lambda(z) = \frac{e^{-\frac{z^2}{2\sigma^2}}}{\sqrt{2\pi\sigma}} \frac{f}{1 + R_{56}\delta'(z) + T_{566}\delta''(z) + U_{5666}\delta'''(z)}, \quad \text{where } f \text{ is a scaling factor.}$$

non-caustic region

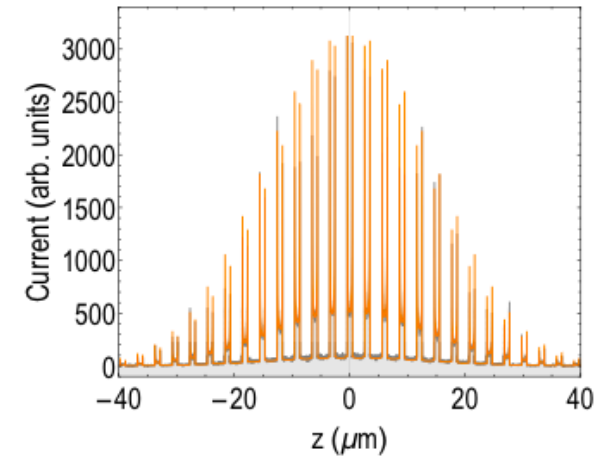
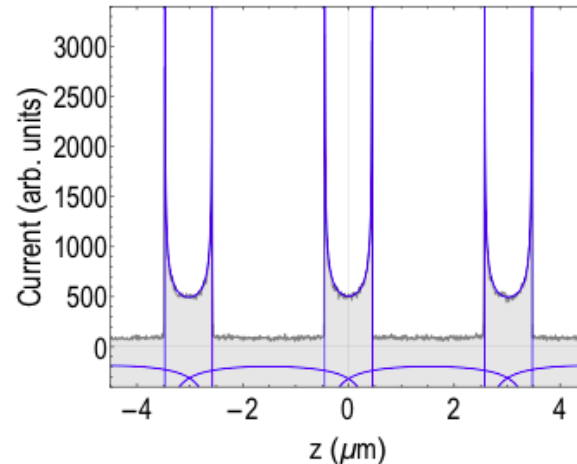
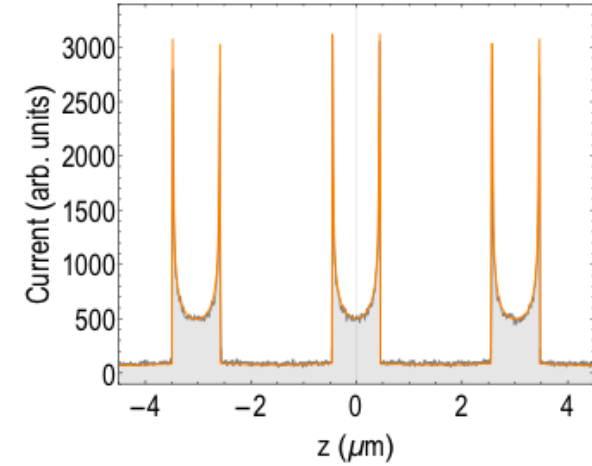
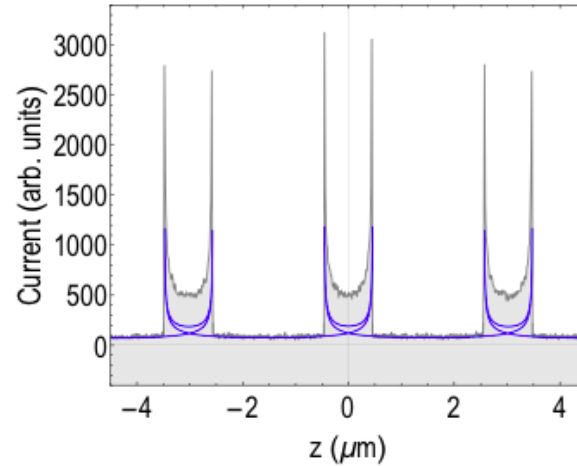


caustic region



Current profile analytical expressions – caustic region

Piecewise analytical functions (orange) can model the caustic current profiles.
(These are mono-energetic, longitudinal plane only.)



We're looking to hire a PhD student!

The screenshot shows a PhD project listing on the FindaPhD.com website. The title is "Microbunching Instability Suppression for Improved FEL performance". The project is located at the University of Liverpool, Cockcroft Institute. The project is supervised by Dr T Charles, Dr P Williams, and Dr S Thorin. Applications are accepted all year round, and it is a funded PhD project for students worldwide. The project is categorized under Applied Physics and Atomic Physics. The "About the Project" section describes recent advances in Free Electron Lasers (FELs) and the potential to image atomic structures. The right-hand side of the listing includes the University of Liverpool logo, a link to "About the Project" with "Funding Notes", a prominent red "Email institution" button, and icons for "Institution website", "Add to shortlist", and "Institution profile". A "COVID-19 Information" button is also present.

< Search PhDs

Microbunching Instability Suppression for Improved FEL performance

University of Liverpool > Cockcroft Institute

Dr T Charles , Dr P Williams , Dr S Thorin

Applications accepted all year round

Funded PhD Project (Students Worldwide)

Liverpool United Kingdom Applied Physics Atomic Physics

About the Project

Recent advances in Free Electron Lasers (FELs) have seen peak X-ray brightness increase by several orders of magnitude, and pulse durations decrease from 100 fs down to <10 fs. With these advancements, a new world of possibilities has been afforded researchers to image atomic structure of proteins and explore dynamical processes in timescales on the order of

UNIVERSITY OF LIVERPOOL

> About the Project

Funding Notes

Email institution

Institution website Add to shortlist Institution profile

COVID-19 Information

Details [here](#)

Or email me:

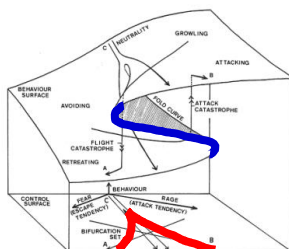
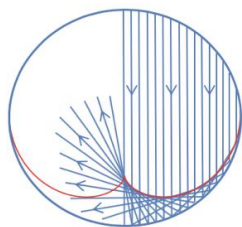
tessa.charles@liverpool.ac.uk

<https://www.findaphd.com/phds/project/microbunching-instability-suppression-for-improved-fel-performance/?p125125>

Conclusions ...

Caustics are a useful way that we can look at various types of focusing.

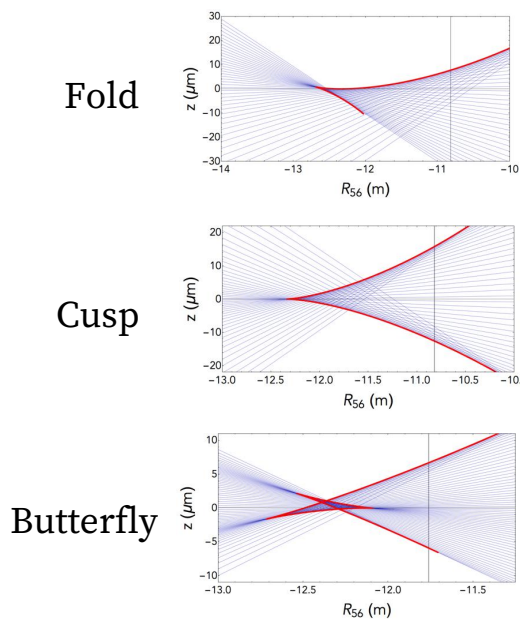
Caustics are commonplace in optics, they are utilised in electron microscopy, and they are also seen in accelerator physics.



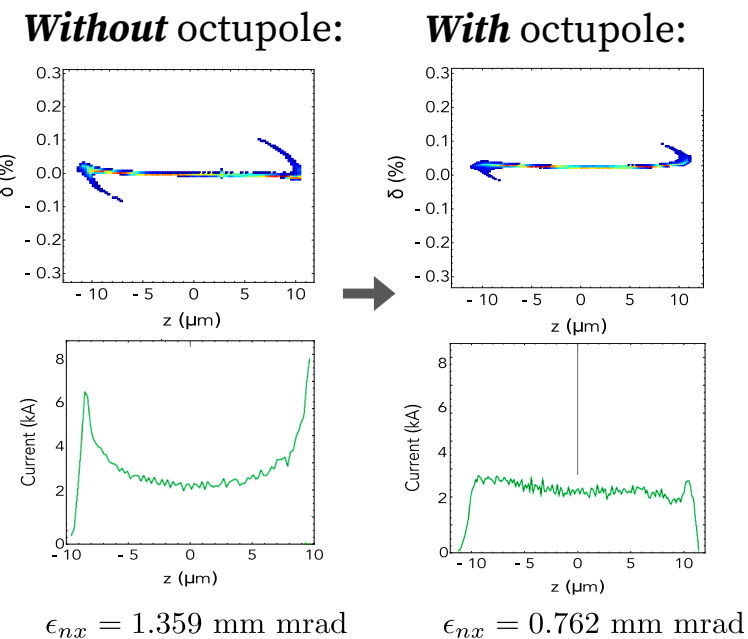
Applied to accelerator physics, we can explore the high-order focusing.

$$\tilde{z}_c(z_i) = z_i + \frac{\delta(z_i)(-1 + T_{566}(-2 + \delta(z_i))\delta'(z_i) + U_{5666}(-3 + \delta(z_i)^2)\delta'(z_i))}{\delta'(z_i)}$$

$$\tilde{R}_{56}(z_i) = \frac{-1 - 2T_{566}\delta'(z_i) - 3U_{5666}\delta'(z_i)}{\delta'(z_i)}$$



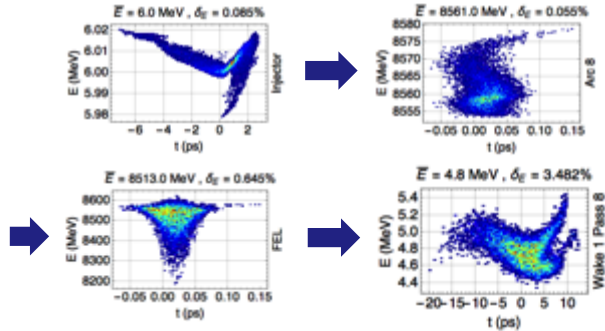
Current horns (often seen in FELs) can be suppressed by considering the underlying caustics, resulting in 63% reduction in the CSR-induced emittance growth.



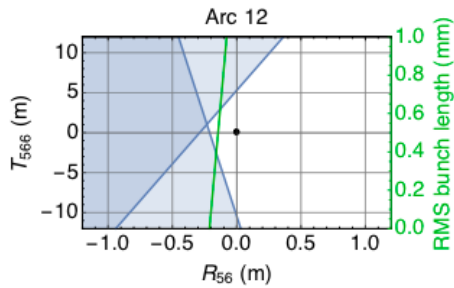
Conclusions

Caustics are a useful way that we can look at various types of focusing.

Longitudinal phase space manipulation in recirculating & energy recovery machines

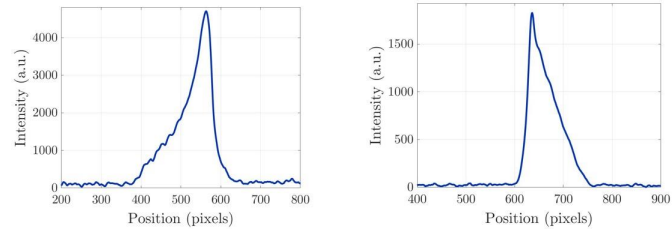


Caustic exclusion plots can be used to pair down viable parameter space.

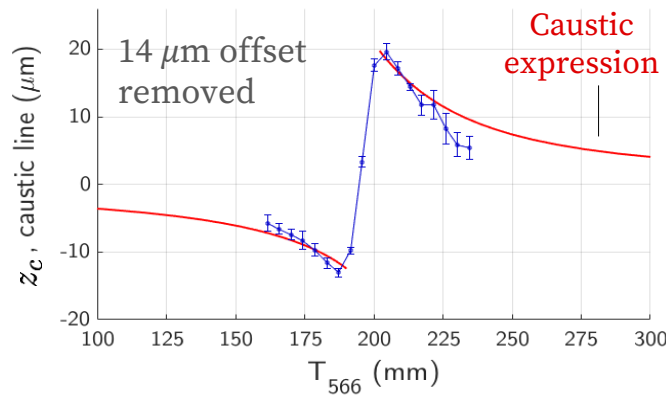


Exclusion plots identify regions where caustics of different codimension exist

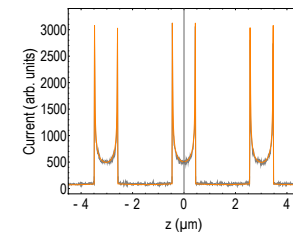
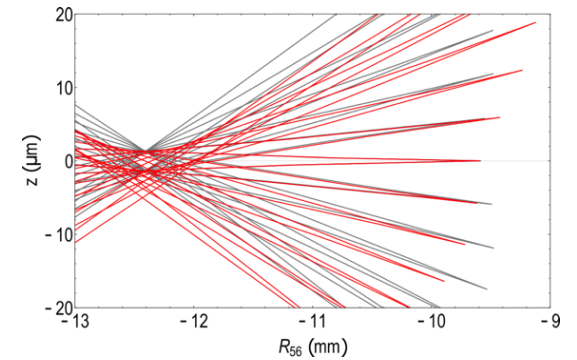
Experimental demonstration of linearly-ramped current profiles and caustics!



Linearly-ramped current profile achieved through T566 variation.



Microbunching is also a caustic phenomenon and can be used to better model microbunching.



Bifurcated current peaks

Acknowledgements

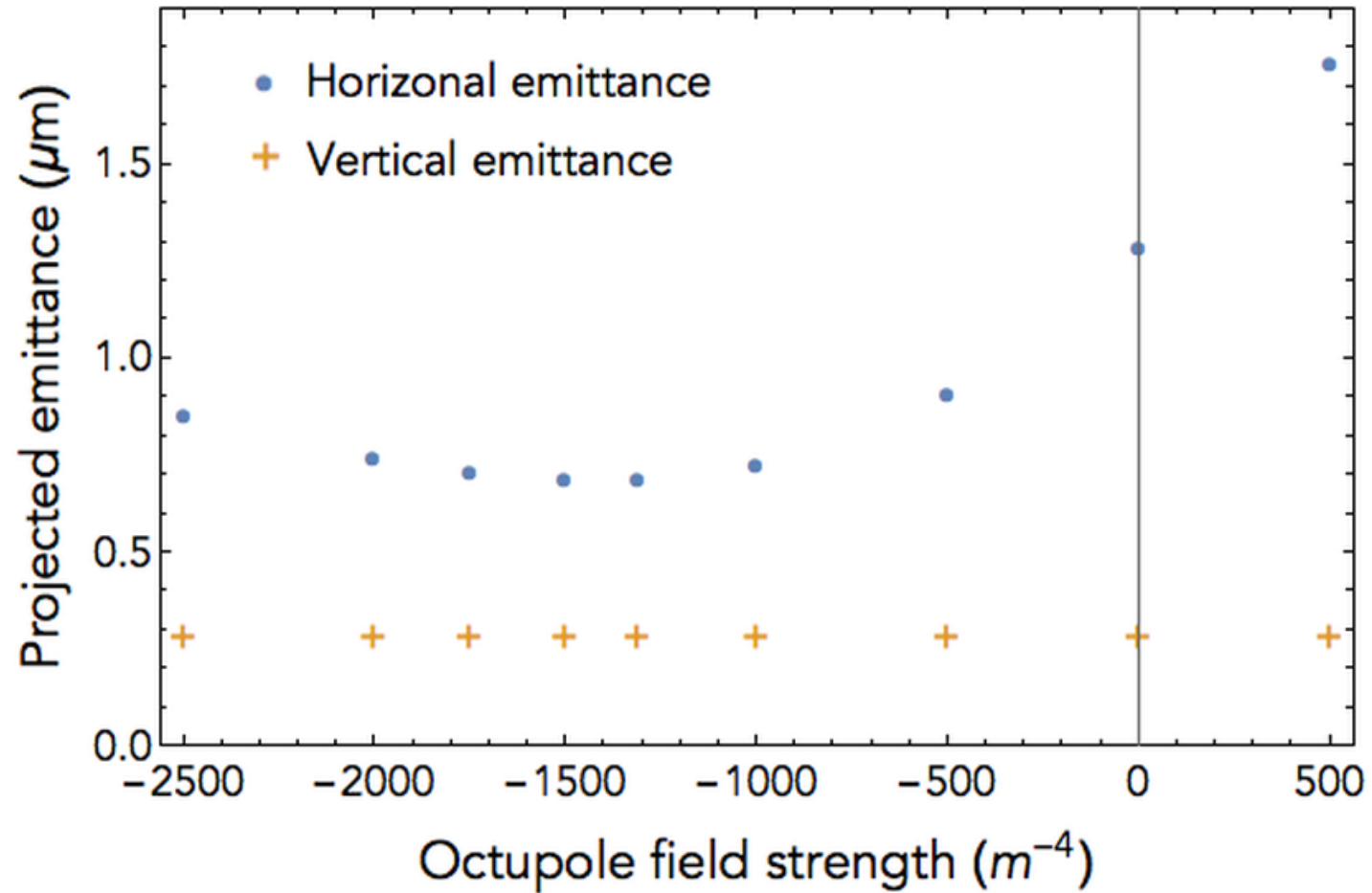
With acknowledgments and thanks to the people who have supported and contributed to this work:

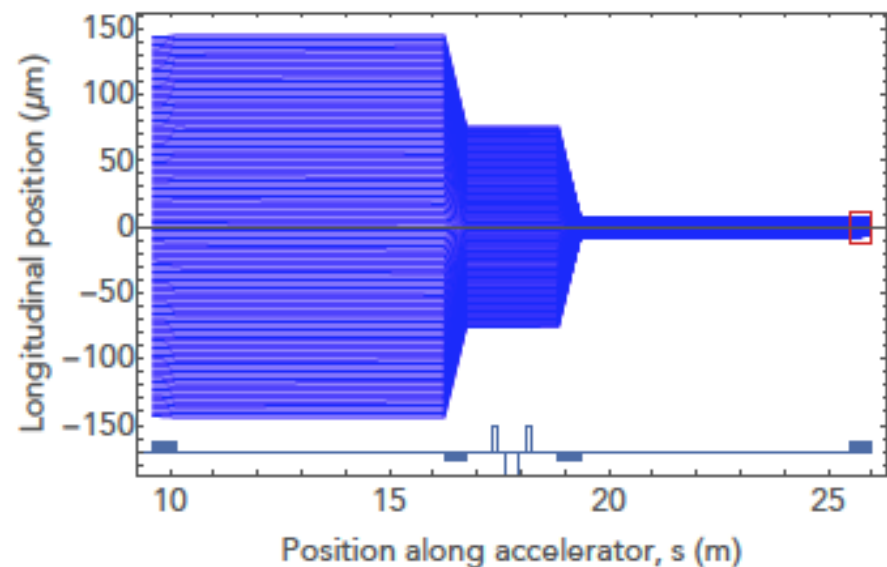
- Sara Thorin, Jonas Bjorklund Svensson, and Joel Andersson (MAX IV)
- Andrea Latina and Frank Zimmermann (CERN)
- Rohan Dowd (Australian Synchrotron)
- David Paganin (Monash University)
- Mark Boland (Canadian Light Source)
- Peter Williams (Daresbury Laboratory)
- Dave Douglas (J-Lab)
- In memory of Greg LeBlanc (Australian Synchrotron)

Thank you

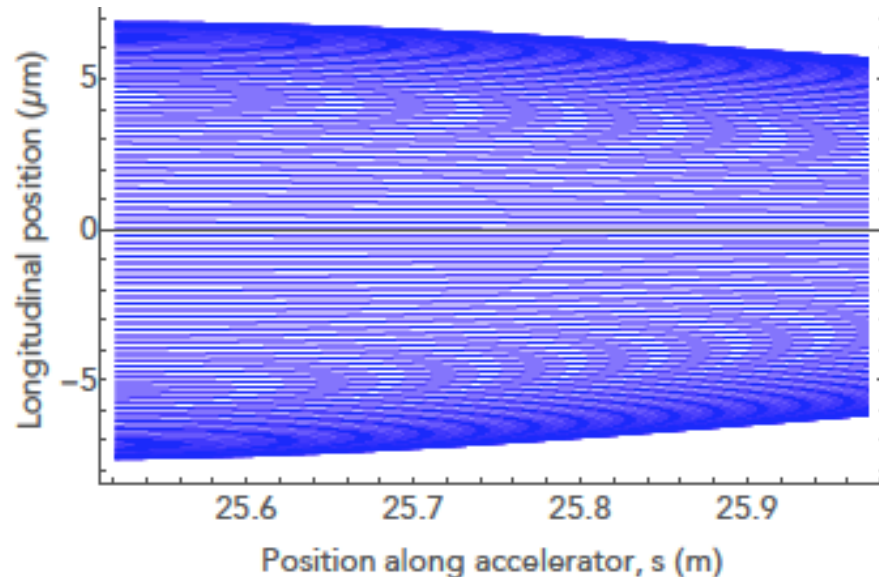
Back up slides

What about chromatic and geometric aberrations?





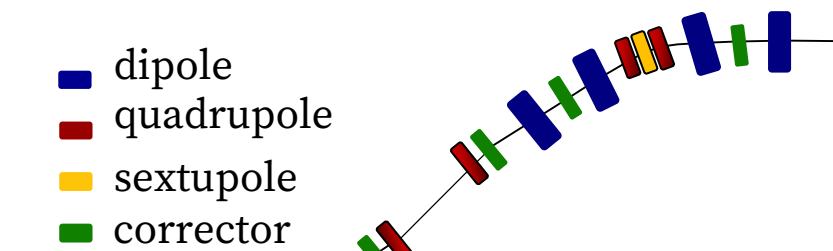
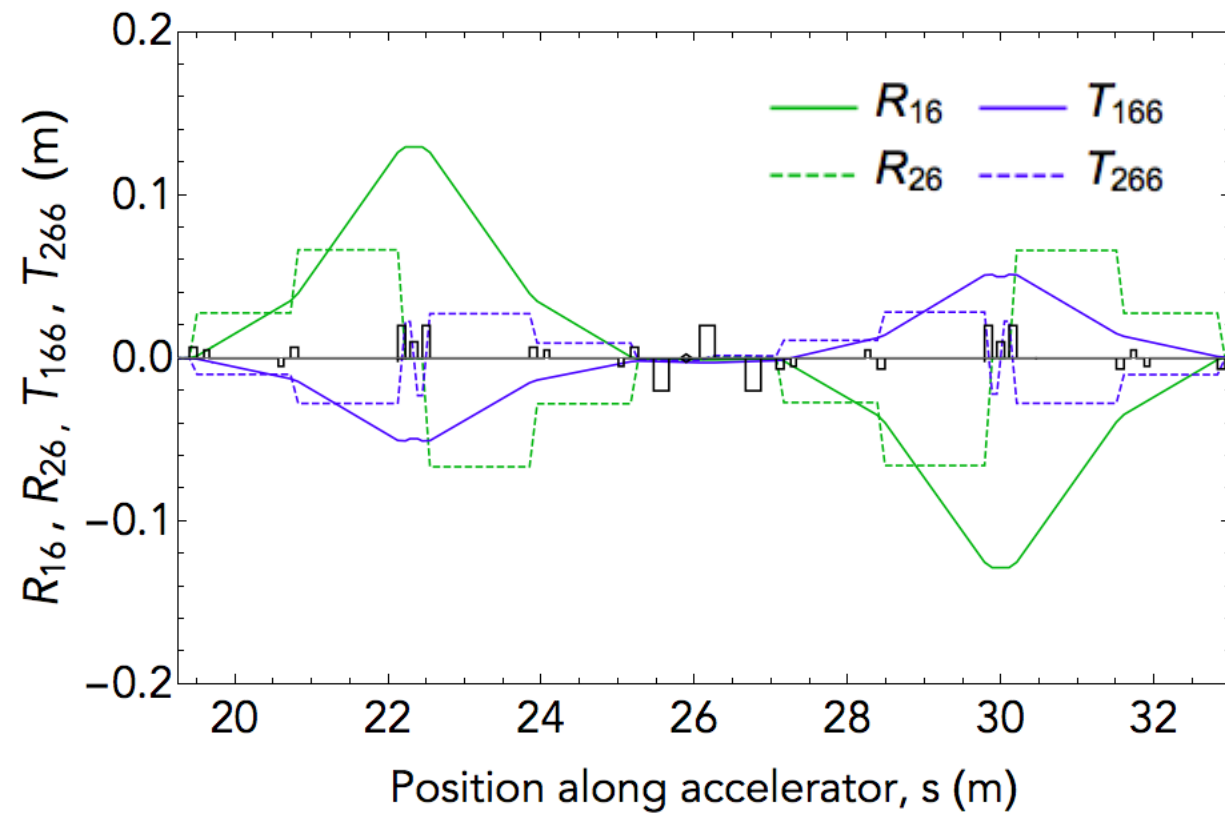
(a)



(b)

Figure 6.8: Electron trajectories (in s - z space) through a bunch compressor. (b) shows a close up of the trajectories through the fourth dipole (i.e. region outlined with a red box in (a)). Caustics can be seen forming at head and tail of the bunch in (b).

MAX IV Bunch Compressors



Intro: Caustics in accelerator physics 1

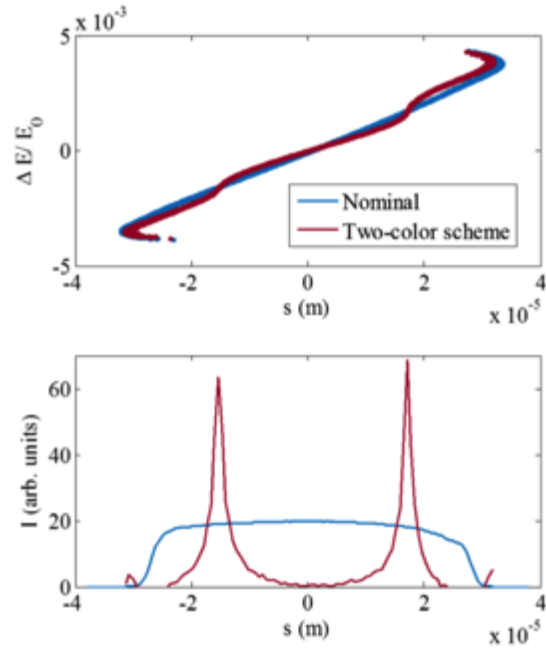


FIG. 2. Comparison of the beam longitudinal phase space at the entrance of BC1 (top) and current longitudinal profile at the entrance of BC2 (bottom) corresponding to the nominal operation mode of SwissFEL and the one assuming an opportune wakefield source.

S. Bettoni et al, Phys. Rev. AB (2016) **19** 050702

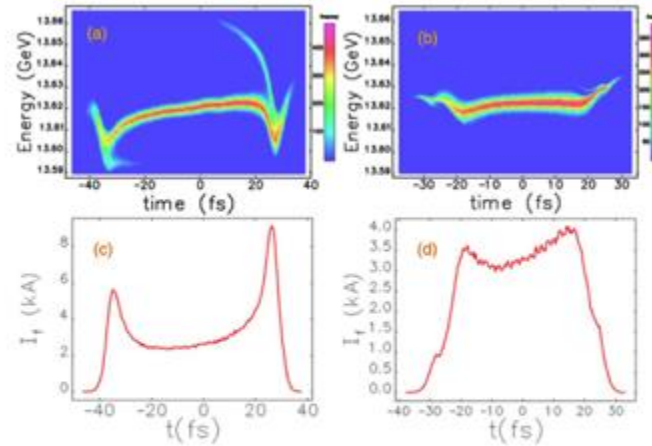


FIG. 1. Simulated electron beam phase space and current profile at the entrance of the LCLS undulator. (a) and (c) are for regular compression setup with full charge of 250 pC without collimation; (b) and (d) show the collimated beam cutting down to about 150 pC using the BCI collimator. We see clearly the reduced current horns and flat phase space with the truncation mode.

F. Zhou et al, Phys. Rev. ST AB (2016) **18** 050702

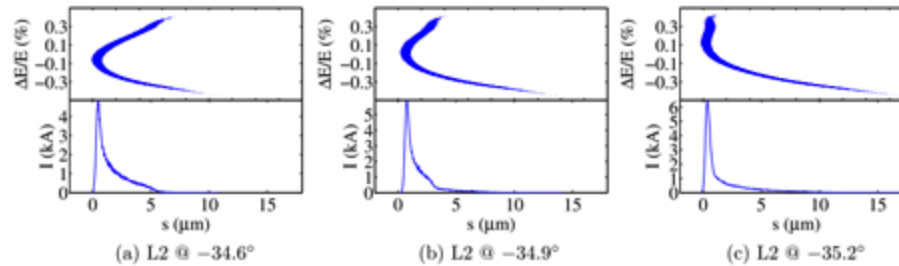


FIG. 2. LiTRACK simulations for electron bunch distribution in the longitudinal phase space (upper) and its current profile (lower) at the LCLS undulator entrance. The L2 rf phase is adjusted from -34.6° (a) to -35.2° (c), which rotates the longitudinal phase space while maintaining a relatively constant current spike. The LIS rf phase is -27° , and the LIS phase and amplitude are -180° and 15 MV, respectively. For the phase space and current plots in this figure and throughout the paper, the bunch head is to the left.

S. Huang et al, Phys. Rev. AB (2014) **17** 120703

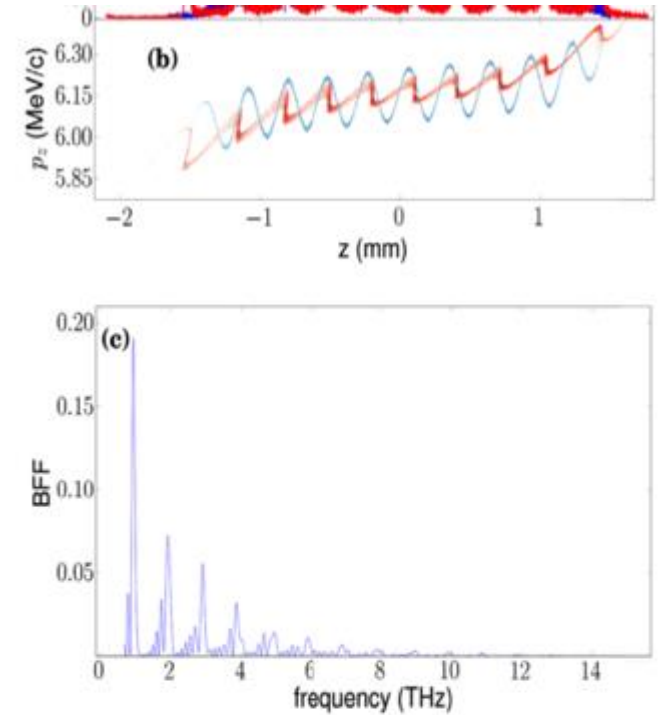


FIG. 6. Current profiles (a) and associated longitudinal phase spaces (LPS) (b) simulated at the exit of the DLW (blue trace) and at the location of maximum bunching (red trace) $z = 1.3$ m from the photocathode. Bunch form factor (BFF) (c) obtained at $z = 1.3$ m from the photocathode. The simulations correspond to the parameters listed under the S-band column in Table I.

F. Lemery et al, Phys. Rev. AB (2014) **17** 112804

Intro: Caustics in accelerator physics 2

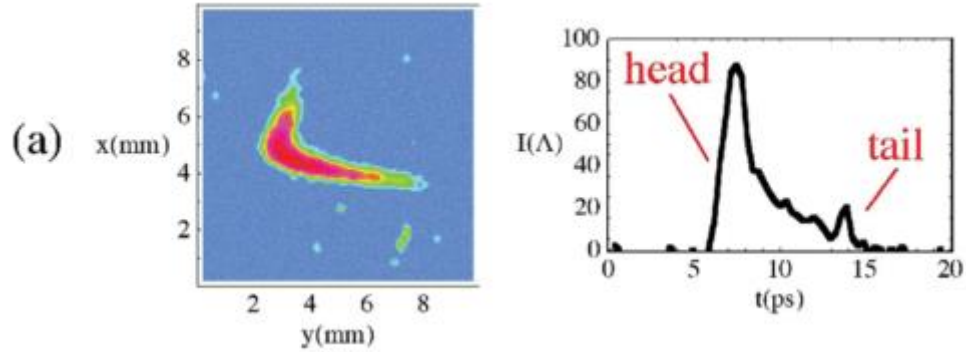


FIG. 5 (color). Deflecting cavity streaks (left) and current profile reconstructions (right) of an initially chirped electron beam for five different sextupole field values: (a) $\kappa = 0$, (b) $\kappa = 547 \text{ m}^{-3}$, (c) $\kappa = 1094 \text{ m}^{-3}$, (d) $\kappa = 1641 \text{ m}^{-3}$, and (e) $\kappa = 2188 \text{ m}^{-3}$.

R. England et al, Phys. Rev. Lett. (2008) **100** 214802

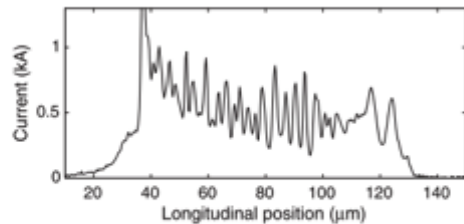


FIG. 3. Current taken from a projection of the upper left image in Fig. 2. Strong modulations show that MBI is nearly saturated without the laser heater.

D. Ratner et al, Phys. Rev. AB (2015) **18** 030704

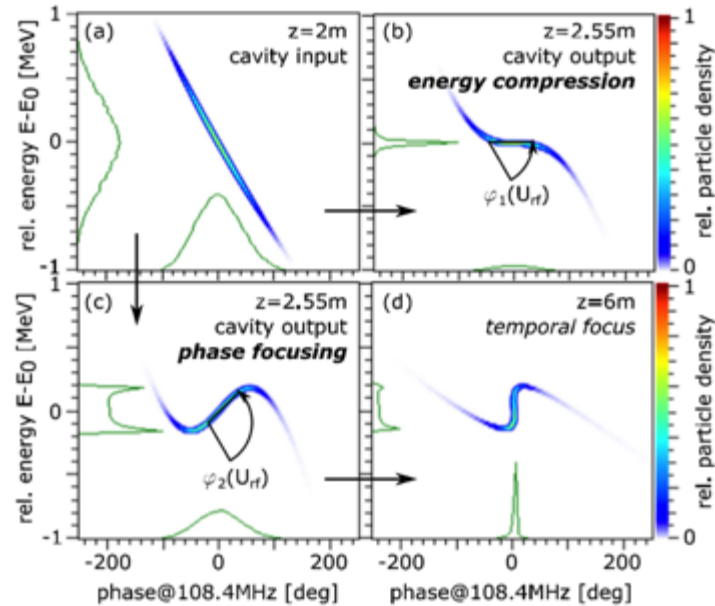


Figure 2. Illustration of phase rotation in longitudinal phase space via applied rf. The input beam is shown for reference in (a) and the two operational modes of interest are depicted in (b) and (c): At an injection phase of $\Phi_s = -90$ deg the bunch is rotated around the central energy by an angle φ in dependency on the rf amplitude U_{rf} . (b) represents the *energy compression mode*, see²⁵ and (c) the *phase focusing mode*, which is described in this paper and leads to (d) a focus of the bunch in the time domain after a certain drift length.

S. Busold et al, Scientific Reports (2015) **5** 12459

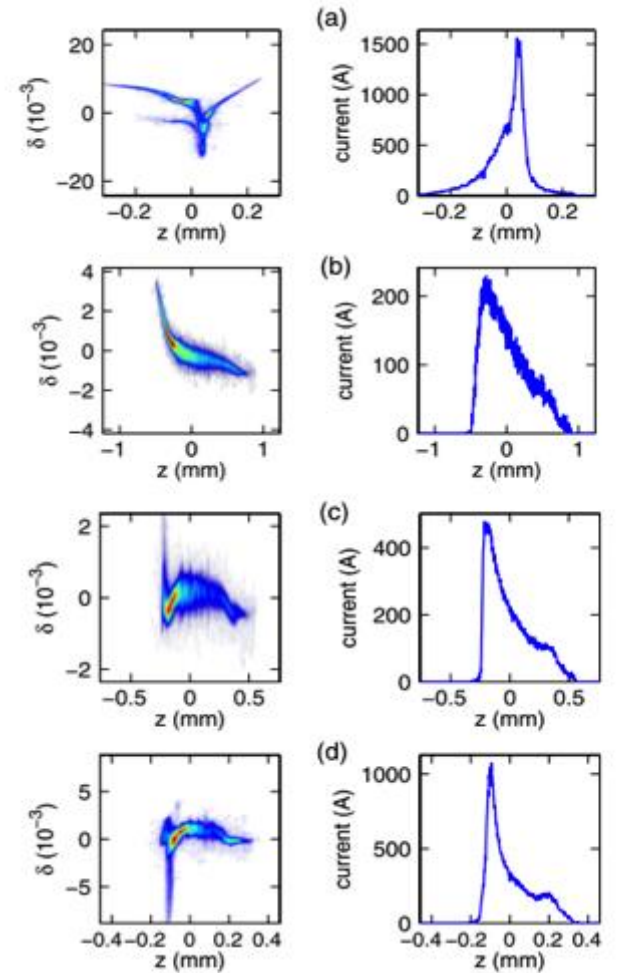
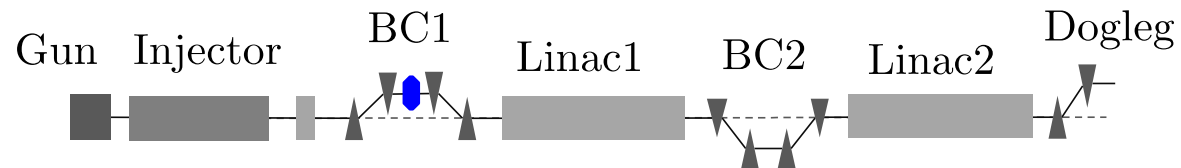


FIG. 4 (color online). Snapshots of the measured longitudinal phase spaces (left column) and associated current profiles (right column) for different settings of the ACC1 and ACC39 accelerating modules. The values $(V_1, \varphi_1, V_3, \varphi_3)$ [in (MV, °; MV, °)] $(150.5, 6.1; 20.7, 3.8)$, $(156.7, 3.8; 20.8, 168.2)$, $(155.6, 3.6; 20.7, 166.7)$, and $(156.8, 4.3; 20.7, 167.7)$ for, respectively, case (b), (c), and (d).

P. Piot et al, Phys. Rev. Lett. (2012) **108** 034801

X-band linac example



$$R_{56} = -82.38 \text{ mm}$$

$$T_{566} = 102.40 \text{ mm}$$

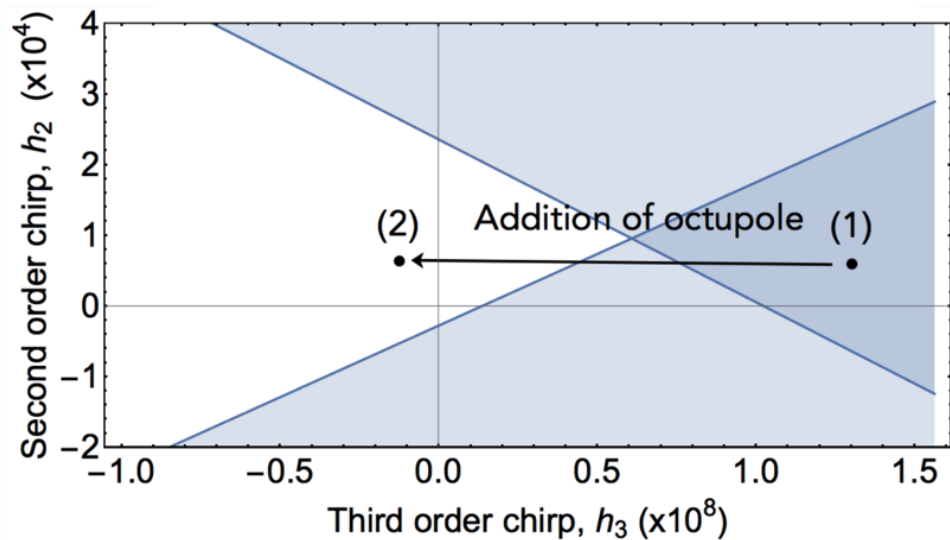
$$U_{5666} = -5.23 \text{ m}$$

$$R_{56} = -11.18 \text{ mm}$$

$$T_{566} = 16.77 \text{ mm}$$

$$U_{5666} = -11.10 \text{ mm}$$

- Non-caustic region
- Region of single fold caustic (single current spike)
- Region of two fold caustics (multiple current spike)

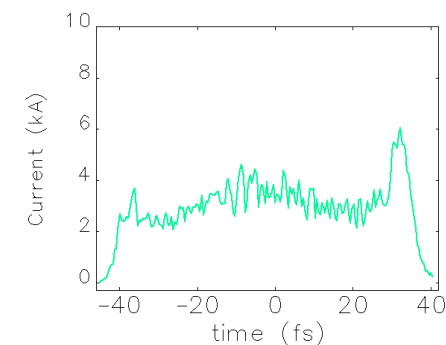
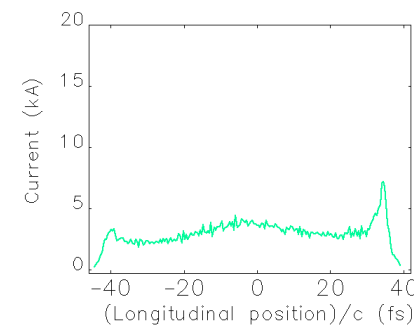
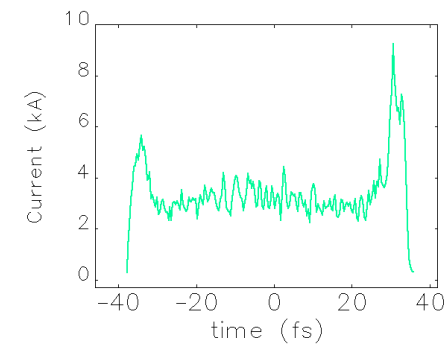
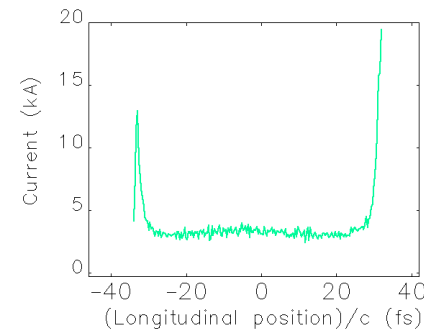


Without octupole:

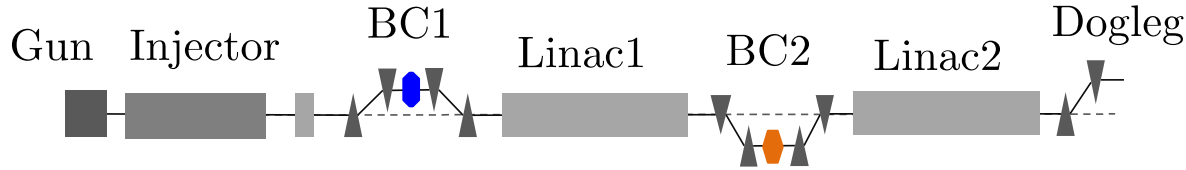
With octupole:

Without CSR:

With CSR:



X-band linac example



$$R_{56} = -82.38 \text{ mm}$$

$$T_{566} = 102.40 \text{ mm}$$

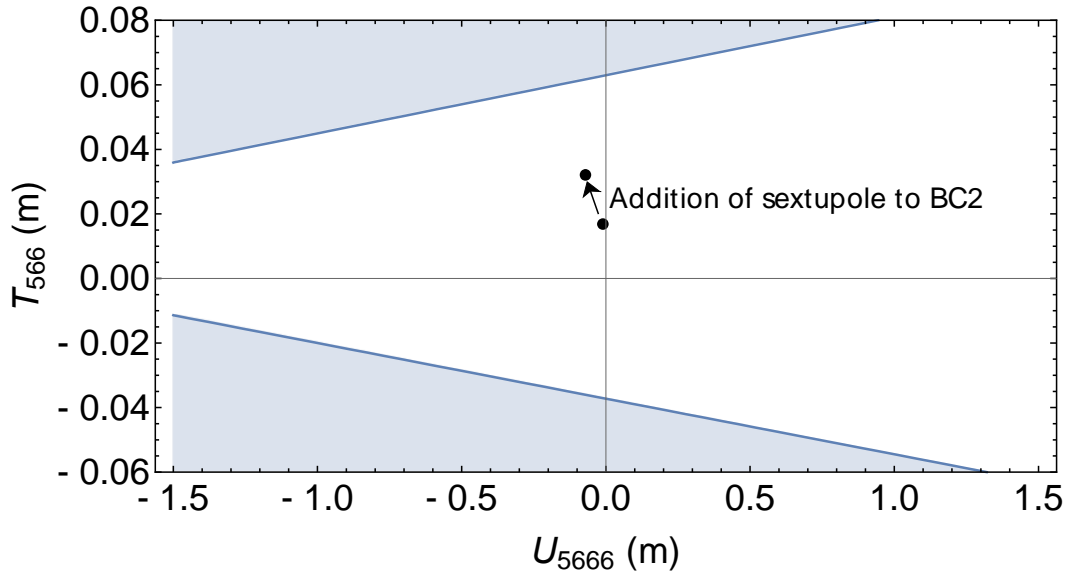
$$U_{5666} = -5.23 \text{ m}$$

$$R_{56} = -11.18 \text{ mm}$$

$$T_{566} = 32.05 \text{ mm}$$

$$U_{5666} = -72.00 \text{ mm}$$

- Non-caustic region
- Region of single fold caustic (single current spike)
- Region of two fold caustics (multiple current spike)

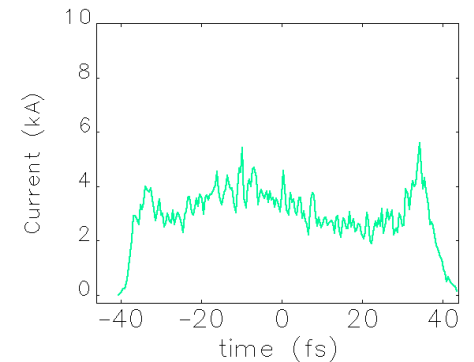
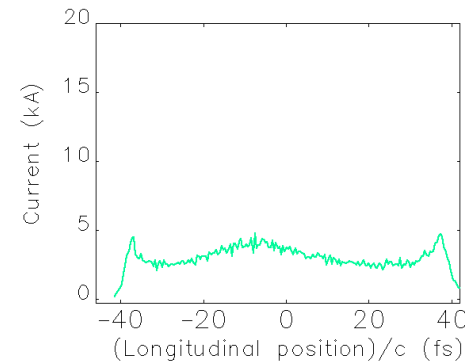
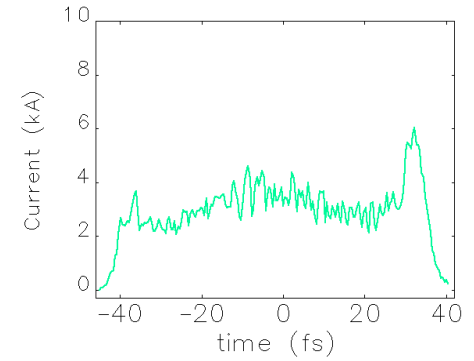
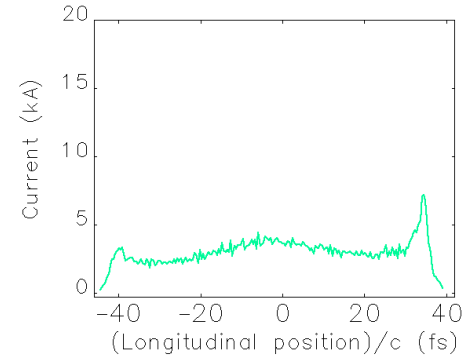


Without sextupole:

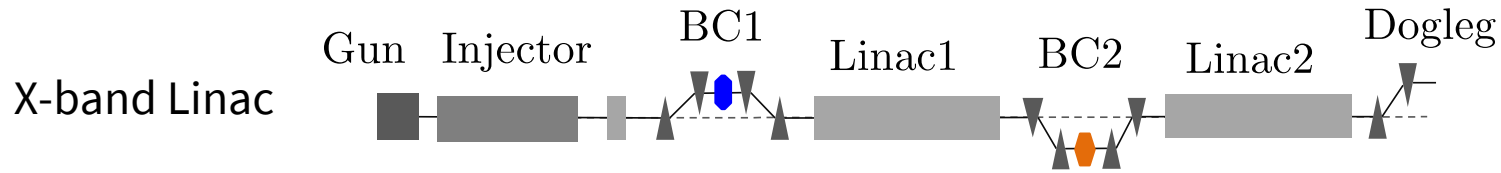
With sextupole:

Without CSR:

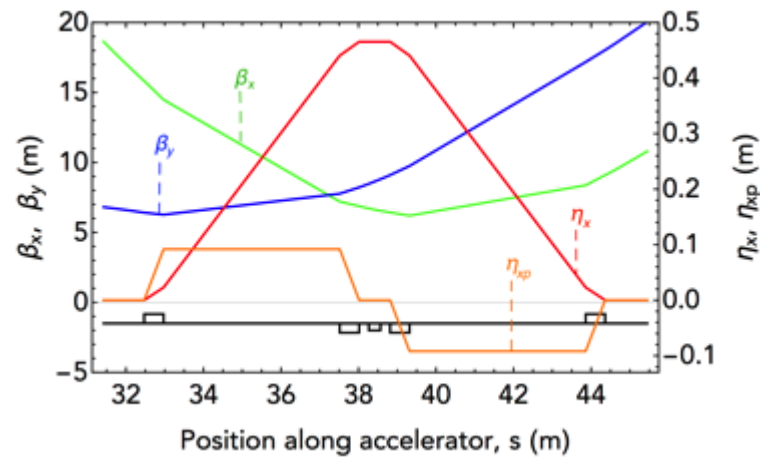
With CSR:



X-band linac example



Bunch Compressor 1



BC1:

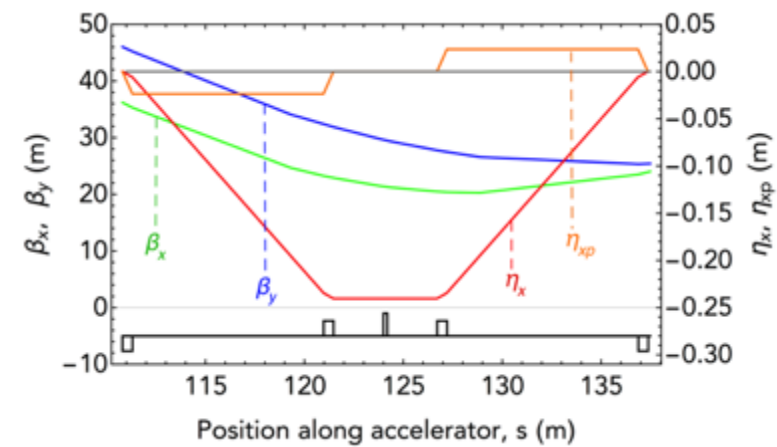
$$R56 = -82.36 \text{ mm}$$

$$T566 = 102.40 \text{ mm}$$

$$U5666 = -5.23 \text{ m}$$

Dipole bending angle, $\theta = 5.25^\circ$
 Octupole strength, $K3 = 2061 \text{ m}^{-4}$

Bunch Compressor 2



BC2:

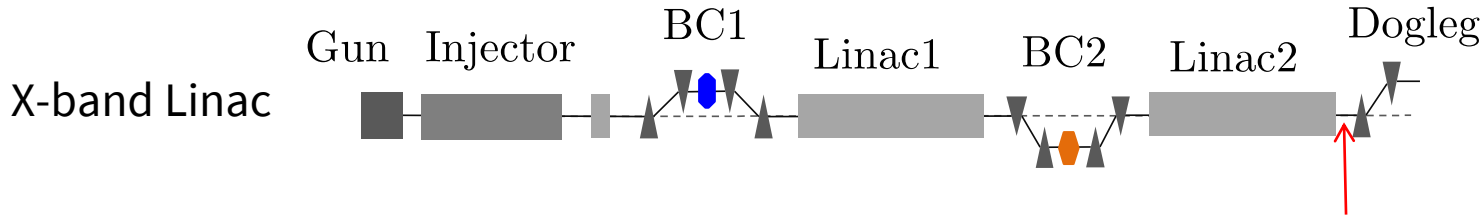
$$R56 = -11.18 \text{ mm}$$

$$T566 = 32.10 \text{ mm}$$

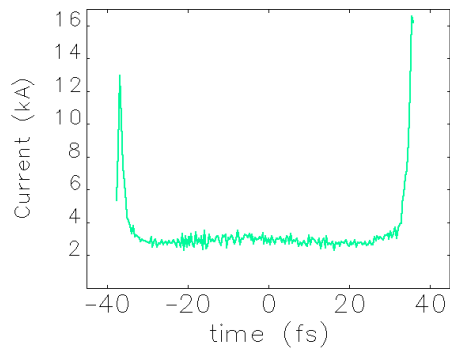
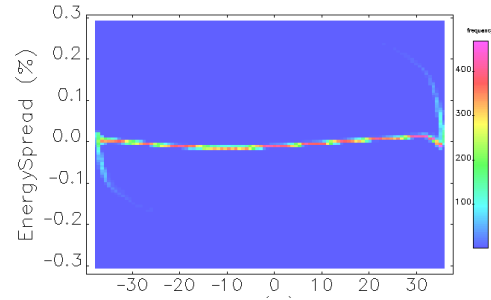
$$U5666 = -72.19 \text{ mm}$$

Dipole bending angle, $\theta = 1.35^\circ$
 Sextupole 1 strength, $K2 = 11.03 \text{ m}^{-2}$

X-band linac example

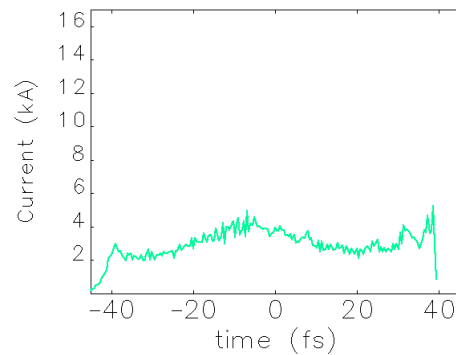
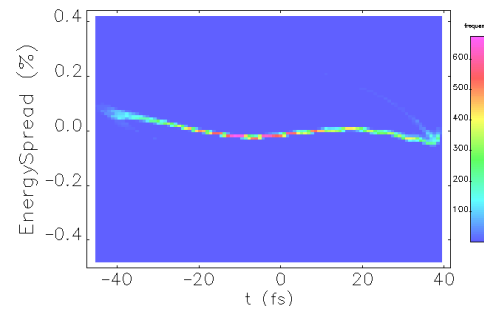


Without octupole & sextupole:



$$\epsilon_{nx} = 1.394 \text{ mm mrad}$$

With octupole & sextupole:



$$\epsilon_{nx} = 0.842 \text{ mm mrad}$$

49% reduction in the
CSR-induced emittance
growth.

T. K. Charles *et al.* (2017)
Phys. Rev. AB, 30, 030705

FFI - X-band linac

TABLE I: Beam properties at the end of the final linac section, for (a) Baseline layout, (b) Layout 1: which includes BC1 octupole magnet (Fig. 6a), (c) Layout 2 which includes BC2 sextupole magnet (Fig. 6b).

Parameter	Symbol	Units	Baseline	Layout 1	Layout 2
Bunch length	σ_z	μm	6.65	6.75	6.68
Horizontal bunch size	σ_x	μm	0.376	0.306	0.267
Vertical bunch size	σ_y	μm	0.161	0.162	0.163
Energy spread	$\sigma_{\Delta E/E}$	%	0.0371 (core)	0.0292	0.0281
Peak current	I_{peak}	kA	3.02 (core)	3.02	3.09
Total compression ratio	CR	-	121.38 ^a	119.6	120.8
Bunch charge	Q	pC	250	250	250
Electron energy	E	GeV	6.16	6.16	6.16
Projected horizontal emittance	$\epsilon_{n,x}$	mm mrad	1.394	0.974	0.842
Mean horizontal slice emittance	$\epsilon_{s,n,x}$	mm mrad	0.386	0.392	0.377
Projected vertical emittance	$\epsilon_{n,y}$	mm mrad	0.274	0.273	0.274
Mean vertical slice emittance	$\epsilon_{s,n,y}$	mm mrad	0.255	0.249	0.246

^a Note the bending angles of BC2 were reduced by less than 0.01% to bring the compression ratio down to be in-line with Layout 1 and Layout 2.

X-band linac, final bunch slice properties

X-band linac

Without octupole: •

With octupole: +

With octupole and sextupole: *

